

**An anti-CD30 immunocytokine
with combined IL-2 and IL-12 domains
enhances anti-tumour immunity**

Dissertation
zur
Erlangung des Doktorgrades (Dr. rer. nat.)
der
Mathematisch-Naturwissenschaftlichen Fakultät
der
Rheinischen Friedrich-Wilhelms-Universität Bonn

vorgelegt von
Martin Zuther
aus
Hamburg

Bonn im Oktober 2009

Bibliografische Information der Deutschen Nationalbibliothek

Die Deutsche Nationalbibliothek verzeichnet diese Publikation in der Deutschen Nationalbibliografie; detaillierte bibliografische Daten sind im Internet über <http://dnb.d-nb.de> abrufbar.

ISBN 978-3-86853-433-7

Angefertigt mit Genehmigung der
Mathematisch-Naturwissenschaftlichen Fakultät
der Rheinischen Friedrich-Wilhelms-Universität Bonn

1. Gutachter: Prof. Dr. Hinrich Abken
Labor für Tumorgenetik
Uniklinik Köln
2. Gutachter: Prof. Dr. Klaus Mohr
Pharmakologie und Toxikologie
Rheinische Friedrich-Wilhelms-Universität Bonn
- Tag der Promotion: 19. März 2010

Cover photograph used with kind permission of André Karwath.

© Verlag Dr. Hut, München 2010
Sternstr. 18, 80538 München
Tel.: 089/66060798
www.dr.hut-verlag.de

Die Informationen in diesem Buch wurden mit großer Sorgfalt erarbeitet. Dennoch können Fehler nicht vollständig ausgeschlossen werden. Verlag, Autoren und ggf. Übersetzer übernehmen keine juristische Verantwortung oder irgendeine Haftung für eventuell verbliebene fehlerhafte Angaben und deren Folgen.

Alle Rechte, auch die des auszugsweisen Nachdrucks, der Vervielfältigung und Verbreitung in besonderen Verfahren wie fotomechanischer Nachdruck, Fotokopie, Mikrokopie, elektronische Datenaufzeichnung einschließlich Speicherung und Übertragung auf weitere Datenträger sowie Übersetzung in andere Sprachen, behält sich der Autor vor.

1. Auflage 2010

See first, think later, then test.
But always see first.
Otherwise you will only see
What you were expecting.

(Douglas Adams)

Meinen Eltern.

Contents

1	Introduction	1
1.1	Classical Hodgkin's lymphoma	2
1.2	Cytokines	3
1.3	Immunocytokines	5
1.4	Objectives of this study	7
2	Materials	9
2.1	Chemicals	9
2.2	Solutions, media and buffers	9
2.3	Sterilisation procedures	9
2.4	DNA plasmids	10
2.5	Synthetic oligonucleotides	13
2.6	Bacterial strains	17
2.7	Primary cells	17
2.8	Cell lines	18
2.9	Antibodies	19
2.10	Sera	23
2.11	Recombinant proteins	23
2.12	Software	24
3	Methods	25
3.1	Bacteria	25
3.1.1	Bacteria culture	25
3.1.2	Generation of chemically competent bacteria	26
3.1.3	Transformation by heat-pulse	26
3.2	Plasmid DNA	27
3.2.1	Preparation of plasmid DNA	27
3.2.2	Quantification of DNA	27
3.2.3	Ethanol precipitation of DNA	27

3.2.4	Agarose gel electrophoresis	28
3.2.5	Isolation of DNA from agarose gels	28
3.2.6	Digestion of DNA	28
3.2.7	Ligation of DNA	29
3.2.8	Polymerase chain reaction	29
3.2.9	Colony PCR	30
3.2.10	Dideoxy DNA sequencing	30
3.3	Tissue culture	31
3.3.1	Mammalian tissue culture	31
3.3.2	Insect tissue culture	32
3.3.3	Passage of adherent cells	32
3.3.4	Passage of cells growing in suspension	33
3.3.5	Subcloning	33
3.3.6	Cryoconservation	33
3.3.7	Calcium phosphate co-precipitation of DNA	33
3.3.8	Lipofection	34
3.3.9	Selection of stably transfected cells	36
3.3.10	FibraStage™ bioreactor	36
3.3.11	Isolation of PBMCs	38
3.3.12	Magnetic cell separation	39
3.4	Proteins	41
3.4.1	Preparation of affinity chromatography media	41
3.4.2	Affinity chromatography	43
3.4.3	Quantification of proteins	44
3.4.4	Radiolabelling of immunocytokines	44
3.4.5	Thin layer chromatography of radiolabelled immunocytokines	46
3.4.6	Desalting of radiolabelled immunocytokines	46
3.4.7	Affinity chromatography of radiolabelled immunocytokines	47
3.5	Assays	47
3.5.1	Enzyme-linked immunosorbent assay	47
3.5.2	Binding inhibition	50
3.5.3	Radioimmunoassay	50
3.5.4	Immunofluorescence	51
3.5.5	Proliferation of PBMCs	52
3.5.6	Cytolysis of tumour cells	53

3.5.7 Phosphorylation of STAT4	54
3.6 Experiments on mice	55
3.6.1 Biodistribution	55
3.6.2 Tumour growth in mice	55
3.6.3 Serum samples	56
3.7 Statistics	56
4 Results	59
4.1 Immunocytokines are expressed in insect cells	59
4.1.1 Generation of the plasmid pBullet HRS3scFv-CD3 ζ (#1078)	60
4.1.2 Generation of the plasmid pMT/BiP HRS3scFv-Fc (#1082)	60
4.1.3 Generation of the plasmid pMT/BiP HRS3scFv-Fc-hi-IL12 (#1083)	62
4.1.4 Generation of the plasmid pMT/BiP HRS3scFv-Fc-IL2 (#1086)	62
4.1.5 Generation of the plasmid pMT/BiP HRS3scFv-hi-IL12-Fc-IL2 (#1100)	65
4.1.6 Generation of the plasmid pMT/BiP SCA431scFv-Fc (#1103)	68
4.1.7 Generation of the plasmid pMT/BiP SCA431scFv-Fc-IL7 (#1117)	68
4.1.8 Generation of the plasmid pMT/BiP SCA431scFv-Fc-IL15 (#1118)	70
4.1.9 Evaluation of transfection efficiency in insect cells . .	70
4.1.10 Insect cells are stably transfected to express immunocytokines	75
4.2 Purified immunocytokines specifically bind to CD30	75
4.2.1 Detection of the individual domains of purified immunocytokines	76
4.2.2 Immunocytokines specifically bind to the anti-idiotypic antibody 9G10	78
4.2.3 CD30 competes with the anti-idiotypic antibody 9G10 in binding to immunocytokines	80
4.2.4 Immunocytokines specifically bind to CD30 ⁺ tumour cells	80

4.3	Purified immunocytokines exhibit cytokine activity	82
4.3.1	Immunocytokines induce proliferation and IFN- γ secretion in PBMCs	87
4.3.2	The IL-12 domain of immunocytokines induces phosphorylation of STAT4 in T cells	90
4.3.3	Immunocytokines induce NK cells to lyse tumour cells	92
4.4	Immunocytokines accumulate at the tumour site	96
4.4.1	Immunocytokines retain specificity of binding after radiolabelling	96
4.4.2	Immunocytokines accumulate at the tumour site . . .	100
4.4.3	Biological half-life of immunocytokines	104
4.5	Immunocytokine HRS3scFv-hi-IL12-Fc-IL2 inhibits tumour growth in immunocompetent mice	105
4.5.1	Immunocytokine HRS3scFv-hi-IL12-Fc-IL2 inhibits tumour growth	107
4.5.2	Immunocytokine HRS3scFv-hi-IL12-Fc-IL2 accumulates in serum	109
4.5.3	Mice raise antibodies directed against the immunocytokine HRS3scFv-hi-IL12-Fc-IL2	112
5	Discussion	115
6	Summary	127
7	Acknowledgements	129
A	Abbreviations	131
B	DNA sequence data	137
B.1	pBullet HRS3scFv-CD3 ζ (#1078)	137
B.2	pMT/BiP HRS3scFv-Fc (#1082)	140
B.3	pMT/BiP HRS3scFv-Fc-hi-IL12 (#1083)	143
B.4	pMT/BiP HRS3scFv-Fc-IL2 (#1086)	148
B.5	pMT/BiP HRS3scFv-hi-IL12-Fc-IL2 (#1100)	151
B.6	pMT/BiP SCA431scFv-Fc (#1103)	156
B.7	pMT/BiP SCA431scFv-Fc-IL7 (#1117)	159
B.8	pMT/BiP SCA431scFv-Fc-IL15 (#1118)	162

C	äктаPrime™ methods	165
C.1	Purification of immunocytokines	166
C.1.1	1 ml HiTrap™ HP column (Conditioning)	166
C.1.2	1 ml HiTrap™ HP column (Elution)	167
C.1.3	5 ml HiTrap™ HP column (Conditioning)	168
C.1.4	5 ml HiTrap™ HP column (Elution)	169
C.1.5	C10/10™ column packed with Sepharose™ beads (Conditioning)	170
C.1.6	C10/10™ column packed with Sepharose™ beads (Elution)	171
C.2	Purification of antibodies	172
C.2.1	C10/10™ column (Conditioning)	172
C.2.2	C10/10™ column (Elution)	173

List of Figures

1.1	Expression cassettes of anti-CD30 immunocytokines	8
3.1	FibraStage™ culture parameters	37
3.2	Purity of isolated lymphocyte subsets	40
3.3	The asinh ₁₀ transformation	52
4.1	Generation of the plasmid pBullet HRS3scFv-CD3ζ (#1078) .	61
4.2	Generation of the plasmid pMT/BiP HRS3scFv-Fc (#1082) . .	63
4.3	Generation of the plasmid pMT/BiP HRS3scFv-Fc-hi-IL12 (#1083)	64
4.4	Generation of the plasmid pMT/BiP HRS3scFv-Fc-IL2 (#1086)	66
4.5	Generation of the plasmid pMT/BiP HRS3scFv-hi-IL12-Fc- IL2 (#1100)	67
4.6	Generation of the plasmid pMT/BiP SCA431scFv-Fc (#1103)	69
4.7	Generation of the plasmid pMT/BiP SCA431scFv-Fc-IL7 (#1117)	71
4.8	Generation of the plasmid pMT/BiP SCA431scFv-Fc-IL15 (#1118)	72
4.9	Comparison of transfection procedures for insect cells	73
4.10	Transfected insect cells secrete immunocytokines	74
4.11	Detection of the individual domains of purified immunocy- tokines	77
4.12	Immunocytokines specifically bind to the anti-idiotypic anti- body 9G10	79
4.13	CD30 competes with the anti-idiotypic antibody 9G10 in binding to immunocytokines	81
4.14	Immunocytokines bind to CD30 ⁺ L540 cells	83
4.15	Immunocytokines do not bind to CD30 ⁻ MeWo cells	84

4.16 Immunocytokines bind to 9G10 hybridoma cells	85
4.17 Immunocytokines bind to CD30 ⁺ tumour cells	86
4.18 Immunocytokines induce proliferation in PBMCs	88
4.19 Immunocytokines induce IFN- γ secretion in PBMCs	89
4.20 Murine IL-12 induces phosphorylation of STAT4 in human T cells	91
4.21 The IL-12 domain of immunocytokines induces phosphoryl- ation of STAT4 in T cells	93
4.22 Characterisation of modified MC38 and C15A3 cells	94
4.23 Immunocytokines induce NK cells to lyse tumour cells	95
4.24 Desalting of radiolabelled immunocytokines	97
4.25 Purification of radiolabelled immunocytokine HRS3scFv-hi- IL12	98
4.26 Radiolabelled immunocytokines specifically bind to the anti- idiotypic antibody 9G10	99
4.27 L540Cy cells express CD30	101
4.28 Immunocytokine HRS3scFv-hi-IL12 accumulates at the tu- mour site	102
4.29 Immunocytokine HRS3scFv-Fc-hi-IL12 accumulates at the tumour site	103
4.30 Biological half-life of immunocytokines	106
4.31 Dose escalation of immunocytokine HRS3scFv-hi-IL12-Fc- IL2 in mice	108
4.32 Immunocytokine HRS3scFv-hi-IL12-Fc-IL2 inhibits tumour growth in mice	110
4.33 Immunocytokine HRS3scFv-hi-IL12-Fc-IL2 accumulates in serum.	111
4.34 Mice raise antibodies directed against the immunocytokine HRS3scFv-hi-IL12-Fc-IL2	112

1 Introduction

Cancer is the third leading cause of death worldwide. Of the estimated 60 million deaths that occurred worldwide in 2004, 13% have been attributed to cancer, following cardiovascular diseases (29%) and infectious or parasitic diseases (16%). Moreover, the number of deaths caused by cancer is expected to nearly double by 2030 (World Health Organization, 2008). Cancer is a genetic disease thought to develop by clonal selection after a series of mutation events. Thus, tumour specimens derived from the same tissue show considerable heterogeneity of mutated genes, and each tumour is unique and responds differently to therapy (Sjöblom *et al.*, 2006). In the process of clonal selection, malignant cells often lose regulation of cell growth, become resistant to apoptosis, down-regulate molecules that allow detection of aberrant cells by the immune system or start to secrete soluble factors such as cytokines. In advanced stages of cancer, malignant cells can also migrate to other tissues and grow metastases.

Resection, radiation and chemotherapeutic agents are still the treatment of choice for malignant diseases. However, such therapy is not specific for malignant cells, and systemic application is accompanied by high toxicities. During the last decade, a number of therapeutic agents that specifically target tumour cells, such as monoclonal antibodies and tyrosine kinase inhibitors, have become available and revolutionised cancer therapy (Gerber, 2008; Voltz and Gronemeyer, 2008).

1.1 Classical Hodgkin's lymphoma

Classical Hodgkin's lymphoma is a cancer of the immune system that comprises approximately 0.5% of newly diagnosed cancers. It has a bimodal age-incidence curve with a peak at 15 to 34 years and a second peak at 60 years and above. The neoplastic cells represent the Hodgkin-Reed-Sternberg cells and are of B cell origin. Interestingly, malignant cells comprise only a small fraction of the tumour mass and are surrounded by an inflammatory infiltrate of healthy lymphocytes, eosinophils, fibroblasts, macrophages and plasma cells (Young and Iland, 2007).

While classical Hodgkin's lymphoma is one of the most curable cancers in adults, non-responders, tumour relapses and long-term toxicities of the treatment make it necessary to look for alternative drugs (Fuchs *et al.*, 2006). Current therapeutic schemes for classical Hodgkin's lymphoma do not specifically target the malignant cells, therefore therapies would benefit from drugs that effect a specific anti-tumour response (table 1.1). The surface molecule CD30, a 120kDa glycoprotein belonging to the tumour necrosis factor receptor superfamily, presents a good target for immunotherapy, as it is expressed almost exclusively on the cell surface of activated lymphocytes and malignant lymphoid cells such as the Hodgkin-Reed-Sternberg cells of Hodgkin's lymphoma (Chiarle *et al.*, 1999). CD30 is shed from Hodgkin-Reed-Sternberg cells in large quantities which poses a major problem for targeted immunotherapy. However, shedding can effectively be inhibited by hydroxamate inhibitors of metalloproteases (Matthey *et al.*, 2004).

An overproduction of T_H2 cytokines in the tumour lesion is attributed to suppress an adequate immune response against the malignant Hodgkin-Reed-Sternberg cells (Skinnider and Mak, 2002). The balance between T_H1 and T_H2 cytokines determines which immune response results from infection with a pathogen: T_H1 cells help in eliminating intracellular pathogens, whereas T_H2 cells target extracellular pathogens. Hence, the defective immune response in classical Hodgkin's lymphoma might be turned into an efficient anti-tumour response by administration of T_H1 cytokines, thus tipping the balance in favour of a T_H1 reaction. However, clinically effec-

Table 1.1: Drugs used in the ABVD and BEACOPP protocols for the therapy of classical Hodgkin's lymphoma (Young and Iland, 2007).

Drug	Class	ABVD	BEACOPP
Bleomycin	anthracycline	x	x
Cyclophosphamide	alkylating agent		x
Dacarbazine	alkylating agent	x	
Doxorubicin	anthracycline	x	x
Etoposide	topoisomerase inhibitor		x
Prednisone	glucocorticoid		x
Procarbazine	alkylating agent		x
Vinblastine	mitotic inhibitor	x	
Vincristine	mitotic inhibitor		x

tive doses of recombinant cytokines often lead to severe side effects, thus a means of targeting cytokines to the tumour site needs to be explored.

1.2 Cytokines

Cytokines are low-molecular-weight proteins secreted by cells that, after binding to their receptors, regulate cellular functions in a paracrine or autocrine fashion. Among other functions, cytokines play a significant role in regulating immune responses. Cytokines secreted by T cells are usually termed interleukins (IL), while cytokines induced in response to viral infections are called interferons (IFN) (Murphy *et al.*, 2008; Skinnider and Mak, 2002).

Interleukin-2

Human interleukin-2 (IL-2) is a 15.5 kDa glycoprotein which is mainly produced by activated CD4⁺ lymphocytes of the T_H1 phenotype. IL-2 delivers

potent proliferation signals to T cells, B cells and natural killer (NK) cells *in vitro*. Moreover, IL-2 augments the *in vitro* cytolytic activity of NK cells and monocytes. *In vivo*, IL-2 mainly supports the differentiation of regulatory T cells, thus preventing immune reactions from overshooting. The cytokine may also regulate the *in vivo* expansion of recently activated T cells.

IL-2 receptors are mainly expressed by cells of the immune system and composed from three subunits. The IL-2R α chain (CD25) does not seem to be involved in intramolecular signalling, whereas the IL-2R β chain (CD122), that is shared with the IL-15 receptor, signals via Jak3-, STAT5- and AKT-dependent pathways. The common cytokine receptor γ_c chain (CD132) is shared by a number of cytokine receptors and signals via MAP kinase and PI3 kinase pathways. The IL-2R β and γ_c chains form an intermediate-affinity receptor complex, while all three receptor subunits assemble to a high-affinity receptor (Ma *et al.*, 2006; Thèze, 1999).

Recombinant IL-2 has been approved by the United States Food and Drug Administration for use in adults with metastatic melanoma and metastatic renal cell carcinoma. High-dose IL-2 therapy has shown complete and durable responses in approximately 10% of treatment-naïve patients with advanced renal cell carcinoma. However, systemic administration of IL-2 elicits life-threatening side effects. Grade 3 to 4 toxicities include hypotension, capillary leak syndrome, arrhythmia and neurotoxicity. As of 2001, the incidence of treatment-related mortality has been as high as 1% (Atkins, 2009; Dutcher *et al.*, 2001).

Interleukin-12

Human interleukin-12 (IL-12) is a 70 kDa heterodimeric glycoprotein (p70) composed of two disulfide-linked subunits with molecular weights of 35 kDa (p35) and 40 kDa (p40). The p35 chain shows limited homology with other single-chain cytokines, whereas p40 is homologous to the extracellular domain of the hematopoietic receptor family. Both subunits are required for biologically active IL-12. The expression of p40 determines a cell's ability to secrete IL-12, while p35 controls the absolute amount of

IL-12 produced. IL-12 is mainly produced by phagocytic cells, acts as a pro-inflammatory cytokine, favours the differentiation of T_H1 cells and inhibits the differentiation of T_H2 cells. The cytokine induces proliferation in activated T and NK cells, enhances the cytotoxic activity of NK cells and favours the generation of cytotoxic $CD8^+$ cells. Moreover, IL-12 induces activated T and NK cells to secrete the T_H1 cytokine IFN- γ , which in turn enhances production of IL-12 in granulocytes, thus forming a positive feedback loop. In contrast, the T_H2 cytokines TGF- β and IL-10 are potent inhibitors of IL-12 production.

IL-12 receptors are mainly expressed on activated T and NK cells. The IL-12R β 1 chain (CD212) is shared with the IL-23 receptor, binds to p40 and does not seem to be involved in intramolecular signalling, while the IL-12R β 2 chain interacts with p35 and signals through phosphorylation of Jak2, Tyk2 and the transcription factors STAT1, STAT3, STAT4 and STAT5. The cellular functions of IL-12 are mainly mediated by phosphorylation of STAT4 (Hölscher, 2004; Thèze, 1999; Thomson and Lotze, 2003).

In vivo, IL-12 mediates efficient anti-tumour responses by triggering both innate and adaptive immune responses against tumour cells, and by inhibiting angiogenesis. The anti-tumour effects of IL-12 are mostly mediated by indirect mechanisms, particularly by enhancing the endogenous production of IFN- γ . However, long-term IL-12 monotherapy inhibits IFN- γ production and induces immunosuppression in humans. Moreover, systemic administration of IL-12 elicits severe toxicities. Grade 3 to 4 toxicities include dyspnea, stomatitis, transaminitis and leukopenia. Two treatment-related deaths have been reported (Weiss *et al.*, 2007; Wigginton and Wiltrot, 2002).

1.3 Immunocytokines

One of the major problems of current cancer therapy is that most drugs neither specifically target malignant cells, nor accumulate at the tumour lesion. Unless primary tumour and metastases are directly accessible, drugs

have to be administered systemically and patients generally suffer from side effects, while toxicities lead to the use of suboptimal doses. Cytokines exhibit particularly severe toxicities when administered systemically, as they are highly effective in nanomolar to picomolar concentrations. Moreover, side effects of cytokine administration may be amplified by the induction of cytokine secretion and positive feedback loops.

With the advance of monoclonal antibodies and hybridoma technology (Köhler and Milstein, 1975), a plethora of antibodies have been raised against tumour-associated antigens. Subsequently, such diverse agents as radioactive substances, chemotherapeutic agents, toxins, enzymes and prodrugs have been targeted to malignant cells by conjugation to monoclonal antibodies or single-chain fragment variants (scFv) derived from these antibodies (Schrama *et al.*, 2006). To decrease the severe side effects of systemically administered cytokines, antibodies and single-chain fragment variants have also been conjugated to cytokines. The resulting fusion proteins, termed immunocytokines, accumulate at tumour lesions and display anti-tumour activity *in vivo*. Moreover, immunocytokines that include the Fc domain of an antibody enhance the anti-tumour activity of a cytokine by inducing antibody-dependent cellular cytotoxicity (ADCC) (Davis and Gillies, 2003).

For the therapy of classical Hodgkin's lymphoma, our group has generated an scFv that retains the idiotypic profile of the anti-CD30 monoclonal antibody HRS3 (Hombach *et al.*, 1998). Anti-CD30 immunocytokines have been generated by fusing the HRS3 scFv to human IL-2 or murine single-chain IL-12 using the hinge or Fc regions of human IgG₁ as linkers (Heuser *et al.*, 2003, 2004). Murine IL-12 has been chosen instead of its human counterpart because we want to assess immunocytokine activity on both human lymphocytes and in mouse models. Human IL-12 does not stimulate murine lymphocytes, whereas murine IL-12 is active on human and murine lymphocytes (Schoenhaut *et al.*, 1992). In contrast, human IL-2 stimulates human and murine T cells with similar efficacies (Mosmann *et al.*, 1987).

1.4 Objectives of this study

Researchers have proposed to treat cancer with a combination of IL-2 and IL-12, as these cytokines activate separate pathways, reciprocally up-regulate each other's receptors and induce complimentary biological effects (Wigginton and Wiltout, 2002). *In vivo*, IL-2 and IL-12 show a strong synergistic effect that is mostly attributed to enhanced activation of cytotoxic T and NK cells. Moreover, immunosuppression and inhibition of IFN- γ production during monotherapy with IL-12 can be overcome by concurrent administration of low-dose IL-2. Finally, effective cytokine doses of combination therapy with IL-2 and IL-12 seem to be lower and side effects much reduced compared to therapy with a single cytokine (Weiss *et al.*, 2007).

Accordingly, our group has found that the combination of an immunocytokine with IL-2 domain and an immunocytokine with IL-12 domain enhances activation of resting NK cells and tumour cell lysis *in vitro*, compared to either immunocytokine alone (Hombach *et al.*, 2005). As the simultaneous administration of two immunocytokines may induce problems such as competition on binding to CD30, we have generated the novel anti-CD30 immunocytokine HRS3scFv-hi-IL12-Fc-IL2. This immunocytokine has been designed for the therapy of classical Hodgkin's lymphoma and combines human IL-2 and single-chain murine IL-12 in one molecule. Figure 1.1 gives an overview on the anti-CD30 immunocytokines used in this study.

The objective of this study is to assess whether an immunocytokine with combined IL-2 and IL-12 domains is more suited for the immunotherapy of classical Hodgkin's lymphoma in terms of lymphocyte activation and tumour cell lysis than immunocytokines with each cytokine domain. We aim to explore whether the novel immunocytokine HRS3scFv-hi-IL12-Fc-IL2 augments secretion of the T_H1 cytokine IFN- γ , which may be important for overcoming the misguided T_H2 immune reaction in classical Hodgkin's lymphoma. We will reveal that the insertion of an additional cytokine domain into immunocytokines does not alter avidity and specificity of binding. As the influence of dimerisation mediated by the Fc domain of an an-

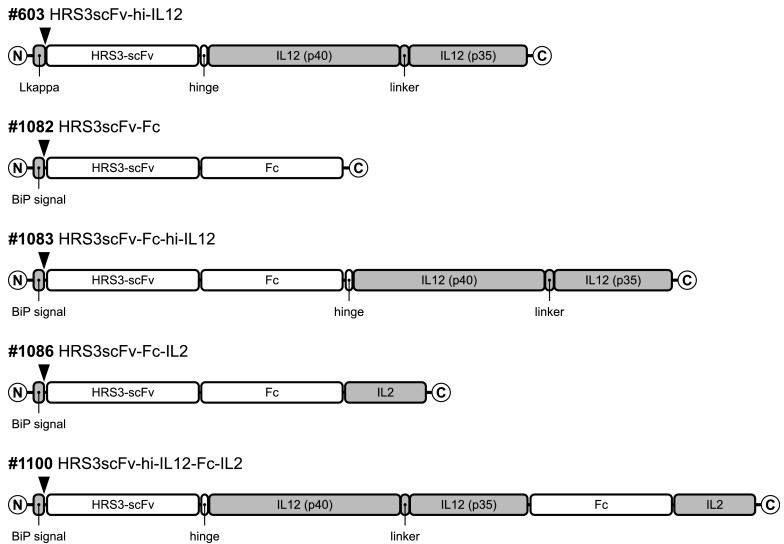


Figure 1.1: Expression cassettes of the anti-CD30 immunocytokines used in this study. Immunocytokines and the fusion protein HRS3scFv-Fc were generated by fusing DNA coding for the anti-CD30 scFv HRS3 to DNA coding for the Fc region of human IgG₁, the hinge region of human IgG₁, human IL-2 or murine single-chain IL-12. **Linker:** (GlySer₄)₃ linker. **Hinge:** hinge region of human IgG₁. **LKappa and BiP signal:** leader sequences needed for protein secretion. **Black triangles:** signal cleavage sites.

tibody on the biodistribution of immunocytokines is not clear, we further want to compare the biodistribution of two anti-CD30 immunocytokines that are identical except for lacking or containing an Fc domain. At the same time, we want to ascertain that anti-CD30 immunocytokines accumulate at the tumour. Finally, we intend to estimate suitability of the immunocytokine HRS3scFv-hi-IL12-Fc-IL2 for use in cancer patients by investigating whether immunocompetent mice tolerate systemic administration of this immunocytokine, and whether tumour growth is inhibited in this setting.

2 Materials

2.1 Chemicals

Chemicals were obtained from Fluka (Neu-Ulm, Germany), Merck (Darmstadt, Germany), Roth (Karlsruhe, Germany) and Sigma-Aldrich (Steinheim, Germany). Na^{131}I was obtained from Polatom (Otwock-Świerk, Poland).

2.2 Solutions, media and buffers

Solutions and media were prepared according to Ausubel (2005) and Coligan (2005) unless mentioned otherwise. All solutions were prepared from double distilled water (ddH_2O). If needed, pH was corrected by addition of 1 M or 5 M solutions of HCl, HOAc or NaOH prior to sterilisation. Thermally unstable ingredients such as antibiotics were added when sterilised solutions had cooled down to 50°C or below.

2.3 Sterilisation procedures

Pipette tips and thermally stable solutions were autoclaved (121°C, 2×10^5 Pa). Thermally unstable solutions were sterilised by filtration through 200nm Sterifix™ filters (B. Braun, Melsungen, Germany). Glassware was heat-sterilised (180°C, ≥ 4 h). Performance of heat-sterilisation

procedures was controlled with heat indicators for every item. Sterilisation efficiency was also tested at regular intervals with spores of *Geobacillus stearothermophilus* (autoclaving) or *Bacillus atrophaeus* (heat-sterilisation).

2.4 DNA plasmids

Table 2.1: List of DNA plasmids used in this study.

ID	Plasmid	Characteristics (Reference)
#435	pBullet-Lk CC49-scFv-Fc-CD3 ζ	contains the mammalian expression cassette of the TAG-72-specific immunoreceptor CC49scFv-Fc-CD3 ζ (Hombach <i>et al.</i> , 1998)
#440	pRSV-Lk HRS3scFv-Fc	contains the mammalian expression cassette of the anti-CD30 immunocytokine HRS3scFv-Fc (Heuser <i>et al.</i> , 2004)
#508	pRSV-Lk HRS3scFv-Fc-IL2	contains the mammalian expression cassette of the anti-CD30 immunocytokine HRS3scFv-Fc-IL2 (Heuser <i>et al.</i> , 2004)
#603	pRSV-Lk HRS3scFv-hi-IL12	contains the mammalian expression cassette of the anti-CD30 immunocytokine HRS3scFv-hi-IL12 (Heuser <i>et al.</i> , 2003)
#619	pRSV-Lk HRS3scFv-Fc-hi-IL12	contains the mammalian expression cassette of the anti-CD30 immunocytokine HRS3scFv-Fc-hi-IL12 (Hombach <i>et al.</i> , 2005)

Table 2.1: List of DNA plasmids used in this study (continued).

ID	Plasmid	Characteristics (Reference)
#653	pGT60 hB7.2	contains the mammalian expression cassettes encoding for the hygromycin resistance gene, the Herpes simplex thymidine kinase and human B7.2 (InvivoGen, Toulouse, France)
#715	pRSV-Lk HRS3scFv-hi-IL12-Fc-IL2	contains the mammalian expression cassette of the anti-CD30 immunocytokine HRS3scFv-hi-IL12-Fc-IL2 (unpublished)
#841	pcDNA3.1 CD30	contains the mammalian expression cassette coding for the surface marker CD30 (unpublished)
#844	pORF IL15	contains DNA coding for human IL-15 (InvivoGen)
#944	pRSV-Lk 763.74-scFv-Fc	contains the mammalian expression cassette of the anti-melanoma immunocytokine 763.74scFv-Fc (unpublished)
#977	pBullet-Lk SCA431-scFv-Fc-CD4tm-CD3 ζ	contains the mammalian expression cassette of the CEA-specific immunoreceptor SCA431scFv-Fc-CD4tm-CD3 ζ (Chmielewski, 2007)
#1024	pJR IL7	contains DNA coding for murine IL-7; kindly provided by Prof. Dr. Thomas Blankenstein, Max-Delbrück-Centrum für Molekulare Medizin, Berlin-Buch, Germany (pBA IL7 in Hock <i>et al.</i> , 1991)

Table 2.1: List of DNA plasmids used in this study (continued).

ID	Plasmid	Characteristics (Reference)
#1041	pcDNA3.1 IL21	contains DNA coding for murine IL-21; kindly provided by Prof. Dr. Naomi Taylor, Institut de Génétique Moléculaire de Montpellier, Montpellier, France
#1070	pMT/BiP V5-His A	Drosophila Expression System™ (Invitrogen, Karlsruhe, Germany); inducible expression of secreted proteins in cells of <i>Drosophila melanogaster</i>
#1078	pBullet HRS3scFv-CD3 ζ	contains DNA coding for anti-CD30-scFv HRS3
#1080	pCoHygro	expression in <i>Drosophila</i> cells; contains expression cassette encoding for the hygromycin resistance gene (Invitrogen)
#1082	pMT/BiP HRS3-scFv-Fc	expression in <i>Drosophila</i> cells; contains expression cassette of the anti-CD30 immunocytokine HRS3scFv-Fc
#1083	pMT/BiP HRS3-scFv-Fc-hi-IL12	expression in <i>Drosophila</i> cells; contains expression cassette of the anti-CD30 immunocytokine HRS3scFv-Fc-hi-IL12
#1086	pMT/BiP HRS3-scFv-Fc-IL2	expression in <i>Drosophila</i> cells; contains expression cassette of the anti-CD30 immunocytokine HRS3scFv-Fc-IL2
#1100	pMT/BiP HRS3-scFv-hi-IL12-Fc-IL2	expression in <i>Drosophila</i> cells; contains expression cassette of the anti-CD30 immunocytokine HRS3scFv-hi-IL12-Fc-IL2

Table 2.1: List of DNA plasmids used in this study (continued).

ID	Plasmid	Characteristics (Reference)
#1103	pMT/BiP SCA431-scFv-Fc	expression in <i>Drosophila</i> cells; contains expression cassette of the anti-CEA immunocytokine SCA431scFv-Fc
#1117	pMT/BiP SCA431-scFv-Fc-IL7	expression in <i>Drosophila</i> cells; contains expression cassette of the anti-CEA immunocytokine SCA431scFv-Fc-IL7
#1118	pMT/BiP SCA431-scFv-Fc-IL15	expression in <i>Drosophila</i> cells; contains expression cassette of the anti-CEA immunocytokine SCA431scFv-Fc-IL15

2.5 Synthetic oligonucleotides

Oligonucleotides were synthesised by Eurogentec (Cologne, Germany), Invitrogen (Karlsruhe, Germany) and MWG-Biotech (Munich, Germany).

Table 2.2: List of synthetic oligonucleotides used in this study. Restriction sites (**sites**) in sequences are indicated by lines. **C**: The oligonucleotide has been used for cloning procedures. **S**: The oligonucleotide has been used for sequencing.

ID	Name	Sites	Sequence (5' to 3')	Usage
#38	HRS3-VL-BamHI-3'	BamHI	ACC TGG <u>ATC</u> CGC CCG TTT GAT TTC	S
#55	IL-2SX	XhoI	TCA <u>ACT CGA</u> GTC GAC TCA AGT CAG TGT TGA GAT GAT	C

Table 2.2: List of synthetic oligonucleotides used in this study (continued).

ID	Name	Sites	Sequence (5' to 3')	Usage
#75	SeqRSV-S		TTG GTG TGC ACC TCC AAG CTC CTC	S
#76	SeqFc-AS		CGG TCC CCC CAG GAG TTC AGG TGC	S
#95	IL12-hi-S	BamHI	TG AAG <u>GAT CCC</u> GCC GAG CCC AAA TCT CCT GAC AAA ACT CAT ACA TGC CCA CCA ATG TGG GAG CTG GAG AAA GAC GTT	S
#111	IL12-Li-AS-1		AGA TCC GCC GCC ACC CGA CCC	S
#113	IL12-Li-AS-2		CTT GAT GTT GAA CTT CAA GTC CAT GTT TC	S
#127	hIgG-Seq-S		C AAC TGG TAC GTG GAC GGC G	S
#128	hIgG-Seq-AS		C ATT GCT CTC CCA CTC CAC GG	S
#135	pBullet-5'- Seq neu		GG ACC TTA CAC AGT CCT GCT GAC CA	S
#136	pBullet-3'- Seq neu		C GTA CTA TAG GCT TCA GCT GGT GAT ATT G	S
#195	5'-Seq-Fc-End		A TGC TCC GTG ATG CAT GAG GCT CT	S

Table 2.2: List of synthetic oligonucleotides used in this study (continued).

ID	Name	Sites	Sequence (5' to 3')	Usage
#238	S-HRS3-hi-Bam	BamHI	GGC ACC AAG CTG GAA ATC AAA CGG GCG GAT CCC GCC	C
#251	mIgG1-S		AAC TGG GAG GCA GGA AAT ACT TTC ACC	S
#253	Seq-p40-S2		ACT CCC CAT TCC TAC TTC TCC CTC	S
#317	Seq-VH#680		TGA GGA GAC GGT GAC CGT GGT	S
#324	SCA431-Vk-Gly-Linker S		TCG GGC GGT GGC GGG TCG GGT GGC GGC GGA TCT GAC ATC CAG CTG ACC CAG TCT CCA GCA ATC A	S
#363	AS-mIgG		AT GGT GAG CAC ATC CTT GGG C	S
#433	HRS3-pMT-S	NcoI	C GAA CCA TGG GTG GCC CAG GTG CAA CTG CAG	C
#469	pMT-BiP Seq-S		C ATC TCA GTG CAA CTA AA	S
#470	pMT-BiP Seq-AS		TAG AAG GCA CAG TCG AGG	S
#471	pMT-SCA431-S	NcoI	G GGG CCA TGG AGA GGT GTC CAC TCC CAG	C

Table 2.2: List of synthetic oligonucleotides used in this study (continued).

ID	Name	Sites	Sequence (5' to 3')	Usage
#472	pMT-SCA431-AS	BstXI, NotI	TTT <u>TGC GGC CGC</u> TCA CTT <u>ACC AGG AGA GTG</u> GGA	C
#490	pMT-mIL7-BstX-S	BstXI	CTC TCC <u>CAC TCT CCT</u> <u>GGT</u> AAG GAG TGC CAC ATT AAA GAC	C, S
#491	pMT-mIL7-Not-AS	NotI, XhoI	<u>AC TCG AGC GGC CGC</u> TCA TAT ACT GCC CTT CAA AAT	C
#492	pMT-hIL15-BstX-S	BstXI	CTC TCC <u>CAC TCT CCT</u> <u>GGT</u> AAG AAC TGG GTG AAT GTA ATA	C, S
#493	pMT-hIL15-Not-AS	NotI, XhoI	<u>AC TCG AGC GGC CGC</u> TCA AGA AGT GTT GAT GAA CAT	C
#495	pMT-mIL21-Not-AS	NotI, XhoI	<u>AC TCG AGC GGC CGC</u> TCA GGA GAG ATG CTG ATG AAT	C
#496	mIgG1-S2		GTG CCC AGG GAT TGT GGT TGT	S
#512	pMT-mIL21-shortSP-BstX-S	BstXI	CTC TCC <u>CAC TCT CCT</u> <u>GGT</u> AAG CCA GAT CGC CTC CTG ATT	C
#513	pRSV-Seq-AS		TCA CAA ATT TCA CAA	S

2.6 Bacterial strains

The following bacterial strains were used for cloning, transformation and the amplification of plasmids:

- *Escherichia coli* DH5 α (Hanahan, 1985)
Genotype: F⁻ endA hsdR17 supE44 thi-1 recA1 gyrA relA1 Δ (lacZYA-argF) Φ 80d lacZ Δ M15
- *Escherichia coli* One ShotTM INV110 (Invitrogen)
Genotype: F' {tra Δ 36 proAB lacI^q lacZ Δ M15} rpsL (Str^R) thr leu endA thi-1 lacY galK galT ara tonA tsx dam dcm supE44 Δ (lac-proAB) Δ (mcrC-mrr)102::Tn10 (Tet^R)

2.7 Primary cells

Human peripheral blood mononuclear cells

Human peripheral blood mononuclear cells (PBMC) were isolated from fresh blood or buffy coats (platelet and leukocyte fraction from blood donations) of healthy donors. Buffy coats were obtained from *Transfusionsmedizin der Uniklinik Köln*.

2.8 Cell lines

Table 2.3: List of cell lines used in this study.

Cell line	Species	Characteristics (Reference)
293T	human	embryonic kidney 293 cell line (ATCC CRL-1573™) stably expressing the SV40 large T antigen; neomycin resistant (DuBridg <i>et al.</i> , 1987)
L540	human	CD30 ⁺ cell line derived from Hodgkin's lymphoma (Diehl <i>et al.</i> , 1982); kindly provided by PD Dr. Hinrich Hansen, Uniklinik Köln, Cologne, Germany
L540Cy	human	CD30 ⁺ mutant subline of L540, recultured from a tumour developing in a cyclophosphamide-treated nude mouse (von Kalle <i>et al.</i> , 1992); kindly provided by PD Dr. Hinrich Hansen
MeWo	human	cell line derived from a metastasis of melanoma (Bean <i>et al.</i> , 1975; ATCC HTB-65™)
C15A3	mouse	MC38 cell line stably expressing CEA; neomycin resistant (Hoffmann <i>et al.</i> , 2001)
MC38	mouse	methylcholanthrene-induced colon carcinoma cell line (Corbett <i>et al.</i> , 1975)
SL2	insect	cell line derived from late embryonic stages of <i>Drosophila melanogaster</i> (Schneider, 1972; ATCC CRL-1963™); kindly provided by Dr. Ralph Willemsen, Erasmus MC, Rotterdam, The Netherlands
1116-NS-19-9	mouse	hybridoma, secretes antibody directed against CA-19-9 (Koprowski <i>et al.</i> , 1979; ATCC HB-8059™)

Table 2.3: List of cell lines used in this study (continued).

Cell line	Species	Characteristics (Reference)
9G10	mouse	hybridoma, secretes anti-idiotypic antibody bearing the internal image of the HRS3-binding epitope (Pohl <i>et al.</i> , 1992)
HRS3	mouse	hybridoma, secretes monoclonal antibody directed against CD30 (Pfreundschuh, 1989)
OKT3	mouse	hybridoma, secretes monoclonal antibody directed against CD3 (Kung <i>et al.</i> , 1979; ATCC CRL-8001™)
T84.66A3.1A.1F2	mouse	hybridoma, secretes antibody directed against CEA (Wagener <i>et al.</i> , 1983; ATCC HB-8747™)

2.9 Antibodies

Table 2.4: List of antibodies used in this study.

Antibody	Species, Isotype	Conjugate	Clone	Source
anti-human IgG	goat	–	poly-clonal	Southern Biotech (Birmingham, AL, USA)
anti-human IgG	goat	biotin	poly-clonal	Southern Biotech
anti-human IgG, F(ab') ₂	goat	PE	poly-clonal	Southern Biotech

Table 2.4: List of antibodies used in this study (continued).

Antibody	Species, Isotype	Conjugate	Clone	Source
anti-mouse IgG	goat	–	poly-clonal	Southern Biotech
anti-mouse IgG	goat	biotin	poly-clonal	Southern Biotech
anti-mouse IgG₁	goat	PE	poly-clonal	Southern Biotech
anti-human IL-2	mouse IgG _{1κ}	–	5344.111	BD Pharmingen (Heidelberg, Germany)
anti-human IL-2	mouse IgG _{1κ}	biotin	B33-2	BD Pharmingen
anti-mouse IL-12 (p40/p70)	rat IgG ₁	–	C15.6	BD Pharmingen
anti-mouse IL-12 (p40/p70)	rat IgG _{2a}	biotin	C17.8	BD Pharmingen
anti-human IFN-γ	mouse IgG _{1κ}	–	NIB42	BD Pharmingen
anti-human IFN-γ	mouse IgG _{1κ}	biotin	B133.5	Pierce Endogen (Rockford, IL, USA)
anti-human CD3	mouse mIgG _{2a}	–	OKT3	purified from hybridoma supernatants

Table 2.4: List of antibodies used in this study (continued).

Antibody	Species, Isotype	Con- jugate	Clone	Source
anti-human CD3	mouse IgG _{1κ}	FITC	UCHT1	Dako (Hamburg, Germany)
anti-human CD30	mouse IgG ₁	–	HRS3	purified from hybridoma supernatants
anti-human CD30	mouse IgG ₁	PE	HRS4	Immunotech (Praha, Czech Republic)
anti-human CD56	mouse IgG _{1κ}	PE	MY31	BD Pharmingen
anti-763.74	mouse IgG ₁	–	MK2-72. 8854	kindly provided by Soldano Ferrone, University of Pittsburgh Cancer Institute, Pittsburgh, PA, USA
anti-human CEA	mouse IgG _{1κ}	–	T84.66A3. 1A.1F2	purified from hybridoma supernatants
anti-HRS3	mouse IgG ₁	–	9G10	purified from hybridoma supernatants

Table 2.4: List of antibodies used in this study (continued).

Antibody	Species, Isotype	Conjugate	Clone	Source
anti-HMW-MAA	mouse IgG ₁	PE	EP-1	Miltenyi Biotech (Bergisch-Gladbach, Germany)
anti-human pSTAT4 (pY693)	mouse IgG _{2bκ}	PE	38/p-STAT4	BD Pharmingen
anti-BrdU, Fab	mouse	peroxidase	BMG 6H8	Roche Diagnostics, Penzberg, Germany
human IgG	human IgG	–	polyclonal	Southern Biotech
murine IgG₁	mouse IgG ₁	–	1116-NS-19-9	purified from hybridoma supernatants
murine IgG₁	mouse IgG _{1κ}	FITC	DAK-G01	Dako
murine IgG₁	mouse IgG _{1κ}	PE	679.1 Mc7	Immunotech
murine IgG_{2b}	mouse IgG _{2bκ}	PE	27-35	BD Pharmingen

2.10 Sera

Foetal calf serum (FCS) was obtained from Biochrom (Berlin, Germany). Normal mouse serum was obtained from Dako.

2.11 Recombinant proteins

Table 2.5: List of recombinant proteins used in this study. According to the manufacturer, 1.8×10^7 IU Proleukin™ S correspond to 1.1 mg human IL-2.

Protein	Produced in	MW	Source
human Fc	293T	50 kDa (SDS-PAGE)	kindly provided by PD Dr. Hinrich Hansen
des-alanyl-1, serine-125 human IL-2	<i>Escherichia coli</i>	15.6 kDa	Proleukin™ S (Novartis Pharma, Nürnberg, Germany)
murine IL-12	<i>Spodoptera frugiperda</i>	54 kDa	EMD Chemicals (Darmstadt, Germany)
human IFN-γ_{1b}	<i>Escherichia coli</i>	38 kDa	Imukin™ (Boehringer Ingelheim Pharma, Ingelheim am Rhein, Germany)
human CD30-Fc	293T	200 kDa (SDS-PAGE)	kindly provided by PD Dr. Hinrich Hansen

2.12 Software

Ubuntu™ Linux (Canonical, Douglas, Isle of Man, UK)

The statistical language *R* 2.9 (R Development Core Team, 2009) was used to plot graphs and calculate statistics. Absorption curves from ELISA experiments were fitted to three-parameter logistic models using the *R* add-on package *drc* 1.7 (Ritz and Streibig, 2005). Data from flow cytometry experiments were analysed using *flowViz* from the *R* add-on package *Bioconductor* 2.4 (Gentleman *et al.*, 2004). Input files for use in *R* were exported from spreadsheets generated in *OpenOffice.org* 2.x and 3.0 (Sun Microsystems, Santa Clara, CA, USA). Figures were drawn in *Inkscape* 0.46. Source files were edited using *GNU Emacs* 22.x (Free Software Foundation, Boston, MA, USA). This document was typeset using *pdfTeX* 1.4 and *KOMA-Script* 3.0. References were managed in *JabRef* 2.4.

Windows™ (Microsoft Corporation, Redmond, WA, USA)

DNA sequences were analysed in *Vector NTI Advance* 10.3 (Invitrogen). Parameters of the äktaPrime™ chromatograph were monitored in real-time using the application *UNICORN* 4.0 (Amersham Biosciences, Freiburg, Germany). Absorption data of microtitre plates were read using *SoftMax Pro* 1.2 (Molecular Devices, Sunnyvale, CA, USA). Flow cytometer data were read using *FACSDiva* 5.0 (BD Biosciences, Heidelberg, Germany).

3 Methods

Methods were performed or adapted according to Ausubel (2005) and Coligan (2005). The fusion proteins HRS3scFv-Fc and SCA431scFv-Fc lack a cytokine domain and therefore do not match the term “immunocytokine”. In order to simplify the description of methods, use of the term “immunocytokine” in this chapter is extended to include these fusion proteins. Amounts of substance and related units were always calculated for the non-dimerised state of immunocytokines in order to make calculations and figures less confusing. If handled differently, 10 pmol of dimerised immunocytokine would require 20 pmol cytokine standard for equivalence.

3.1 Bacteria

Bacteria cells were handled in gene technology labs of security level *S1*.

3.1.1 Bacteria culture

Bacteria cells were cultured overnight at 37°C, either in liquid LB medium (rotated at 200 rpm) or on LB plates. Genetically modified bacteria were selected by adding 200 µg/ml ampicillin or 50 µg/ml kanamycin to media. LB plates were stored at 4°C for up to two weeks. For long-term storage, 700 µl bacteria cultures were mixed with 300 µl of 87% (v/v) glycerol and stored at –80°C.

3.1.2 Generation of chemically competent bacteria (Hanahan, 1983)

Bacteria colonies were inoculated in 500 ml of LB medium and cultured (37°C, 200 rpm) until the suspension reached an OD_{600nm} of 0.5. The suspension was chilled on ice for 15 min and cells were centrifuged for 15 min (3000×g, 4°C). The pellet was immediately suspended in 60 ml of ice-cold Tfb I buffer. The suspension was incubated on ice for 10 min and centrifuged again for 15 min (3000×g, 4°C). The pellet was suspended in 4 ml of ice-cold Tfb II buffer and stored at -80°C in 100µl aliquots. Transformation of 1 ng plasmid DNA resulted in approximately 1 × 10³ bacterial colonies.

Tfb I buffer

100 mM RbCl, 50 mM MnCl₂, 30 mM KOAc, 10 mM CaCl₂ and 15% (v/v) glycerol were dissolved in ddH₂O, adjusted to pH 5.8 and filter-sterilised (prepared fresh)

Tfb II buffer

10 mM RbCl, 10 mM MOPS, 75 mM CaCl₂ and 15% (v/v) glycerol were dissolved in ddH₂O, adjusted to pH 6.8 and filter-sterilised (prepared fresh)

3.1.3 Transformation by heat-pulse (Hanahan, 1983)

Competent bacteria were thawed on ice and 10 ng to 100 ng plasmid DNA were added. The suspension was mixed and incubated on ice for 20 min. Bacteria were heat-pulsed for 90 s (42°C), chilled for 60 s, diluted in 500µl LB medium and incubated for 60 min (37°C, 200 rpm) to express antibiotic resistance. Finally, bacteria were cultured overnight on LB plates with antibiotics.

3.2 Plasmid DNA

3.2.1 Preparation of plasmid DNA

Plasmid DNA was prepared from fresh bacteria cultures by anion-exchange chromatography following alkaline lysis. DNA was eluted with sterile 10 mM TRIS buffer and stored at -20°C . The following reaction kits were used according to the manufacturer's recommendations:

- peqGOLD™ Plasmid Miniprep Kit I (Peqlab, Erlangen, Germany)
- QIAGEN™ Plasmid Midi Kit (Qiagen, Hilden, Germany)
- QIAGEN™ Plasmid Maxi Kit (Qiagen)

10 mM TRIS buffer

10 mM TRIS were dissolved in ddH₂O, adjusted to pH 8.4, autoclaved and stored at room temperature

3.2.2 Quantification of DNA

DNA concentrations were quantified by means of a spectrophotometer. DNA diluted in 10 mM TRIS buffer was placed in quartz cuvettes and absorbance at the wavelengths 230 nm, 260 nm, 280 nm and 320 nm was determined. 10 mM TRIS buffer was used as blank. Double-stranded DNA in 10 mM TRIS buffer has a specific absorption coefficient $A_{260\text{nm}}$ of 0.020 ml/($\mu\text{g cm}$). Purity was estimated by the ratio between absorbance at 260 nm and 280 nm. Ratios ranging from 1.8 to 1.9 indicated highly purified DNA preparations.

3.2.3 Ethanol precipitation of DNA

For precipitations or buffer exchange, DNA solutions were mixed with 0.1 volumes of 3 M NaOAc (pH 5.2) and 2.5 volumes of ice-cold 96% (v/v)

ethanol. DNA was precipitated at -80°C for 15 min and centrifuged for 5 min ($25\,000\times g$, 4°C). The supernatant was removed, the pellet was washed with 1 ml of 70% (v/v) ethanol and centrifuged again for 5 min ($25\,000\times g$, 4°C). The supernatant was removed and the pellet was vacuum dried in a Concentrator 5301 (Eppendorf, Hamburg, Germany). Finally, the DNA was dissolved in 10 mM TRIS buffer or ddH₂O.

3.2.4 Agarose gel electrophoresis

DNA fragments were separated by electrophoresis in 1% (w/v) agarose gels. Gels were run at 10 V/cm in TAE buffer with 100 ng/ml ethidium bromide. Before electrophoresis, $6\times$ DNA Loading Dye (Fermentas, St. Leon-Rot, Germany) was added to DNA samples. GeneRuler™ 1 kb DNA ladder (Fermentas) was used as size standard. DNA was visualised in a UV transilluminator (254 nm) and photographed.

3.2.5 Isolation of DNA from agarose gels

DNA fragments were separated by agarose gel electrophoresis in presence of ethidium bromide. The DNA bands of interest were then excised with a scalpel under UV light (312 nm). Finally, DNA fragments were isolated from the agarose gel using the QIAquick™ Gel Extraction Kit (Qiagen) according to the manufacturer's recommendations.

3.2.6 Digestion of DNA

DNA was digested using restriction endonucleases (Roche Diagnostics) in the appropriate SuRE/Cut™ buffers (Roche Diagnostics) according to the manufacturer's recommendations. Digestions with two different restriction endonucleases were performed in one step if buffers and reaction conditions were compatible.

3.2.7 Ligation of DNA

DNA fragments were ligated using T4 DNA ligase (1U; Roche Diagnostics) according to the manufacturer's recommendations. Plasmid and insert DNA were added in a molar ratio of 1 : 3 to yield 100 ng plasmid DNA. The ligation mixture was incubated overnight at 14 °C and transformed into bacteria.

3.2.8 Polymerase chain reaction

PCR reactions were carried out in 500- μ l reaction tubes using thermal cyclers by Biometra (Göttingen, Germany) and Eppendorf. The following reaction mix was used:

Template DNA:	1 ng to 100 ng
Upstream primer oligonucleotide:	200 nM
Downstream primer oligonucleotide:	200 nM
PCR Nucleotide Mix ¹:	200 μ M of each dNTP
10 \times Polymerase buffer ^{1 2}:	5 μ l
Pwo DNA polymerase ¹:	2.5 U
ddH₂O:	ad 50 μ l

¹ Roche Diagnostics

² 100 mM TRIS-HCl, 20 mM MgSO₄, 50 mM (NH₄)₂SO₄, 250 mM KCl, pH 8.85

To minimise condensation or evaporation of samples, the thermal cycler's lid was heated to 104 °C during PCR. The following thermal cycler program was routinely used:

Initialisation:	96 °C	240 s	} 30 cycles
Denaturation:	96 °C	60 s	
Annealing:	55 °C	60 s	
Elongation:	72 °C	60 s	
Final elongation:	72 °C	240 s	

Elongation time was adjusted to the length of the amplified fragment (Pwo polymerase: \approx 1000 bp/min, Taq polymerase: \approx 2000 bp/min). In case a reaction did not yield amplified DNA, annealing temperature was optimised by means of a gradient thermal cycler.

3.2.9 Colony PCR

Colony PCR allows to screen for recombinant plasmid DNA in bacterial clones. Individual clones were picked and cultured overnight on LB plates with antibiotics. Bacteria of each clone were picked with a pipette tip and dipped for 2 min into 500- μ l reaction tubes filled with the following reaction mix:

Upstream primer oligonucleotide:	200 nM
Downstream primer oligonucleotide:	200 nM
PCR Nucleotide Mix ¹:	200 μ M of each dNTP
10 \times Polymerase buffer ^{1 2}:	1 μ l
Taq DNA polymerase ¹:	0.25 U
ddH₂O:	ad 10 μ l

¹ Roche Diagnostics

² 100 mM TRIS-HCl, 15 mM MgCl₂, 500 mM KCl, pH 8.3

The pipette tips were removed and a standard PCR was carried out using the same oligonucleotides and thermal cycler program as during cloning. During the initialisation step (96 °C, 240 s), DNA is both released from the bacteria cells and denatured. Finally, PCR products were separated by agarose gel electrophoresis and visualised in a UV transilluminator.

3.2.10 Dideoxy DNA sequencing

DNA was sequenced by the dideoxy chain termination method using the “BigDye™ Terminator v3.1 Cycle Sequencing Kit” (Applied Biosystems,

Warrington, UK) and a thermal cycler (Eppendorf). The following reaction mix was used:

Template DNA:	150 ng
Sequencing primer oligonucleotide:	2 μ M
5 \times BigDye Sequencing Buffer ¹:	2 μ l
2.5 \times Ready Reaction Premix ¹:	4 μ l
ddH₂O:	ad 10 μ l

¹ Applied Biosystems

The PCR was performed using the following thermal cycler program:

Initialisation:	96 °C	60 s	90 cycles
Denaturation:	96 °C	30 s	
Annealing:	50 °C	15 s	
Elongation:	60 °C	240 s	

After PCR, 10 μ l ddH₂O were added to each sample. Finally, samples were analysed at the Cologne Centre for Genomics (University of Cologne) using a 3730 DNA Analyser (Applied Biosystems).

3.3 Tissue culture

Tissue culture was carried out in gene technology labs of security level *S1* using laminar flow cabinets of *Sicherheitsklasse II* (Heraeus, Hanau, Germany).

3.3.1 Mammalian tissue culture

Mammalian cells were cultured in a humidified atmosphere with 5% (v/v) CO₂ at 37°C. The culture medium “RPMI 1640 with GlutaMAX I™” (Gibco, Karlsruhe, Germany) was supplemented with 10% (v/v) FCS, 25IU/ml

penicillin G and 25 µg/ml streptomycin (Gibco). Media were stored at 4 °C.

3.3.2 Insect tissue culture

Insect cells were cultured either in a humidified atmosphere at 28 °C or in a FibraStage™ bioreactor (New Brunswick Scientific, Nürtingen, Germany) at room temperature. The culture medium “Schneider’s Insect Medium (Revised)” (Gibco) was supplemented with 10% (v/v) heat-inactivated FCS, 25 IU/ml penicillin G and 25 µg/ml streptomycin (Gibco). Protein production in cells transfected with *Drosophila* Expression System™ plasmids (Invitrogen) was induced by addition of CuSO₄ in a final concentration of 500 µM. Media were stored at 4 °C.

Heat inactivation of serum

Serum was heated for 30 min in a water bath (56 °C) and stored at 4 °C.

3.3.3 Passage of adherent cells

To passage adherent cells, culture supernatants were removed and cells were washed once with 10 ml PBS. Cells were detached by adding 500 µg/ml trypsin and 200 µg/ml EDTA in a volume sufficient to cover the entire tissue culture surface. After 2 to 5 min, trypsin was blocked by resuspending the detached cells in 10 ml fresh growth medium. A small volume of conditioned medium was added and the cell suspension was diluted with fresh medium in a ratio of 1 : 2 to 1 : 10, depending on the cell line.

3.3.4 Passage of cells growing in suspension

To passage cells growing in suspension, cells were centrifuged for 5 min (300×g). Supernatants were removed while retaining a small volume of conditioned growth medium. The cell suspension was then diluted with fresh medium in a ratio of 1 : 2 to 1 : 10, depending on the cell line.

3.3.5 Subcloning

Cells were passaged, plated in microtitre plates (5 cells/ml to 500 cells/ml, 200µl/well) and cultured for a few weeks until clones appeared. Supernatants from each well were screened by ELISA for secreted protein. Clones producing high amounts of protein were expanded and cryoconserved.

3.3.6 Cryoconservation

For long-time storage of cell lines, 5×10^6 to 1×10^7 cells were centrifuged for 5 min (300×g) and resuspended in a mixture of 450µl conditioned growth medium and 450µl fresh growth medium. The cell suspension was placed in a cryovial and 100µl of the cryoprotectant DMSO were slowly run down the vial's wall. The cryovial was placed in a "Cryo 1°C Freezing Container"TM (Nalgene, Roskilde, Denmark) that had been pre-chilled to -20°C, and the freezing container was transferred to a -80°C freezer. On the following day, the cryovial was transferred to and stored in liquid nitrogen.

3.3.7 Calcium phosphate co-precipitation of DNA

- (A) SL2 cells were seeded in six-well-plates (3×10^6 cells, 3ml medium) and incubated overnight. In a reaction tube, 19µg plasmid DNA coding for an immunocytokine and 1µg DNA of the hygromycin

B resistance plasmid pCoHygro (#1080) were mixed and ethanol-precipitated. Precipitated DNA was dissolved in 270µl ddH₂O and 30µl of a 2.5 M CaCl₂ solution were added.

(B) 293T cells were seeded in six-well-plates (2×10^6 cells, 3 ml medium) and incubated overnight. In a reaction tube, 19µg plasmid DNA coding for the protein of interest and 1µg DNA of the hygromycin B resistance plasmid pGT60 hB7.2 (#653) were mixed and ethanol-precipitated. Precipitated DNA was dissolved in 270µl ddH₂O and 30µl of a 2.5 M CaCl₂ solution were added.

A 15-ml tube was set up with 300µl $2 \times$ HeBS buffer. While bubbling the $2 \times$ HeBS buffer with a 1-ml pipette attached to a mechanical pipettor, the DNA solution from **A** or **B** was added dropwise. The tube was immediately vortexed for 5 s and incubated for 20 min at room temperature to allow precipitate formation. Cells were washed twice with PBS, resuspended in 3 ml medium and the calcium phosphate co-precipitate was added. Cells were incubated for 8 hours and washed twice with medium.

2.5 M CaCl₂

2.5 M tissue-culture grade CaCl₂ (Sigma-Aldrich) were dissolved in ddH₂O, filter-sterilised and stored at -20°C

$2 \times$ HeBS buffer

280 mM NaCl, 50 mM HEPES and 1.5 mM Na₂HPO₄ were dissolved in ddH₂O, adjusted to pH 7.05, filter-sterilised and stored at 4°C for up to one month

3.3.8 Lipofection

The negatively charged plasmid DNA forms complexes with cationic lipids. Such complexes are then able to cross the membranes of cells and cell nuclei (Felgner *et al.*, 1987).

FectoFly™ II (Polyplus, Illkirch, France)

SL2 cells were seeded in six-well-plates (2×10^6 cells, 1.6ml medium) and incubated for 3 hours. In a reaction tube, 9µg plasmid DNA coding for an immunocytokine were mixed with 0.45µg DNA of the hygromycin B resistance plasmid pCoHygro (#1080) and 100µl of a 150mM NaCl solution. In a second tube, 9µl FectoFly™ II were mixed with 100µl of a 150mM NaCl solution. The contents of the second tube were added to the first tube, vortexed for 10s and incubated for 30min at room temperature to allow complex formation. Finally, cells were transfected by adding the DNA complexes and incubated overnight.

Fugene™ HD (Roche Diagnostics)

SL2 cells were seeded in six-well-plates (2×10^6 cells, 1.6ml medium) and incubated for 3 hours. In a reaction tube, 2µg plasmid DNA coding for an immunocytokine were mixed with 0.1µg DNA of the hygromycin B resistance plasmid pCoHygro (#1080). Sterile ddH₂O was added to a final volume of 100µl. To allow complex formation, 5µl Fugene™ HD were added, thoroughly mixed for 2s and incubated for 15min at room temperature. Finally, cells were transfected by adding the DNA complexes and incubated overnight.

Insectogene™ (Biontex, Planegg, Germany)

SL2 cells were seeded in six-well-plates (2×10^6 cells, 1.6ml medium) and incubated for 3 hours. In a reaction tube, 5µg plasmid DNA coding for an immunocytokine were mixed with 0.25µg DNA of the hygromycin B resistance plasmid pCoHygro (#1080). Serum-free medium was added to a final volume of 100µl. In a second tube, 32µl Insectogene™ were mixed with 68µl serum-free medium. The contents of the first tube were added to the second tube, mixed and incubated for 15min at room temperature to al-

low complex formation. Cells were washed with medium, transfected by adding the DNA complexes and incubated overnight.

3.3.9 Selection of stably transfected cells

Stably transfected clones were selected by adding hygromycin B (300 µg/ml; InvivoGen) to the medium 24 hours after transfection. Cells were cultured until colonies appeared and subcloned.

3.3.10 Fibrastage™ bioreactor

The Fibrastage™ system (New Brunswick Scientific) is a bioreactor for up to four Fibrastage™ bottles. Each bottle is a closed system that can be filled with 500ml medium and contains 10g of Fibrastage™ disks with a total surface area of 12000cm² for cell adhesion. Bottles are locked in a holder and medium is pumped through the Fibrastage™ disk layer by the programmable vertical motion of a platform. SL2 cells stably transfected with plasmid DNA coding for an immunocytokine were cultured in the Fibrastage™ system at room temperature with the programs given in table 3.1. Medium was replaced by 450ml fresh medium three times a week.

A Fibrastage™ bottle was inoculated with 2×10^8 SL2 cells suspended in 30ml conditioned medium, and 470ml fresh medium were added. The Fibrastage™ system was programmed for “inoculation” and started immediately. After 4 hours, the Fibrastage™ system was switched to the “growth” program. Protein production was induced after 6 days by addition of CuSO₄ in a final concentration of 500 µM, and the Fibrastage™ system was switched to the “production” program. Three to five weeks later, Fibrastage™ bottle and cells were discarded. Culture parameters for an initial run of the Fibrastage™ bioreactor are given in figure 3.1. In contrast to the information given in the manufacturer’s protocol, cell growth in Fibrastage™ bottles couldn’t be monitored.

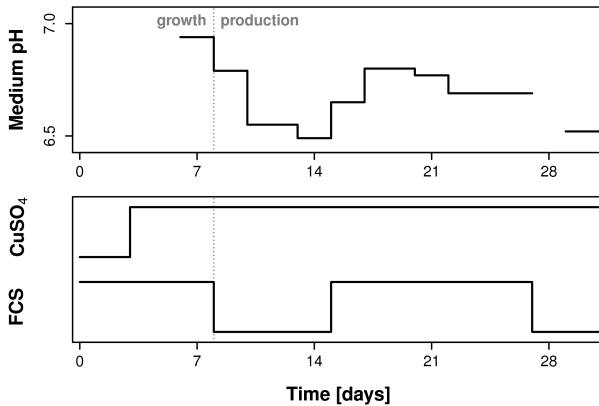


Figure 3.1: Fibrastage™ culture parameters. A Fibrastage™ bottle was inoculated with SL2 cells (2×10^8 cells, 30ml growth medium). Fresh growth medium (470ml) was added immediately and the Fibrastage™ system was run with the “growth” program. After 8 days, the system was switched to the “production” program. Medium was replaced every few days by 450ml fresh growth medium and pH of culture supernatants was determined. Protein production was induced after 3 days by adding CuSO₄ (final concentration: 500μM). In growth phase and from days 15 to 27, culture medium was supplemented with 10% (v/v) heat-inactivated FCS. **Lower figure:** graphical representation of supplements that were added to the culture medium.

Table 3.1: Fibrastage™ programs for the cultivation of SL2 cells. The programs given in this table control the vertical movement of a platform pumping medium through Fibrastage™ bottles. The speed parameters control mixing of the medium, whereas the delay parameters influence gas and nutrient exchange.

Program	Duration	Up Speed	Top Delay
		Down Speed	Bottom Delay
Inoculation	4 h	2.0 mm/s	20 s
		2.0 mm/s	0 s
Growth	6 d	1.0 mm/s	10 s
		1.0 mm/s	180 s
Production	<i>ad libitum</i>	1.0 mm/s	10 s
		1.0 mm/s	1800 s

3.3.11 Isolation of peripheral blood mononuclear cells

Human peripheral blood mononuclear cells (PBMC) were isolated from fresh blood or buffy coats of healthy donors by density gradient centrifugation on an isosmotic polysaccharide solution with a density of 1.077 g/ml. Erythrocytes and polymorphonuclear leukocytes migrate through the gradient and serum remains above the gradient, while monocytes, lymphocytes and platelets accumulate at the boundary between blood sample and gradient.

Buffy coats were diluted 1 : 2 with PBS, whereas fresh blood was used undiluted. In a 50-ml tube, 25 ml blood were layered over 15 ml Lymphoprep™ (Axis-Shield, Oslo, Norway). The centrifuge's brake was turned off and the tube was centrifuged for 30 min (700×g, 20°C). PBMCs were collected, washed three times with PBS and either magnetically separated or incubated in RPMI 1640 medium supplemented with 10% (v/v) FCS, 1000 IU/ml human IL-2 and 100 ng/ml of the anti-CD3 antibody OKT3. After 48 hours, PBMCs were cultured in medium supplemented with 10% (v/v) FCS and 400 IU/ml human IL-2.

3.3.12 Magnetic cell separation (MACS™)

T cells or natural killer cells were isolated from PBMCs using “MACS™ Isolation Kits” (Miltenyi Biotech). Erythrocytes and all non-matching lymphocyte subsets were labelled with a cocktail of biotinylated antibodies and bound to magnetic “Anti-Biotin MicroBeads”. Bound cells were then depleted (negative selection) on columns set-up in a strong magnetic field, thus yielding highly purified and unlabelled lymphocyte subsets.

MACS™ buffer

0.5% (w/v) BSA were dissolved in “autoMACS™ Rinsing Solution” (2 mM EDTA in PBS, pH 7.2; Miltenyi Biotech), filter-sterilised and chilled to 4°C (prepared fresh)

Isolation of T cells (MACS™ Pan T Cell Isolation Kit II)

To isolate human T cells, 2×10^8 freshly isolated human PBMCs were centrifuged for 10 min ($300 \times g$) and resuspended in 800 μ l MACS™ buffer. B cells, NK cells, dendritic cells, monocytes, granulocytes and erythroid cells were labelled with 200 μ l “Pan T Cell Biotin-Antibody Cocktail” for 10 min (4°C) and 600 μ l MACS™ buffer were added. Labelled cells were bound to 400 μ l “Anti-Biotin MicroBeads” for 15 min (4°C). The cells were washed with MACS™ buffer and resuspended in 1 ml MACS™ buffer. An LS Column™ (Miltenyi Biotech) pre-rinsed with 3 ml MACS™ buffer was placed in a strong magnetic field on top of a sterile 15-ml tube. The cell suspension was applied and the column was washed three times with 3 ml MACS™ buffer. Complete effluent was collected and contained approximately 1×10^8 T cells (figure 3.2). Isolated T cells were washed three times with PBS and incubated in RPMI 1640 medium supplemented with 400 IU/ml human IL-2 and 5 μ g/ml leucoagglutinin (PHA-L). After 48 hours, cells were washed twice with medium, transferred to a new flask and incubated in medium supplemented with 1000 IU/ml human IL-2.

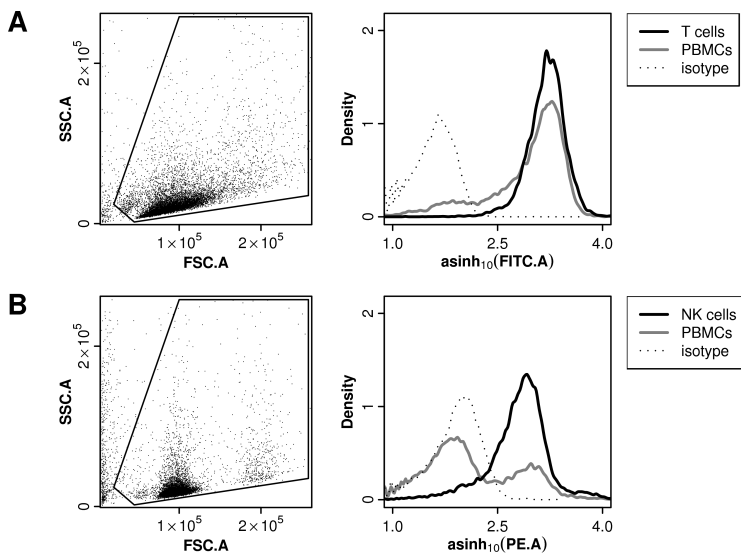


Figure 3.2: Purity of isolated lymphocyte subsets. T cells were isolated from human peripheral blood using the “MACS™ Pan T Cell Isolation Kit II”. Isolated T cells (2×10^5 cells; **black line**) and peripheral blood mononuclear cells as control (2×10^5 cells; **grey line**) were stained with the anti-CD3-FITC antibody or an isotype-matched FITC-conjugated antibody (**dotted line**) as control (A). NK cells were isolated from human peripheral blood using the “MACS™ NK Cell Isolation Kit, human”. Isolated NK cells (2×10^5 cells; **black line**) and peripheral blood mononuclear cells as control (2×10^5 cells; **grey line**) were stained with the anti-CD56-PE antibody or an isotype-matched PE-conjugated antibody (**dotted line**) as control (B). Finally, cells were analysed by flow-cytometry. **Insets:** scatter plots of the isolated lymphocyte subsets.

Isolation of natural killer cells (MACS NK Cell Isolation Kit, human)

To isolate human NK cells, 1×10^8 freshly isolated human PBMCs were centrifuged for 10 min ($300 \times g$) and resuspended in $400 \mu\text{l}$ MACS™ buffer. T cells, B cells, stem cells, dendritic cells, monocytes, granulocytes and erythroid cells were labelled with $100 \mu\text{l}$ “NK Cell Biotin-Antibody Cocktail, human” for 10 min (4°C) and $300 \mu\text{l}$ MACS™ buffer were added. Labelled cells were bound to $200 \mu\text{l}$ “NK Cell Anti-Biotin MicroBead Cocktail, human” for 15 min (4°C). The cells were washed with MACS™ buffer and resuspended in $500 \mu\text{l}$ MACS™ buffer. An LS Column™ (Miltenyi Biotech) pre-rinsed with 3 ml MACS™ buffer was placed in a strong magnetic field on top of a sterile 15-ml tube. The cell suspension was applied and the column was washed three times with 3 ml MACS™ buffer. Complete effluent was collected and contained approximately 8×10^6 NK cells (figure 3.2). Isolated NK cells were washed three times with PBS, resuspended in RPMI 1640 medium and used directly.

3.4 Proteins

3.4.1 Preparation of affinity chromatography media

Antibodies and immunocytokines were affinity-purified using either agarose or Sepharose™ coupled to antibodies. Anti-m-IgG agarose was obtained from Sigma-Aldrich and packed into C10/10™ columns (Amersham Biosciences). Polyclonal anti-h-IgG antibodies or the anti-HRS3 anti-idiotypic antibody 9G10 were coupled to NHS-activated Sepharose™ (GE Healthcare, Freiburg, Germany) as described below. Coupled media and packed columns were stored at 4°C and used for up to 25 purifications.

Blocking buffer A

500 mM 2-aminoethanol and 500 mM NaCl were dissolved in ddH_2O , adjusted to pH 8.3 and degassed (prepared fresh)

Blocking buffer B

100 mM NaOAc and 500 mM NaCl were dissolved in ddH₂O, adjusted to pH 4.0 and degassed (prepared fresh)

Coupling of antibodies to HiTrap™ HP columns

A “HiTrap™ NHS-activated HP column” (1 ml or 5 ml column volume; GE Healthcare) was prepared for coupling by washing with six column volumes of ice-cold 1 mM HCl. One column volume of PBS containing 1 mg/ml antibody was injected and incubated for 60 min at room temperature.

Uncoupled NHS-groups were blocked by washing with six column volumes blocking buffer A, six column volumes blocking buffer B and six column volumes blocking buffer A. After incubation for 30 min at room temperature, the column was washed with six column volumes blocking buffer B, six column volumes blocking buffer A and six column volumes blocking buffer B. Finally, the column was washed with two column volumes PBS containing 0.1 % (w/v) sodium azide and stored at 4 °C.

Coupling of antibodies to Sepharose™ beads

Sepharose™ beads were sedimented by centrifugation at 6000×g for 10 min.

For coupling, 10 ml “NHS-activated Sepharose™ 4 FastFlow” (GE Healthcare) were washed with 150 ml of ice-cold 1 mM HCl. After washing with 50 ml of ice-cold PBS, the beads were resuspended in 20 ml PBS containing 5 mg antibody and incubated overnight at 4 °C in a moving roller bottle. Uncoupled NHS-groups were blocked by incubation with 30 ml blocking buffer A for 4 hours at room temperature. The beads were then washed six times, alternately with 30 ml blocking buffer B and 30 ml blocking buffer A. Finally, coupled beads were washed with 30 ml PBS, resuspended in 20 ml PBS containing 0.1 % (w/v) sodium azide and stored at 4 °C.

3.4.2 Affinity chromatography

Tissue culture supernatants containing antibodies or immunocytokines were centrifuged for 5 min ($1000\times g$) and stored at -20°C until use.

Frozen supernatants (1.5l) containing either antibodies or immunocytokines were thawed in a water bath of 37°C and centrifuged for 10 min ($6000\times g$, 4°C) to clear from cellular debris. Supernatants were transferred to clean tubes, centrifuged again for 60 min ($6000\times g$, 4°C) and vacuum-filtered through Durapore™ membranes (450 nm , $4\mu\text{g}/\text{cm}^2$ protein binding; Millipore, Schwalbach, Germany).

- (A) Supernatants were pumped through a column packed with antibody-coupled medium (1 ml/min, 4°C).
- (B) Supernatants were incubated with antibody-coupled Sepharose™ beads in a moving roller bottle for 4 hours (4°C). Beads were collected three times by centrifugation ($6000\times g$, 10 min) and packed into a C10/10™ column (Amersham Biosciences).

The column from **A** or **B** was connected to an äktaPrime™ chromatograph (ambient temperature: 10°C ; Amersham Biosciences). After washing with PBS, protein bound to the column was eluted with 100 mM glycine buffer (pH 3.0) and collected in 1.5-ml tubes pre-loaded with $100\mu\text{l}$ of $10\times$ PBS. Finally, the column was washed with PBS containing 0.1% (w/v) sodium azide. The process was completely automated to ensure consistent purification results (appendix C). Absorbance at 280 nm and conductivity of effluent were monitored in real-time. Fractions containing protein were determined from absorbance measurements, pooled in Visking™ dialysis membranes (size 2; MWCO: 12 kDa to 14 kDa; Medicell International, London, UK) and dialysed overnight against PBS at 4°C .

The dialysed protein solution was concentrated to approximately 1 ml using Vivaspin™ 15 concentrators (4°C ; MWCO: 30 kDa; Sartorius, Göttingen, Germany). Finally, the protein solution was supplemented with

3% (v/v) of either heat-inactivated FCS or heat-inactivated normal mouse serum and stored at -80°C in aliquots of 50 μl .

100 mM glycine buffer

100 mM glycine were dissolved in ddH₂O, adjusted to pH 3.0, filter-sterilised and stored at 4°C for up to one month

3.4.3 Quantification of proteins (Pace *et al.*, 1995)

The molar absorption coefficient of a protein depends on the content of tryptophan, tyrosine and cystine (disulfide bonds). $\epsilon_{280\text{nm}}$ can be predicted reliably for proteins containing tryptophan residues:

$$\epsilon_{280\text{nm}} = 5500 * \sum \text{Trp} + 1490 * \sum \text{Tyr} + 125 * \sum \text{cystine}$$

Concentrations of protein solutions were determined by blanking a spectrophotometer with the solvent and measuring absorbance at 330 nm and 280 nm. Absorbance values were corrected for light scattering and protein concentrations were calculated using the Beer-Lambert law:

$$A_{\text{corr}} = A_{280\text{nm}} - 1.929 * A_{330\text{nm}}$$

$$c = \frac{A_{\text{corr}}}{\epsilon_{280\text{nm}} * d}$$

3.4.4 Radiolabelling of immunocytokines

Experiments involving work with radionuclides were supervised by PD Dr. Stefan Guhlke and carried out at the *Klinik und Poliklinik für Nuklearmedizin* in Bonn. Jan-Philipp Hering assisted in biodistributions experiments.

Radiolabelling buffer

0.2 M NaOAc was dissolved in ddH₂O, adjusted to pH 5.0 and stored at room temperature

1 M NaHCO₃ buffer

1 M NaHCO₃ was dissolved in ddH₂O and stored at room temperature

Rudinger reagent solution

380 μM (2,5-dioxopyrrolidin-1-yl) 3-(4-hydroxyphenyl) propanoate (Rudinger reagent; Pierce Endogen) was dissolved in DMSO (prepared fresh)

Chloramine-T solution A

180 μM chloramine-T was dissolved in ddH₂O (prepared fresh)

Chloramine-T solution B

1.05 mM chloramine-T was dissolved in radiolabelling buffer (prepared fresh)

Radiolabelling in presence of chloramine-T (Greenwood *et al.*, 1963)

Immunocytokines were radiolabelled by dissolving approximately 20 MBq Na¹³¹I in 10 μl PBS and adding 1.7 nmol immunocytokine (10 mM in PBS) and 15 μl chloramine-T solution A. After incubation for 90 s at room temperature, a sample was taken to determine labelling efficiency by thin layer chromatography (section 3.4.5) and the labelled immunocytokine was immediately desalted (section 3.4.6) and affinity-purified (section 3.4.7).

Coupling to Bolton-Hunter reagent (Bolton and Hunter, 1973)

Bolton-Hunter reagent was freshly prepared by dissolving approximately 50 MBq Na¹³¹I in 100 μl radiolabelling buffer and adding 10 μl Rudinger reagent solution and 10 μl chloramine-T solution B. After incubation for

120s at room temperature, 300µl ddH₂O were added and Bolton-Hunter reagent was extracted with 600µl benzene. Bolton-Hunter reagent was then condensed to a plastic reaction tube by evaporating 100µl benzene extract in an air stream. Coupling was started by adding 1.2 nmol immunocytokine (8mM in PBS) and 30µl of 1 M NaHCO₃ buffer. After incubation for 60min at room temperature, labelling efficiency was determined by thin layer chromatography (section 3.4.5) and the radiolabelled immunocytokine was desalted (section 3.4.6).

3.4.5 Thin layer chromatography of radiolabelled immunocytokines

Efficiency of radiolabelling was determined by thin layer chromatography. A few microlitres of radiolabelled immunocytokine were spotted on an ITLC-SGTM strip (Pall, Dreieich, Germany), the strip was placed in an elution chamber and chromatographed using normal saline (B. Braun) as mobile phase. When the solvent front had reached the end of the strip, the ITLC-SGTM strip was removed from the chamber, cut at an R_F of 0.5 and radioactivity of both halves was counted by means of a Curiemeter. Bound radionuclide elutes at an R_F below 0.5, whereas unbound radionuclide elutes at an R_F above 0.5. Labelling efficiency was calculated as follows:

$$\text{Labelling efficiency} = \frac{\text{cpm}_{(R_F < 0.5)}}{\text{cpm}_{\text{total}}}$$

3.4.6 Desalting of radiolabelled immunocytokines

Radiolabelled protein was desalted to remove chemical reagents and unbound radioactivity. The protein solution was diluted in PBS to a final volume of 500µl and applied to a PD-10TM column (Amersham Biosciences). The tube used for labelling was washed with 500µl PBS, which was also applied to the column, and the column was eluted with 9 ml PBS. Effluent was

collected in 1 ml-fractions and radioactivity of each fraction was counted by means of a Curiemeter. Fraction #4 contained the main amount of radiolabelled protein and was used for biodistribution experiments. Elution of unbound radioactivity started at fraction #8.

3.4.7 Affinity chromatography of radiolabelled immunocytokines

Radiolabelled immunocytokine was affinity-purified using the anti-idiotypic antibody 9G10 coupled to a HiTrap™ HP column (column volume: 1 ml). Desalted immunocytokine was applied to the column and the tube that had contained the immunocytokine was washed with 1 ml PBS, which was also applied to the column. Effluent was twice re-applied to the column to ensure quantitative binding of the immunocytokine. The column was then washed with PBS until radioactivity of 1 ml effluent was below 0.001 MBq (Curiemeter). Bound immunocytokine was eluted with 100 mM glycine buffer (pH 3.0) in steps of 250 µl (first 5 ml) or 1 ml and radioactivity of each fraction was counted by means of a γ -counter. To raise pH to 7.2, 12.5 µl of 1 M NaHCO₃ buffer were added to the first twenty fractions. Fractions #7 and #8 were pooled and used for biodistribution experiments. Finally, the column was washed with 25 ml PBS containing 0.1% (w/v) sodium azide and stored at 4 °C.

3.5 Assays

3.5.1 Enzyme-linked immunosorbent assay (ELISA; Engvall and Perlmann, 1971)

Unless mentioned otherwise, incubations were carried out at room temperature on a shaker.

MaxiSorp™ microtitre plates (Nunc, Langensfeld, Germany) were coated with capture antibody for 120 min (1 µg/ml in PBS, 50 µl/well). To block unspecific binding, plates were incubated overnight with 3% (w/v) BSA dissolved in PBS (200 µl/well, 4°C, not shaken) and washed five times with PBS-T (200 µl/well). Plates were incubated with supernatants or serial dilutions of samples for 60 min (50 µl/well) and washed five times with PBS-T (200 µl/well). Wells were then incubated with biotinylated detection antibody for 60 min (200 ng/ml to 500 ng/ml in PBS, 50 µl/well) and plates were washed five times with PBS-T (200 µl/well). Bound detection antibodies were conjugated to streptavidin- β -peroxidase for 30 min (50 mU/ml in PBS, 50 µl/well; Roche Diagnostics) and plates were washed five times with PBS-T (200 µl/well). Finally, conjugated antibodies were visualised by incubation with the substrate ABTS (1 mg/ml in ABTS Buffer, 50 µl/well; Roche Diagnostics) and detected by means of a microtitre plate reader (405 nm with 490 nm as reference). Concentrations of samples were calculated by one of the following methods:

- (A) The absorption curve of a standard with known concentration was fitted to a three-parameter logistic model. Sample concentrations were then calculated by comparing the absorption of a sample with the fitted standard curve.
- (B) Absorption curves of each sample were fitted to a three-parameter logistic model. ED_{50} values were calculated from fitted curves and compared with the ED_{50} value of a standard with known concentration.

The following ELISA tests were carried out:

Antigen	Capture antibody¹	Detection antibody²	Detection limit
human IgG / human Fc γ ₁	anti-human IgG ³	anti-human IgG (biotin) ^{3 4}	1 ng/ml
murine IgG / murine Fc γ ₁	anti-mouse IgG ³	anti-mouse IgG (biotin) ³	500 pg/ml
human IL-2	anti-human IL-2	anti-human IL-2 (biotin)	10IU/ml
murine IL-12	anti-mouse IL-12	anti-mouse IL-12 (biotin)	500pg/ml
human IFN- γ	anti-human IFN- γ	anti-human IFN- γ (biotin)	20 pg/ml
immunocytokine	9G10 (anti-idiotypic)	anti-human IgG (biotin) ³	30pM
immunocytokine	9G10 (anti-idiotypic)	anti-human IL-2 (biotin)	60pM
immunocytokine	9G10 (anti-idiotypic)	anti-mouse IL-12 (biotin)	30pM
murine IgG (in sera)	HRS3scFv-Fc	anti-mouse IgG (biotin) ^{3 4}	15ng/ml

¹ 1 μ g/ml in PBS

² 500 ng/ml in PBS

³ polyclonal antibody

⁴ 200 ng/ml in PBS

PBS-T

0.1 % (v/v) polysorbate 20 (Tween™ 20; Merck) was dissolved in PBS and stored at room temperature

3.5.2 Binding inhibition

Binding inhibition was determined by means of ELISA. MaxiSorp™ microtitre plates (Nunc) were coated with capture antibody and unspecific binding was blocked as described in section 3.5.1. Serial dilutions of a competitor or PBS as control (50µl/well) were mixed with a constant amount of immunocytokine (50µl/well). Plates were incubated for 60 min on a shaker (50µl/well, room temperature) and washed five times with PBS-T (200µl/well). Plates were then incubated with detection antibody, streptavidin-β-peroxidase and ABTS as described in section 3.5.1. Absorption of each well was detected by means of a microtitre plate reader (405 nm with 490 nm as reference). Binding inhibition was calculated as follows:

$$\text{Inhibition} = 1 - \frac{A_{\text{immunocytokine with competitor}}}{A_{\text{immunocytokine without competitor}}}$$

3.5.3 Radioimmunoassay (RIA; Yalow and Berson, 1960)

Unless mentioned otherwise, incubations were carried out at room temperature on a shaker.

PolySorp™ tubes (Nunc) were coated with capture antibody for 120 min (2µg/ml in PBS, 400µl/tube). To block unspecific binding, tubes were incubated overnight with 3% (w/v) BSA dissolved in PBS (3 ml/tube, 4°C, not shaken) and washed five times with PBS (3 ml/tube). Tubes were then incubated with serial dilutions of radiolabelled immunocytokine for 60 min (400µl/tube). After washing five times with PBS (3 ml/tube), radioactivity in each tube was counted by means of a γ-counter.

Alternatively, PolySorp™ LockWell™ strips (Nunc) were coated with capture antibody for 120 min (1µg/ml in PBS, 50µl/well). To block unspecific binding, strips were incubated overnight with 3% (w/v) BSA dissolved in PBS (200µl/well, 4°C, not shaken) and washed five times with PBS-T (200µl/well). Strips were then incubated with serial dilutions of radiola-

belled immunocytokine for 60 min (50 μ l/well). After washing five times with PBS-T (200 μ l/well), strips were broken apart and radioactivity in each well was counted by means of a γ -counter.

3.5.4 Immunofluorescence

Unless mentioned otherwise, incubations were carried out at 4 °C in the dark. PBS for washing was pre-chilled to 4 °C. Antibodies were diluted according to the manufacturer's instructions.

- (A) For immunofluorescence, 2×10^5 cells were washed with PBS, stained with a fluorochrome-conjugated antibody for 30 min and washed three times with PBS.
- (B) For indirect immunofluorescence, 2×10^5 cells were washed with PBS, stained with an antibody for 30 min and washed three times with PBS. Bound antibody was detected by incubation with a fluorochrome-conjugated antibody for 30 min. Finally, cells were washed three times with PBS.
- (C) To determine binding of immunocytokines to cells, 2×10^5 cells were washed with PBS, incubated with 4 pmol immunocytokine for 30 min on ice and washed three times with PBS. Bound immunocytokine was detected by incubation with the anti-h-IgG₁-PE antibody for 30 min. Finally, cells were washed three times with PBS.

Stained cells from **A**, **B** or **C** were analysed by means of a FACSCanto™ flow cytometer (BD Biosciences). Immunofluorescence data were analysed by plotting two-dimensional scatter plots and gating the relevant cell subsets. Density curves with a fixed area of 1 were then calculated from the detected fluorescence of gated cells. The smoothing bandwidth of density curves was adapted to each experiment. Data were transformed using the *asinh*₁₀ transformation (figure 3.3).

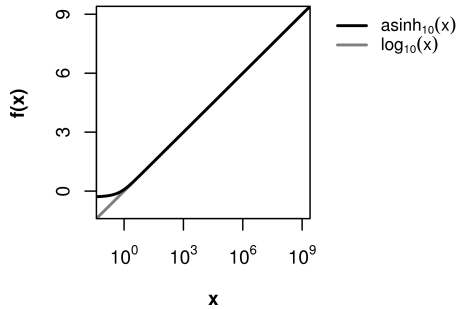


Figure 3.3: The $asinh_{10}$ transformation. In flow-cytometry analysis, an $asinh$ transformation was used instead of logarithmic transformations to avoid problems for values $x \leq 0$. The transformation $asinh(x)/\ln(10) - \log_{10}(2)$ was termed $asinh_{10}$ to indicate that values are close to $\log_{10}(x)$ for $x > 1$ and identical for $x > 1000$.

3.5.5 Proliferation of peripheral blood mononuclear cells

Proliferation of activated peripheral blood mononuclear cells (PBMC) was determined by incorporation of the thymidine analogue 5-bromo-2'-deoxyuridine (BrdU) and subsequent detection by ELISA. MaxiSorp™ microtitre plates that were used to culture PBMCs were handled aseptically.

Pre-activated PBMCs were washed three times with growth medium, transferred to a new flask and cultured in fresh medium without added IL-2. After 24 hours, PBMCs were washed three times with medium and used. MaxiSorp™ microtitre plates (Nunc) were coated with capture antibody for 120 min on a shaker (5 µg/ml in PBS, 50 µl/well, room temperature). To block unspecific binding, plates were incubated overnight with 10% (v/v) FCS in RPMI 1640 medium (200 µl/well, 4 °C) and washed three times with PBS (200 µl/well). One plate was incubated with 4 pmol filter-sterilised immunocytokine dissolved in growth medium for 60 min on a shaker (100 µl/well, room temperature) and washed three times with PBS. Each well was then filled with 100 µl medium. A second plate was incubated with 4 pmol filter-sterilised immunocytokine dissolved in medium for 60 min

on a shaker (100µl/well, room temperature). PBMCs were added to both plates (2.5×10^4 cells/well, 100µl/well) and cultured for up to 96 hours. As blank, one well of each plate was incubated with 200µl medium alone. BrdU (Roche Diagnostics) dissolved in PBS was added to the plates in a final concentration of 10nM and PBMCs were cultured for an additional 8 to 12 hours. Plates were centrifuged for 10 min ($300 \times g$) and supernatants were removed by suction. The empty plates were dried for 15 min using a hair-dryer and stored at 4°C for up to 7 days.

The following incubations were carried out at room temperature on a shaker. PBMCs were fixed by incubation with FixDenat™ for 30 min (100µl/well; Roche Diagnostics) and plates were emptied by flicking. Incorporated BrdU was detected by incubation with the peroxidase-conjugated anti-BrdU antibody for 90 min (50µl/well) and plates were washed three times with PBS. Bound conjugated antibody was visualised by incubation with the substrate ABTS (1 mg/ml in ABTS Buffer, 50µl/well; Roche Diagnostics) and detected by means of a microtitre plate reader (405 nm with 490 nm as reference).

3.5.6 Cytolysis of tumour cells (Jost *et al.*, 1992)

To determine cytolysis of tumour cells mediated by immunocytokines, 5×10^4 tumour cells were suspended in 100µl filter-sterilised RPMI 1640 medium containing 5 ng immunocytokine. After incubation for 60 min on ice, cells were washed three times with medium and resuspended in 100µl medium. Tumour cells were plated in one well of a round-bottom microtitre plate and 100µl RPMI 1640 medium containing either 4×10^4 human NK cells or no cells were added. Plates were cultured for 24 hours and 100µl supernatant were removed from each well. Viability of NK cells and tumour cells was visualised by adding 50µl medium, 50µl XTT reagent solution and 1µl electron coupling reagent solution to each well. Plates were incubated at 37°C and absorption was detected after 30 min, 60 min and 90 min by means of a microtitre plate reader (450 nm with 650 nm as reference).

Cytolysis was calculated as follows:

$$\text{Cytolysis} = 1 - \frac{A_{\text{tumour cells with NK cells}} - A_{\text{NK cells}}}{A_{\text{tumour cells}} - A_{\text{medium}}}$$

Electron coupling reagent solution

1.25 mM phenazine methylsulfate was dissolved in PBS, filter-sterilised and stored at -20°C

XTT reagent solution

1 mg/ml XTT sodium salt (Biomol, Hamburg, Germany) was dissolved in RPMI 1640 medium containing 10% (v/v) FCS, filter-sterilised and stored at -20°C

3.5.7 Phosphorylation of STAT4 (Uzel *et al.*, 2001)

Pre-activated human T cells were washed twice with serum-free medium, transferred to a new flask and cultured in serum-free medium. After 24 hours, T cells were washed with medium, 2×10^5 T cells were resuspended in 100 μl PBS containing 2% (v/v) FCS and 10 μl of 20 nM immunocytokine or murine IL-12 were added. Reaction tubes were incubated for 30 min in a water bath of 37°C , 110 μl pre-warmed “BD Cytotfix Buffer” (BD Pharmingen) were added and the reaction tubes were returned to the water bath for 10 min. Cells were washed with ice-cold PBS, suspended in 1 ml ice-cold “Phosflow™ Perm Buffer III” (BD Pharmingen) and permeabilised for 30 min on ice. Cells were washed twice with ice-cold “Stain Buffer FBS” (BD Pharmingen) and stained with 20 μl of the anti-pSTAT4-PE antibody for 30 min (room temperature, in the dark). Cells were washed with ice-cold “Stain Buffer FBS” and fluorescence was determined by means of a FACSCanto™ flow cytometer (BD Biosciences).

3.6 Experiments on mice

Experiments on mice were approved by *Bezirksregierung Köln*. Mice were obtained from Charles River Laboratories (Sulzfeld, Germany) and 8 to 12 weeks old. The animals were maintained at 20°C under SPF conditions. Injections were carried out by Samir-Ghali Tawadros. For calculations, we assumed that the blood volume of an average mouse (20g) amounted to 1.5ml.

3.6.1 Biodistribution

Female SCID mice received *s.c.* injections of 3×10^7 L540Cy cells in one flank. When the animals had developed tumours after three to five weeks, immunocytokine was radiolabelled (section 3.4.4). Mice received injections of radiolabelled immunocytokine into the tail vein and were sacrificed after 12, 24, 48 or 72 hours. Organs were recovered, weighed and radioactivity was counted by means of a γ -counter. Detected counts were compensated for radioactive decay. For every organ and point in time, the injected dose per gram of tissue (% ID/g) was calculated:

$$\% \text{ ID/g} = \frac{A_{\text{organ}}}{A_{\text{injected}} * m_{\text{organ}}} * 100 \%$$

Tissue retention was calculated as % ID/g (72h) divided by % ID/g (24h).

3.6.2 Tumour growth in mice

Tumour cells were suspended in 200 μ l of sterile PBS and *s.c.* injected. To show that cells were viable and free of contaminations, tumour cells remaining from injections were re-cultured for a week. Tumour size was

measured three to seven times a week by means of a calliper and calculated as follows:

$$V_{\text{tumour}} = \frac{\text{height} * \text{width} * \text{depth}}{2}$$

After mice had been sacrificed, tumour tissue was recovered, embedded in “Tissue-Tek™ O.C.T Compound” (Sakura Finetek, Staufen, Germany) and frozen at -80°C .

3.6.3 Serum samples

Blood samples from mice were taken after warming the tail under infrared light. The tail was disinfected with 70% (v/v) ethanol and the dilated tail vein was cut with a sterile scalpel. Blood drops were caught in a reaction tube and bleeding was stopped by applying gentle pressure with a gauze pad. The tube was transferred to a refrigerator and blood was allowed to clot overnight at 4°C . After centrifugation for 15 min ($600\times g$, room temperature), serum was transferred to a new reaction tube and stored at -80°C .

3.7 Statistics

The statistical language *R* 2.9 (R Development Core Team, 2009) was used to plot graphs and calculate statistics. Absorption curves from ELISA experiments were fitted to three-parameter logistic models using the *R* add-on package *drc* 1.7 (Ritz and Streibig, 2005) and fitting was visually controlled.

Normal distribution of samples was assumed. To determine significance of a difference between two groups, samples were tested by an unpaired two-sided Welch-corrected t-test. The null hypothesis that there was no difference between groups was rejected for p-values of 0.05 and below. Binding

inhibition (section 3.5.2) and cytolysis of tumour cells (section 3.5.6) were calculated prior to statistical analysis. Control values marked with an asterisk were averaged before use:

$$\text{Cytolysis} = 1 - \frac{A_{\text{tumour cells with NK cells}} - A_{\text{NK cells}}^*}{A_{\text{tumour cells}}^* - A_{\text{medium}}^*}$$

$$\text{Inhibition} = 1 - \frac{A_{\text{immunocytokine with competitor}}}{A_{\text{immunocytokine without competitor}}}$$

All experiments were repeated at least once with similar results, except for the cytolysis of tumour cells and experiments on mice.

4 Results

4.1 Immunocytokines are expressed in insect cells

The objective of this study was to compare the novel anti-CD30 immunocytokine HRS3scFv-hi-IL12-Fc-IL2 (combined IL-2 and IL-12 domains) with the immunocytokines HRS3scFv-Fc-hi-IL12 (IL-12 domain), HRS3scFv-Fc-IL2 (IL-2 domain) and the fusion protein HRS3scFv-Fc (without cytokine domains). An experimental prerequisite was the production of large amounts of purified protein within a reasonable time frame. Traditional cell culture methods were laborious and unlikely to yield the required protein concentrations. We used the FibraStage™ bioreactor for bulk protein production, as it allowed cell culture in high densities and simultaneous expression of up to four different recombinant proteins, while still being easy to handle.

We expressed immunocytokines in Schneider's *Drosophila* line 2 (SL2) cells. Therefore, expression cassettes coding for immunocytokines were inserted into the *Drosophila* Expression System™ DNA vector pMT/BiP V5-His A (#1070). Finally, a transfection method for stable expression in SL2 cells was established.

The DNA plasmids pMT/BiP SCA431scFv-Fc (#1103), pMT/BiP SCA431scFv-Fc-IL7 (#1117) and pMT/BiP SCA431scFv-Fc-IL15 (#1118) were solely generated for the “Adoptive engineered T cell targeting to activate cancer killing” (ATTACK) project of the European Union. As these plasmids have been used to determine a suitable transfection method for insect cells, however, their generation is described in sections 4.1.6 to 4.1.8.

4.1.1 Generation of the plasmid pBullet HRS3scFv-CD3 ζ (#1078)

To ease insertion of existing expression cassettes into the *Drosophila* Expression System™ DNA vector, DNA coding for the anti-CD30 scFv HRS3 was flanked by restriction sites needed for subsequent cloning procedures and inserted into the DNA vector pBullet.

DNA coding for the anti-CD30 scFv HRS3 was amplified from the plasmid pRSV-Lk HRS3scFv-Fc (#440) by PCR using the oligonucleotides HRS3-pMT-S and S-HRS3-hi-Bam. The amplified DNA was thereby flanked with the restriction sites NcoI at the 5' end and BamHI at the 3' end. The 0.75 kb DNA fragment was purified and digested by the restriction enzymes NcoI and BamHI. The plasmid DNA pBullet-Lk CC49scFv-Fc-CD3 ζ (#435) was also digested by the restriction enzymes NcoI and BamHI, thereby deleting the Lk CC49-Fc DNA. The two DNA fragments were purified and ligated to generate the new plasmid pBullet HRS3scFv-CD3 ζ (#1078; figure 4.1). The newly generated plasmid was transformed into *Escherichia coli* for amplification and the recombined expression cassette was verified by DNA sequencing (appendix B.1).

4.1.2 Generation of the plasmid pMT/BiP HRS3scFv-Fc (#1082)

To allow expression of the anti-CD30 fusion protein HRS3scFv-Fc in insect cells, an expression cassette coding for the fusion protein was inserted into the DNA vector pMT/BiP V5-His A (#1070).

DNA coding for the scFv HRS3 was isolated from the plasmid pBullet HRS3scFv-CD3 ζ (#1078) by digestion with NcoI and BamHI. DNA coding for the Fc region of human IgG₁ was isolated by digesting the plasmid pRSV-Lk HRS3scFv-Fc (#440) with BamHI and XhoI. The vector DNA pMT/BiP V5-His A (#1070) was digested by the restriction enzymes NcoI and XhoI to allow insertion of the expression cassette into the MCS. The three DNA fragments were purified and ligated to generate the new

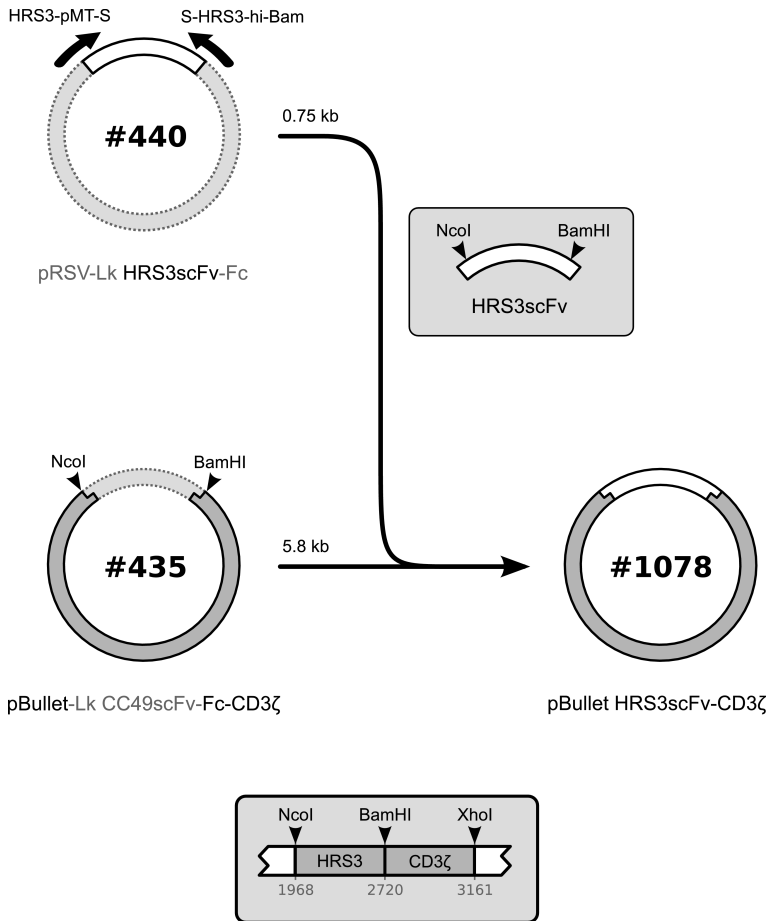


Figure 4.1: Generation of the plasmid pBullet HRS3scFv-CD3ζ (#1078). DNA coding for the anti-CD30 scFv HRS3 was amplified from the plasmid pRSV-Lk HRS3scFv-Fc (#440) by PCR using the oligonucleotides HRS3-pMT-S and S-HRS3-hi-Bam. The 0.75 kb DNA fragment was purified and digested by NcoI and BamHI. The plasmid DNA pBullet-Lk CC49scFv-Fc-CD3ζ (#435) was also digested by NcoI and BamHI. The two DNA fragments were purified and ligated to generate the new plasmid pBullet HRS3scFv-CD3ζ (#1078).

plasmid pMT/BiP HRS3scFv-Fc (#1082; figure 4.2). The newly generated plasmid was transformed into *Escherichia coli* for amplification and the recombinant expression cassette was verified by DNA sequencing (appendix B.2).

4.1.3 Generation of the plasmid pMT/BiP HRS3scFv-Fc-hi-IL12 (#1083)

To allow expression of the anti-CD30 immunocytokine HRS3scFv-Fc-hi-IL12 in insect cells, an expression cassette coding for the immunocytokine was inserted into the DNA vector pMT/BiP V5-His A (#1070).

DNA coding for the scFv HRS3 was isolated from the plasmid pBullet HRS3scFv-CD3 ζ (#1078) by digestion with NcoI and BamHI. DNA coding for the Fc region of human IgG₁, the hinge region of human IgG₁ and murine single-chain IL-12 (p40-p35) was isolated by digesting the plasmid pRSV-Lk HRS3scFv-Fc-hi-IL12 (#619) with BamHI and XhoI. The vector DNA pMT/BiP V5-His A (#1070) was digested by the restriction enzymes NcoI and XhoI to allow insertion of the expression cassette into the MCS. The three DNA fragments were purified and ligated to generate the new plasmid pMT/BiP HRS3scFv-Fc-hi-IL12 (#1083; figure 4.3). The newly generated plasmid was transformed into *Escherichia coli* for amplification and the recombinant expression cassette was verified by DNA sequencing (appendix B.3).

4.1.4 Generation of the plasmid pMT/BiP HRS3scFv-Fc-IL2 (#1086)

To allow expression of the anti-CD30 immunocytokine HRS3scFv-Fc-IL2 in insect cells, an expression cassette coding for the immunocytokine was inserted into the DNA vector pMT/BiP V5-His A (#1070).

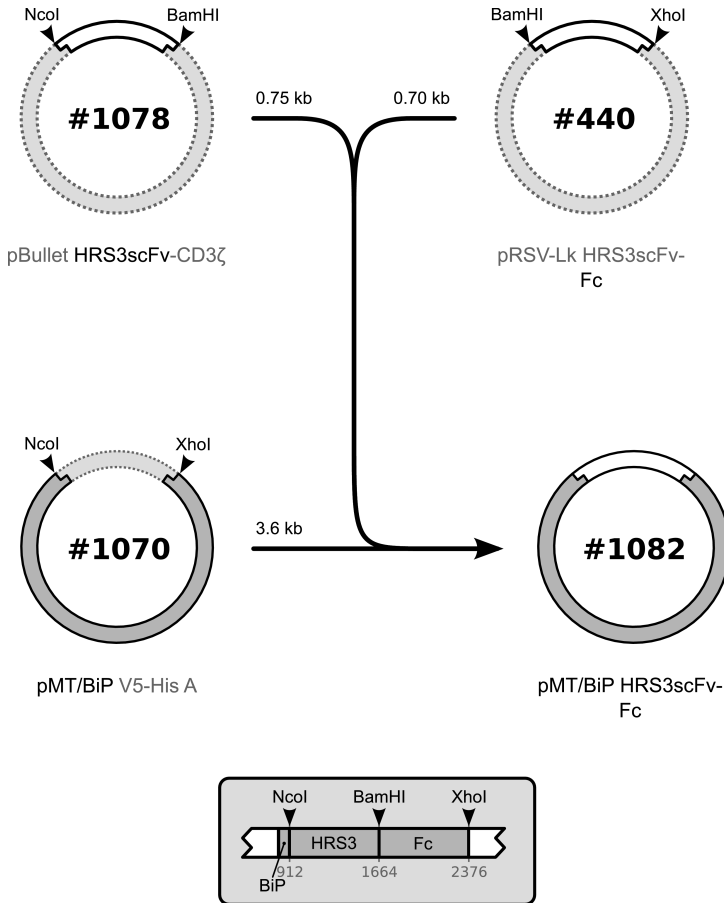


Figure 4.2: Generation of the plasmid pMT/BiP HRS3scFv-Fc (#1082). DNA coding for the scFv HRS3 was isolated from the plasmid pBullet HRS3scFv-CD3 ζ (#1078) by digestion with NcoI and BamHI. DNA coding for the Fc region of human IgG₁ was isolated by digesting the plasmid pRSV-Lk HRS3scFv-Fc (#440) with BamHI and XhoI. The vector DNA pMT/BiP V5-His A (#1070) was digested by NcoI and XhoI. The three DNA fragments were purified and ligated to generate the new plasmid pMT/BiP HRS3scFv-Fc (#1082).

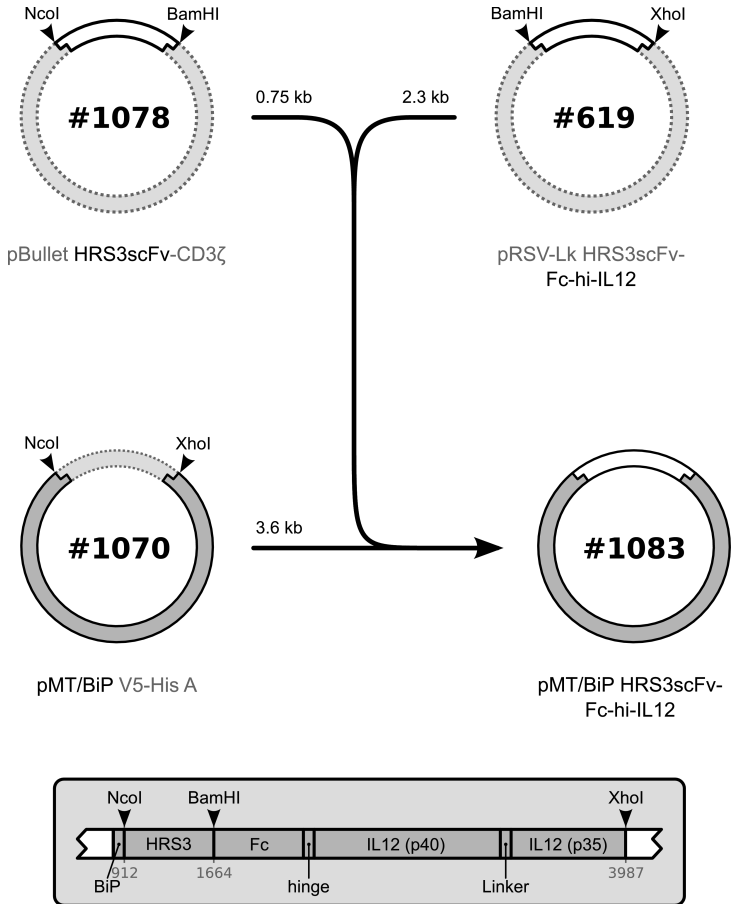


Figure 4.3: Generation of the plasmid pMT/BiP HRS3scFv-Fc-hi-IL12 (#1083). DNA coding for the scFv HRS3 was isolated from the plasmid pBullet HRS3scFv-CD3ζ (#1078) by digestion with *NcoI* and *BamHI*. DNA coding for the Fc region of human IgG₁, the hinge region of human IgG₁ and murine single-chain IL-12 (p40-p35) was isolated by digesting the plasmid pRSV-Lk HRS3scFv-Fc-hi-IL12 (#619) with *BamHI* and *XhoI*. The vector DNA pMT/BiP V5-His A (#1070) was digested by *NcoI* and *XhoI*. The three DNA fragments were purified and ligated to generate the new plasmid pMT/BiP HRS3scFv-Fc-hi-IL12 (#1083).

DNA coding for the scFv HRS3, the Fc region of human IgG₁ and human IL-2 was amplified from the plasmid pRSV-Lk HRS3scFv-Fc-IL2 (#508) by PCR using the oligonucleotides HRS3-pMT-S and IL-2SX. The amplified DNA was thereby flanked with the restriction sites NcoI at the 5' end and XhoI at the 3' end. The 1.9kb DNA fragment was purified and digested by the restriction enzymes NcoI and XhoI. The vector DNA pMT/BiP V5-His A (#1070) was also digested by the restriction enzymes NcoI and XhoI to allow insertion of the expression cassette into the MCS. The two DNA fragments were purified and ligated to generate the new plasmid pMT/BiP HRS3scFv-Fc-IL2 (#1086; figure 4.4). The newly generated plasmid was transformed into *Escherichia coli* for amplification and the recombined expression cassette was verified by DNA sequencing (appendix B.4).

4.1.5 Generation of the plasmid pMT/BiP HRS3scFv-hi-IL12-Fc-IL2 (#1100)

To allow expression of the anti-CD30 immunocytokine HRS3scFv-hi-IL12-Fc-IL2 in insect cells, an expression cassette coding for the immunocytokine was inserted into the DNA vector pMT/BiP V5-His A (#1070).

DNA coding for the scFv HRS3, the hinge region of human IgG₁, murine single-chain IL-12 (p40-p35), the Fc region of human IgG₁ and human IL-2 was amplified from the plasmid pRSV-Lk HRS3scFv-hi-IL12-Fc-IL2 (#715) by PCR using the oligonucleotides HRS3-pMT-S and IL-2SX. The amplified DNA was thereby flanked with the restriction sites NcoI at the 5' end and XhoI at the 3' end. The 3.5kb DNA fragment was purified and digested by the restriction enzymes NcoI and XhoI. The vector DNA pMT/BiP V5-His A (#1070) was also digested by the restriction enzymes NcoI and XhoI to allow insertion of the expression cassette into the MCS. The two DNA fragments were purified and ligated to generate the new plasmid pMT/BiP HRS3scFv-hi-IL12-Fc-IL2 (#1100; figure 4.5). The newly generated plasmid was transformed into *Escherichia coli* for amplification and the recombined expression cassette was verified by DNA sequencing (appendix B.5).

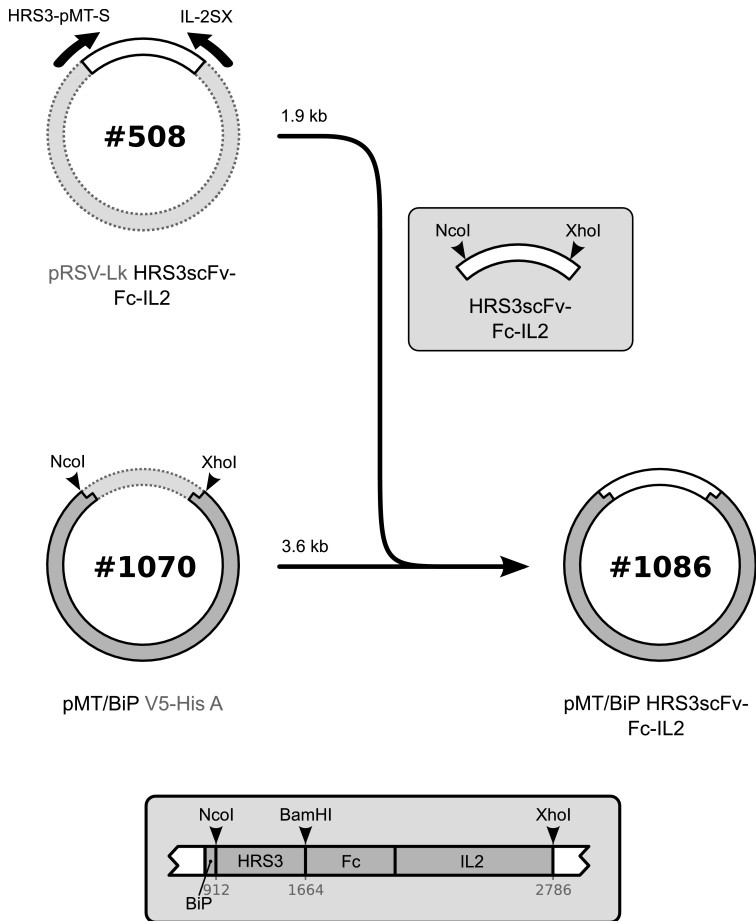


Figure 4.4: Generation of the plasmid pMT/BiP HRS3scFv-Fc-IL2 (#1086). DNA coding for the scFv HRS3, the Fc region of human IgG₁ and human IL-2 was amplified from the plasmid pRSV-Lk HRS3scFv-Fc-IL2 (#508) by PCR using the oligonucleotides HRS3-pMT-S and IL-2SX. The 1.9kb DNA fragment was purified and digested by NcoI and XhoI. The vector DNA pMT/BiP V5-His A (#1070) was also digested by NcoI and XhoI. The two DNA fragments were purified and ligated to generate the new plasmid pMT/BiP HRS3scFv-Fc-IL2 (#1086).

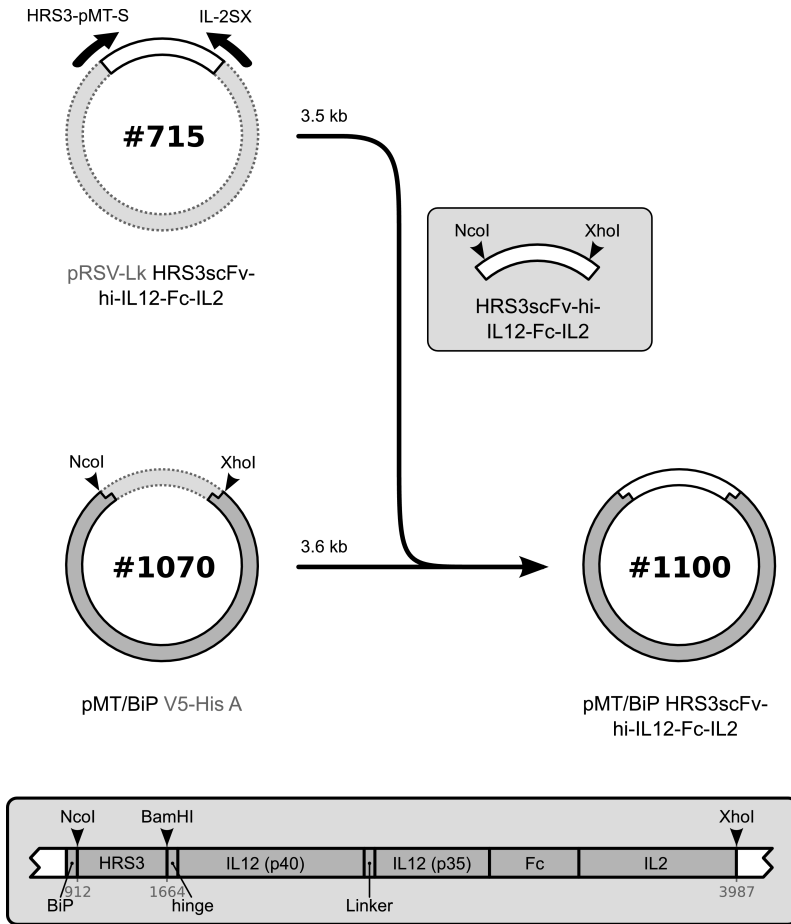


Figure 4.5: Generation of the plasmid pMT/BiP HRS3scFv-hi-IL12-Fc-IL2 (#1100). DNA coding for the the scFv HRS3, the hinge region of human IgG₁, murine single-chain IL-12 (p40-p35), the Fc region of human IgG₁ and human IL-2 was amplified from the plasmid pRSV-Lk HRS3scFv-hi-IL12-Fc-IL2 (#715) by PCR using the oligonucleotides HRS3-pMT-S and IL-2SX. The 3.5 kb DNA fragment was purified and digested by NcoI and XhoI. The vector DNA pMT/BiP V5-His A (#1070) was also digested by NcoI and XhoI. The two DNA fragments were purified and ligated to generate the new plasmid pMT/BiP HRS3scFv-hi-IL12-Fc-IL2 (#1100).

4.1.6 Generation of the plasmid pMT/BiP SCA431scFv-Fc (#1103)

The expression cassette coding for the anti-CEA fusion protein SCA431-scFv-Fc was generated and inserted into the *Drosophila* Expression System™ DNA vector pMT/BiP V5-His A (#1070).

DNA coding for the scFv SCA431 and the Fc region of murine IgG₁ was amplified from the plasmid pBullet-Lk SCA431scFv-Fc-CD4tm-CD3ζ (#977) by PCR using the oligonucleotides pMT-SCA431-S and pMT-SCA431-AS. The amplified DNA was thereby flanked with the restriction sites NcoI at the 5' end and NotI at the 3' end. In addition, the C-terminal lysine of the murine Fc region – that had been changed to isoleucine by previous cloning procedures – was restored. The 1.4kb DNA fragment was purified and digested by the restriction enzymes NcoI and NotI. The vector DNA pMT/BiP V5-His A (#1070) was also digested by the restriction enzymes NcoI and NotI to allow insertion of the expression cassette into the MCS. The two DNA fragments were purified and ligated to generate the new plasmid pMT/BiP SCA431scFv-Fc (#1103; figure 4.6). The newly generated plasmid was transformed into *Escherichia coli* for amplification and the recombined expression cassette was verified by DNA sequencing (appendix B.6).

4.1.7 Generation of the plasmid pMT/BiP SCA431scFv-Fc-IL7 (#1117)

The expression cassette coding for the anti-CEA immunocytokine SCA431-scFv-Fc-IL7 was generated and inserted into the *Drosophila* Expression System™ DNA vector pMT/BiP V5-His A (#1070).

DNA coding for murine IL-7 was amplified from the plasmid pJR IL7 (#1024) by PCR using the oligonucleotides pMT-mIL7-BstX-S and pMT-mIL7-Not-AS. The amplified DNA was thereby flanked with the restriction sites BstXI at the 5' end and NotI at the 3' end. The 0.4kb DNA fragment

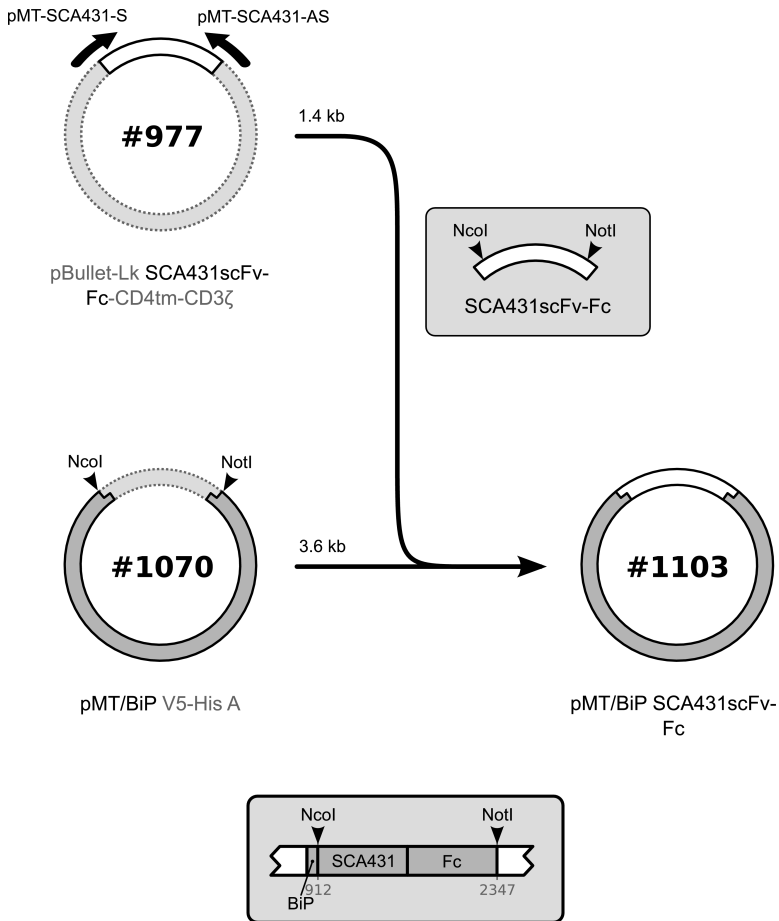


Figure 4.6: Generation of the plasmid pMT/BiP SCA431scFv-Fc (#1103). DNA coding for the scFv SCA431 and the Fc region of murine IgG₁ was amplified from the plasmid pBullet-Lk SCA431scFv-Fc-CD4tm-CD3ζ (#977) by PCR using the oligonucleotides pMT-SCA431-S and pMT-SCA431-AS. The 1.4 kb DNA fragment was purified and digested by NcoI and NotI. The vector DNA pMT/BiP V5-His A (#1070) was also digested by NcoI and NotI. The two DNA fragments were purified and ligated to generate the new plasmid pMT/BiP SCA431scFv-Fc (#1103).

was purified and digested by the restriction enzymes BstXI and NotI. The plasmid DNA pMT/BiP SCA431scFv-Fc (#1103) was also digested by the restriction enzymes BstXI and NotI to allow insertion of the amplified DNA. The two DNA fragments were purified and ligated to generate the new plasmid pMT/BiP SCA431scFv-Fc-IL7 (#1117; figure 4.7). The newly generated plasmid was transformed into *Escherichia coli* for amplification and the recombinant expression cassette was verified by DNA sequencing (appendix B.7).

4.1.8 Generation of the plasmid pMT/BiP SCA431scFv-Fc-IL15 (#1118)

The expression cassette coding for the anti-CEA immunocytokine SCA431-scFv-Fc-IL15 was generated and inserted into the Drosophila Expression System™ DNA vector pMT/BiP V5-His A (#1070).

DNA coding for human IL-15 was amplified from the plasmid pORF IL15 (#844) by PCR using the oligonucleotides pMT-hIL15-BstX-S and pMT-hIL15-Not-AS. The amplified DNA was thereby flanked with the restriction sites BstXI at the 5' end and NotI at the 3' end. The 0.35kb DNA fragment was purified and digested by the restriction enzymes BstXI and NotI. The plasmid DNA pMT/BiP SCA431scFv-Fc (#1103) was also digested by the restriction enzymes BstXI and NotI to allow insertion of the amplified DNA. The two DNA fragments were purified and ligated to generate the new plasmid pMT/BiP SCA431scFv-Fc-IL15 (#1118; figure 4.8). The newly generated plasmid was transformed into *Escherichia coli* for amplification and the recombinant expression cassette was verified by DNA sequencing (appendix B.8).

4.1.9 Evaluation of transfection efficiency in insect cells

High transfection efficiencies of expression plasmids in insect cells were needed to increase the probability to generate high-producer cell clones.

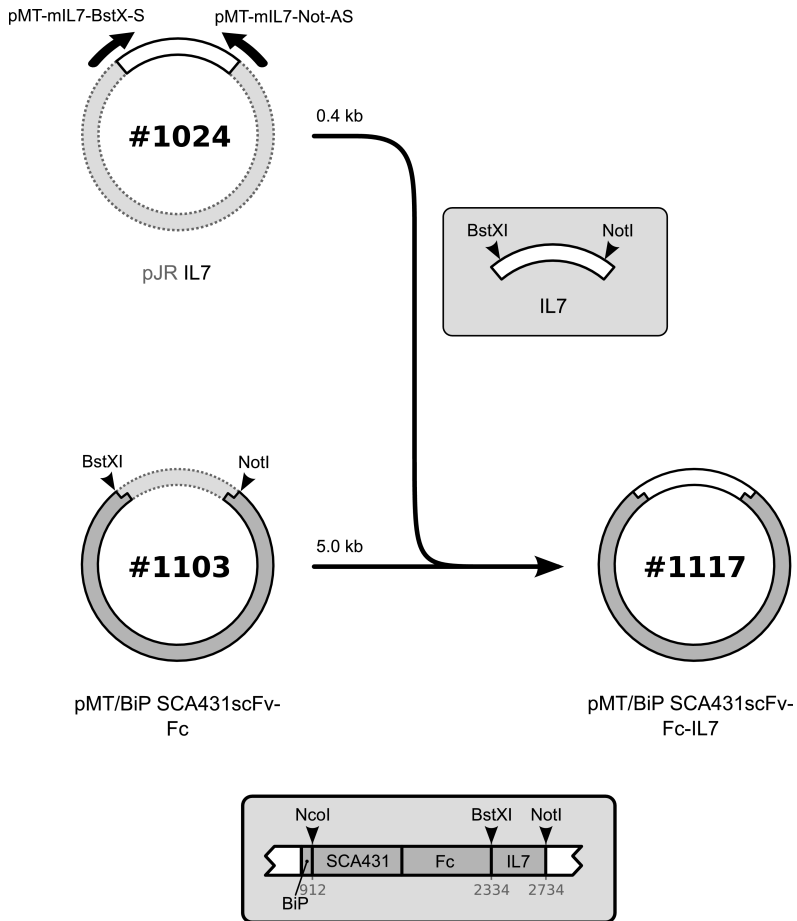


Figure 4.7: Generation of the plasmid pMT/BiP SCA431scFv-Fc-IL7 (#1117). DNA coding for murine IL-7 was amplified from the plasmid pJR IL7 (#1024) by PCR using the oligonucleotides pMT-mIL7-BstX-S and pMT-mIL7-Not-AS. The 0.4 kb DNA fragment was purified and digested by BstXI and NotI. The plasmid DNA pMT/BiP SCA431scFv-Fc (#1103) was also digested by BstXI and NotI. The two DNA fragments were purified and ligated to generate the new plasmid pMT/BiP SCA431-scFv-Fc-IL7 (#1117).

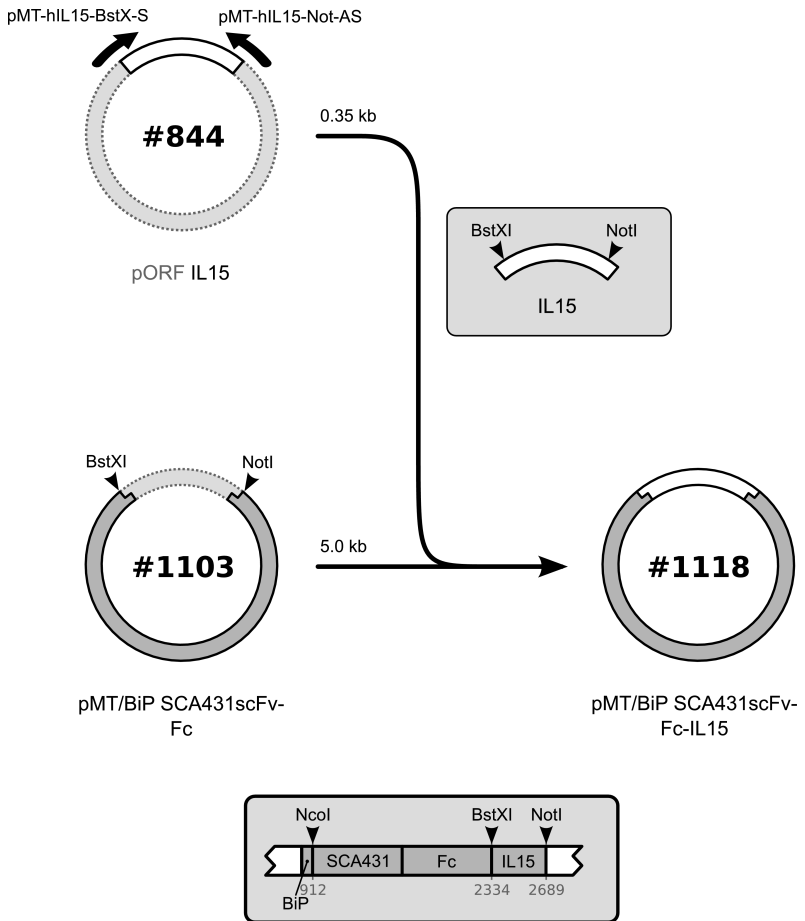


Figure 4.8: Generation of the plasmid pMT/BiP SCA431scFv-Fc-IL15 (#1118). DNA coding for human IL-15 was amplified from the plasmid pORF IL15 (#844) by PCR using the oligonucleotides pMT-hIL15-BstX-S and pMT-hIL15-Not-AS. The 0.35 kb DNA fragment was purified and digested by BstXI and NotI. The plasmid DNA pMT/BiP SCA431scFv-Fc (#1103) was also digested by BstXI and NotI. The two DNA fragments were purified and ligated to generate the new plasmid pMT/BiP SCA431scFv-Fc-IL15 (#1118).

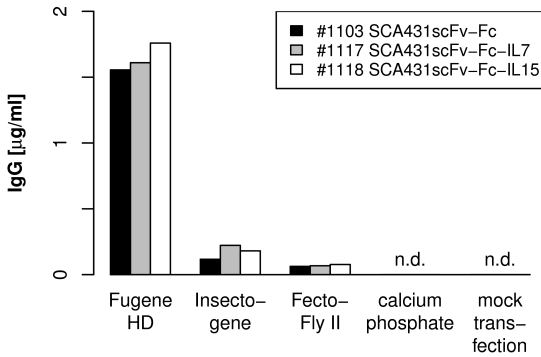


Figure 4.9: Comparison of transfection procedures for insect cells. SL2 cells were co-transfected with plasmid DNA coding for the anti-CEA fusion proteins SCA431-scFv-Fc, SCA431scFv-Fc-IL7 or SCA431scFv-Fc-IL15 by calcium phosphate co-precipitation of DNA or lipofection with the transfection reagents Fugene™ HD, Insectogene™ or FectoFly™ II. Protein production was induced after 24 hours by adding CuSO_4 (final concentration: $500\mu\text{M}$). Two days later, protein concentrations were detected from culture supernatants by ELISA using antibodies directed against the murine IgG domain (**n.d.:** not detected). Each bar corresponds to one sample.

Therefore, we determined the transfection efficiencies of calcium phosphate co-precipitation of DNA or lipofection with the transfection reagents FectoFly™ II, Fugene™ HD or Insectogene™.

SL2 cells were seeded in six-well-plates and transfected with plasmid DNA coding for the anti-CEA fusion proteins SCA431scFv-Fc, SCA431scFv-Fc-IL7 or SCA431scFv-Fc-IL15. Protein production was induced after 24 hours by addition of CuSO_4 . Two days later, concentrations of the respective proteins were determined from supernatants by ELISA of the Fc domain of IgG_1 ($\text{Fc}\gamma_1$) that is present in all of the generated fusion proteins (figure 4.9).

Transfection efficiencies of each transfection reagent were very similar for three different plasmids. Transfection of SL2 cells by Fugene™ HD re-

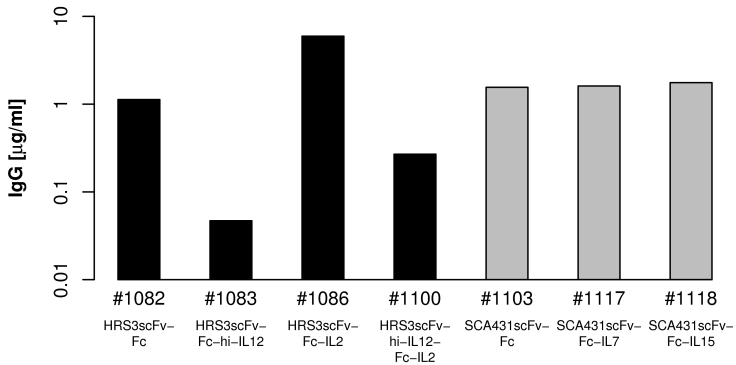


Figure 4.10: Transfected insect cells secrete immunocytokines. SL2 cells were co-transfected with plasmid DNA coding for one of the generated anti-CD30 or anti-CEA fusion proteins and the hygromycin B resistance plasmid pCoHygro (#1080) using Fugene™ HD. After 24 hours, transfected cells were selected by addition of hygromycin B (final concentration: 300 µg/ml) and protein production was induced by adding CuSO₄ (final concentration: 500 µM). After 7 days, protein concentrations were detected from culture supernatants by ELISA using antibodies directed against the human IgG domain (**black bars**) or the murine IgG domain (**grey bars**). Each bar corresponds to one sample.

sulted in a mean protein concentration of 1.6 µg/ml, whereas protein concentrations of cells transfected by FectoFly™ II or Insectogene™ were 10- to 20-fold lower. No protein was detected in SL2 cells transfected by calcium phosphate co-precipitation or mock-transfected cells.

Fugene™ HD was chosen as transfection reagent in further experiments due to its superior transfection efficiency. In addition, the morphology of SL2 cells transfected with Fugene™ HD remained unchanged in contrast to the other transfection reagents.

4.1.10 Insect cells are stably transfected to express immunocytokines

We established high-producer cell clones of insect cells that stably expressed recombinant protein by co-transfection of SL2 cells with the hygromycin B resistance plasmid pCoHygro (#1080) and plasmid DNA coding for one of the anti-CD30 or anti-CEA fusion proteins. After 24 hours, transfected cells were selected by addition of hygromycin B. Resistant clones appeared after four weeks and were subcloned (figure 4.10). Protein production was induced by adding CuSO_4 . After 24 hours, supernatants were screened for expressed protein by ELISA of the $\text{Fc}\gamma_1$ domain that is present in all of the generated fusion proteins. High-producer cell clones were raised and stored in liquid nitrogen.

Concentrations of anti-CD30 fusion protein in culture supernatants were recorded by ELISA using the anti-idiotypic antibody 9G10 and the biotinylated anti-h-IgG antibody which detects the human $\text{Fc}\gamma_1$ domain that is present in all anti-CD30 fusion proteins. Stably transfected SL2 clones that were grown in the FibraStage™ bioreactor at an estimated density of 5×10^6 cells/ml produced 2 mg/l to 8 mg/l recombinant fusion protein within three days. Protein expression was constant over the observation time of four to five weeks.

4.2 Purified immunocytokines specifically bind to CD30

In this study, immunocytokines and fusion proteins that contain the Fc domain of IgG_1 ($\text{Fc}\gamma_1$) were affinity-purified and detected using polyclonal anti-IgG antibodies, whereas the immunocytokine HRS3scFv-hi-IL12 which lacks an $\text{Fc}\gamma_1$ domain was affinity-purified using the monoclonal anti-idiotypic antibody 9G10. We routinely obtained 0.5 mg to 2.0 mg purified protein from 1.5 l of cell culture supernatant. Purified proteins were

stored at -80°C in PBS containing 3% (v/v) of either FCS (*in vitro* studies) or normal mouse serum (studies in mice).

Purified immunocytokines and fusion proteins were analysed for integrity of the protein by binding to the anti-idiotypic antibody 9G10 and detecting the respective $\text{Fc}\gamma_1$ and cytokine domains. Specificity of binding of the anti-CD30 fusion proteins was determined from binding to the anti-idiotypic antibody 9G10 or a control antibody with irrelevant specificity, and by analysing the binding inhibition mediated by CD30. In addition, we assessed binding of the CD30 fusion proteins to CD30^+ and CD30^- tumour cells.

In this study, the anti-idiotypic antibody 9G10 that bears the internal image of the HRS3-binding epitope (Pohl *et al.*, 1992) served as a substitute for immobilised CD30. Validity of this substitute was determined from the binding inhibition experiment.

The experiments described in this and the next section yielded the same results for anti-CD30 fusion proteins that had been expressed in either mammalian 293T cells or SL2 insect cells. Therefore, the study will not distinguish between proteins expressed in either cells.

4.2.1 Detection of the individual domains of purified immunocytokines

To determine whether immunocytokines were intact after purification and storage, the HRS3 scFv of anti-CD30 immunocytokines was captured using the anti-idiotypic antibody 9G10. The human $\text{Fc}\gamma_1$ domain, the human IL-2 domain and the murine IL-12 domain were detected by ELISA using antibodies specific to the respective domain (figure 4.11).

Anti-CD30 fusion proteins bound to the anti-idiotypic antibody 9G10 in a dose-dependant manner. After capturing the HRS3 scFv of purified immunocytokine or the fusion protein HRS3scFv-Fc, all respective protein domains were detected. The resulting curves of the different domains were

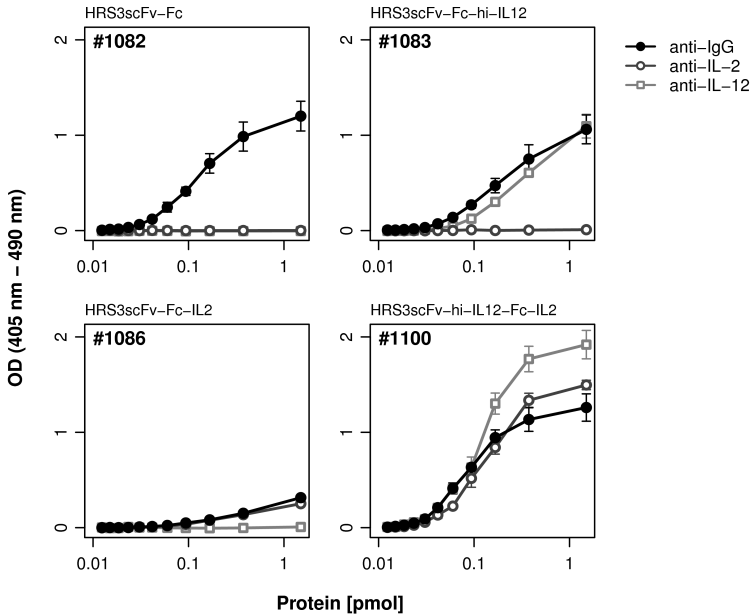


Figure 4.11: Detection of the individual domains of purified immunocytokines. ELISA plates were coated with the anti-idiotypic antibody 9G10 and incubated with serial dilutions of purified immunocytokine or the fusion protein HRS3scFv-Fc. Bound protein was probed with the biotinylated anti-h-IgG, anti-h-IL-2 or anti-m-IL-12 (p40/p70) antibodies and detected by streptavidin- β -peroxidase and ABTS as substrate. Data represent the mean of three samples \pm standard deviation.

similar for each protein in respect to position of half-maximum and shape. Interestingly, binding of the immunocytokine HRS3scFv-Fc-IL2 to the anti-idiotypic antibody 9G10 was 3- to 6-fold lower compared to the other fusion proteins. Detection was specific, as protein domains were only detected in fusion proteins which contained the respective domain.

The fusion proteins bound to the anti-idiotypic antibody 9G10 in a dose-dependant manner. Purified immunocytokines and the fusion protein HRS3scFv-Fc were intact, as all domains of each protein were detected after capturing the HRS3 scFv.

4.2.2 Immunocytokines specifically bind to the anti-idiotypic antibody 9G10

We determined whether binding of anti-CD30 immunocytokines via the HRS3 scFv domain was specific by capturing immunocytokines with either the anti-idiotypic antibody 9G10 or an isotype-matched control antibody. Binding was analysed by ELISA using an antibody directed against the human Fc γ_1 domain that is present in all of the tested proteins (figure 4.12).

Anti-CD30 immunocytokines and the fusion protein HRS3scFv-Fc bound in a dose-dependant manner to the anti-idiotypic antibody 9G10. Maximum binding to the antibody 9G10 was 4- to 8-fold higher compared to the isotype-matched control antibody. These differences in maximum binding were statistically significant. Again, binding of the immunocytokine HRS3scFv-Fc-IL2 to the anti-idiotypic antibody 9G10 was 3- to 4-fold lower compared to the other fusion proteins.

Purified anti-CD30 immunocytokines and the fusion protein HRS3scFv-Fc specifically bound to the anti-idiotypic antibody 9G10.

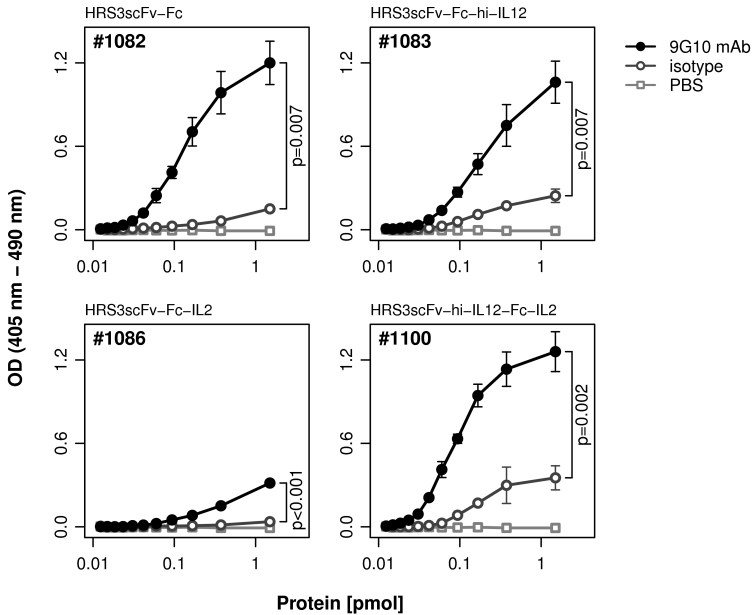


Figure 4.12: Immunocytokines specifically bind to the anti-idiotypic antibody 9G10. ELISA plates were coated with either the anti-idiotypic antibody 9G10 or an isotype-matched control antibody and incubated with serial dilutions of purified immunocytokine, the fusion protein HRS3scFv-Fc or PBS as control. Bound protein was probed with the biotinylated anti-h-IgG antibody and detected by streptavidin- β -peroxidase and ABTS as substrate. Data represent the mean of three samples \pm standard deviation. Significance of differences in binding was determined by an unpaired two-sided Welch-corrected t-test.

4.2.3 CD30 competes with the anti-idiotypic antibody 9G10 in binding to immunocytokines

We determined whether CD30 competed with surface-bound anti-idiotypic antibody 9G10 in binding to the anti-CD30 immunocytokines. Purified anti-CD30 fusion proteins were captured by the anti-idiotypic antibody 9G10 in presence of serial dilutions of CD30-Fc or Fc protein as control. For specificity control, the anti-melanoma fusion protein 763.74scFv-Fc was captured by the anti-763.74 antibody MK2-72.8854 in presence of serial dilutions of CD30-Fc. Bound protein was probed by ELISA using an antibody directed against the human Fc γ ₁ domain that is present in all of the tested anti-CD30 and anti-melanoma fusion proteins (figure 4.13).

Co-incubation of the anti-CD30 fusion proteins with CD30 resulted in dose-dependent binding inhibition. A molar ratio of 1 : 3 between fusion protein and CD30 yielded binding inhibition ranging from 34% (HRS3-scFv-hi-IL12-Fc-IL2) to 54% (HRS3scFv-Fc). Binding inhibition mediated by CD30-Fc was significantly higher compared to binding inhibition mediated by the Fc protein. Moreover, binding inhibition by CD30 was specific, since binding of the anti-HMW-MAA fusion protein 763.74scFv-Fc to the anti-763.74 antibody MK2-72.8854 was not inhibited by CD30.

We conclude that CD30 competed with surface-bound anti-idiotypic antibody 9G10 in binding to anti-CD30 immunocytokines and the fusion protein HRS3scFv-Fc. Furthermore, we infer that the anti-idiotypic antibody 9G10 is a valid substitute for CD30 to capture anti-CD30 fusion proteins.

4.2.4 Immunocytokines specifically bind to CD30⁺ tumour cells

To determine binding of anti-CD30 immunocytokines to tumour cells, CD30⁺ HMW-MAA⁻ L540 cells, HMW-MAA⁺ CD30⁻ MeWo cells or hybridoma cells secreting the anti-idiotypic antibody 9G10 as control were incubated with purified immunocytokine or the fusion protein HRS3scFv-

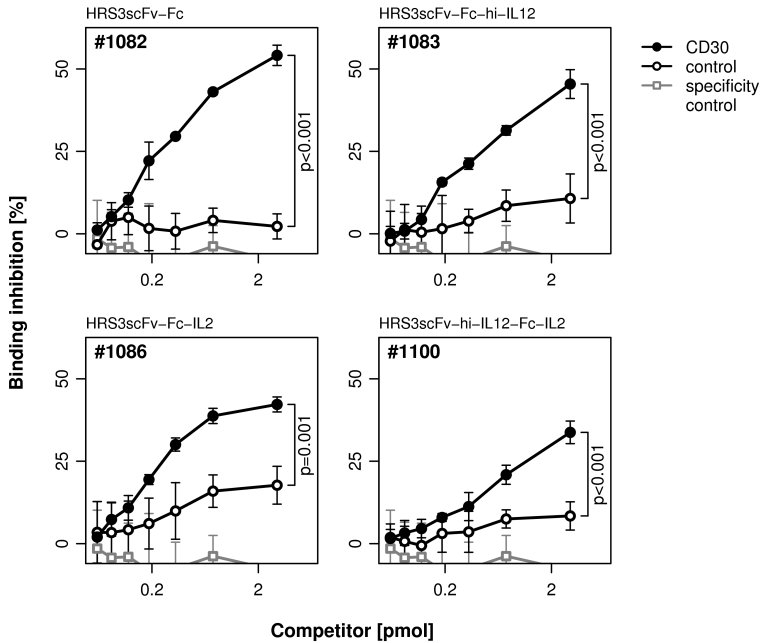


Figure 4.13: CD30 competes with the anti-idiotypic antibody 9G10 in binding to immunocytokines. ELISA plates were coated with the anti-idiotypic antibody 9G10 and incubated with purified anti-CD30 fusion protein (1 pmol) in presence of serial dilutions of CD30-Fc or Fc protein as control (**black lines**). As specificity control, ELISA plates were coated with the anti-763.74 antibody MK2-72.8854 and incubated with the purified anti-melanoma fusion protein 763.74scFv-Fc (1 pmol) in presence of serial dilutions of CD30-Fc (**grey lines**). Bound protein was probed with the biotinylated anti-h-IgG antibody and detected by streptavidin- β -peroxidase and ABTS as substrate. Data represent the mean of four samples \pm standard deviation. Significance of differences in binding inhibition was determined by an unpaired two-sided Welch-corrected t-test.

Fc. The purified anti-melanoma fusion protein 763.74scFv-Fc or PBS served as controls. Bound protein was detected by flow-cytometry using the anti-h-IgG₁-PE antibody which detects the Fcγ₁ domain that is present in all of the tested fusion proteins (figures 4.14 to 4.16). Data were analysed by comparing the ratios of mean fluorescence intensity between incubation with and without protein (figure 4.17).

Anti-CD30 fusion proteins bound to CD30⁺ HMW-MAA⁻ L540 cells and to hybridoma cells secreting the anti-idiotypic antibody 9G10. No binding to HMW-MAA⁺ CD30⁻ MeWo cells was recorded. In contrast, the anti-HMW-MAA fusion protein 763.74scFv-Fc only bound to HMW-MAA⁺ CD30⁻ MeWo cells. The immunocytokine HRS3scFv-Fc-IL2 bound 1.5-fold stronger and the immunocytokine HRS3scFv-hi-IL12-Fc-IL2 bound 3-fold stronger to L540 cells compared to the immunocytokine HRS3scFv-Fc-hi-IL12 and the fusion protein HRS3scFv-Fc. In contrast, binding of the anti-CD30 immunocytokines to hybridoma cells secreting the anti-idiotypic antibody 9G10 was equally strong, except for the immunocytokine HRS3scFv-Fc-IL2 which bound half as strong. Binding was specific, as the anti-CD30 immunocytokines and the fusion protein HRS3scFv-Fc only bound to CD30⁺ HMW-MAA⁻ L540 cells and to hybridoma cells secreting the anti-idiotypic antibody 9G10, whereas the anti-HMW-MAA fusion protein 763.74scFv-Fc only bound to HMW-MAA⁺ CD30⁻ MeWo cells.

In summary, the anti-CD30 fusion proteins specifically bound to CD30⁺ tumour cells and to hybridoma cells that secrete the anti-idiotypic antibody 9G10.

4.3 Purified immunocytokines exhibit cytokine activity

Immunocytokines direct cytokine activity to specific sites of the body in order to modulate immune responses. To determine whether the cytokine domains of purified immunocytokines were active, lymphocytes were co-

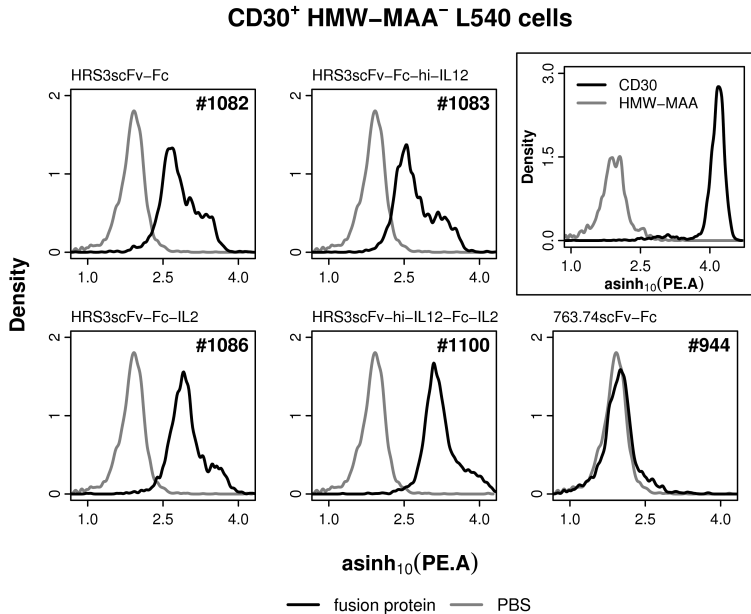


Figure 4.14: Immunocytokines bind to CD30⁺ L540 cells. CD30⁺ HMW-MAA⁻ L540 cells (2×10^5 cells) were incubated for 30 min with purified immunocytokine, the fusion protein HRS3scFv-Fc or the anti-HMW-MAA fusion protein 763.74scFv-Fc as control (4 pmol each; **black lines**). PBS served as control (**grey lines**). Bound protein was detected by flow-cytometry using the anti-h-IgG₁-PE antibody. **Inset:** CD30⁺ HMW-MAA⁻ L540 cells (2×10^5 cells) were stained with the anti-CD30-PE antibody or the anti-HMW-MAA-PE antibody as control and analysed by flow-cytometry.

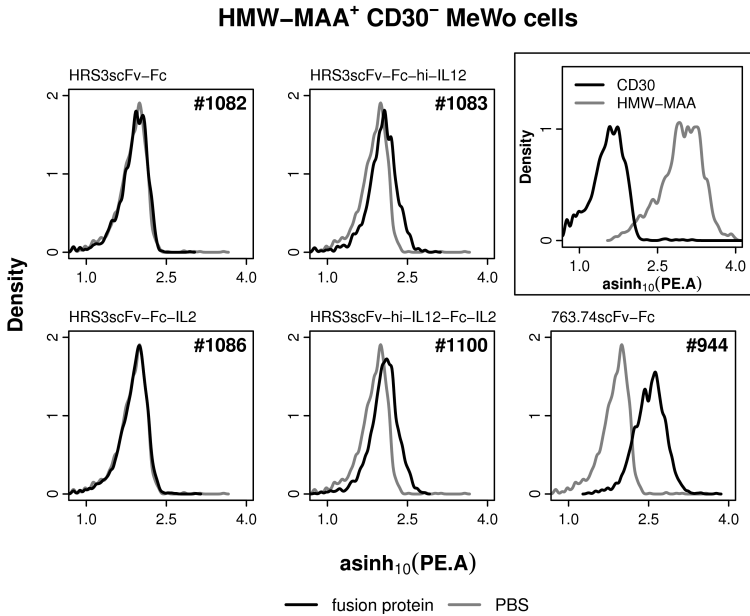


Figure 4.15: Immunocytokines do not bind to CD30⁻ MeWo cells. HMW-MAA⁺ CD30⁻ MeWo cells (2×10^5 cells) were incubated for 30 min with purified immunocytokine, the fusion protein HRS3scFv-Fc or the anti-HMW-MAA fusion protein 763.74scFv-Fc as control (4 pmol each; **black lines**). PBS served as control (**grey lines**). Bound protein was detected by flow-cytometry using the anti-h-IgG₁-PE antibody. **Inset:** HMW-MAA⁺ CD30⁻ MeWo cells (2×10^5 cells) were stained with the anti-CD30-PE antibody or the anti-HMW-MAA-PE antibody as control and analysed by flow-cytometry.

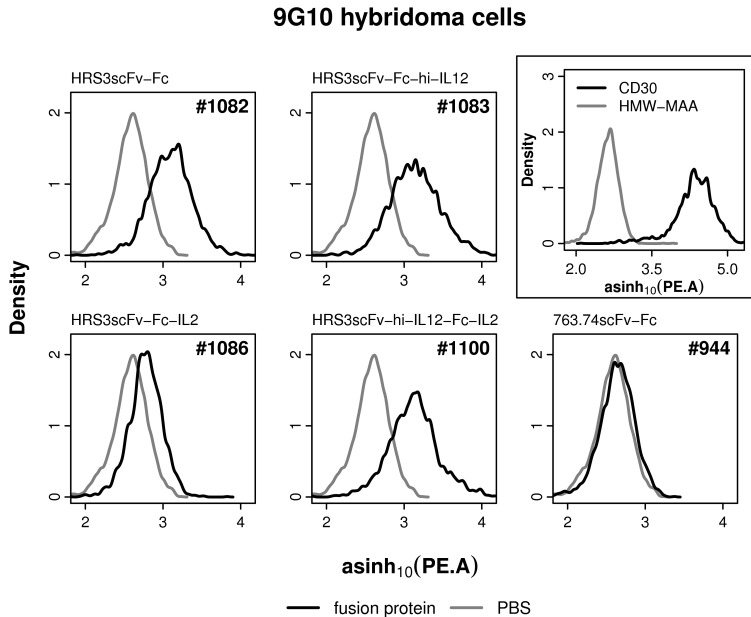


Figure 4.16: Immunocytokines bind to 9G10 hybridoma cells. 9G10 hybridoma cells (clone II-G05; 2×10^5 cells) were incubated for 30 min with purified immunocytokine, the fusion protein HRS3scFv-Fc or the anti-HMW-MAA fusion protein 763.74scFv-Fc as control (4 pmol each; **black lines**). PBS served as control (**grey lines**). Bound protein was detected by flow-cytometry using the anti-h-IgG₁-PE antibody. **Inset:** 9G10 hybridoma cells (clone II-G05; 2×10^5 cells) were stained with the anti-CD30-PE antibody or the anti-HMW-MAA-PE antibody as control and analysed by flow-cytometry.

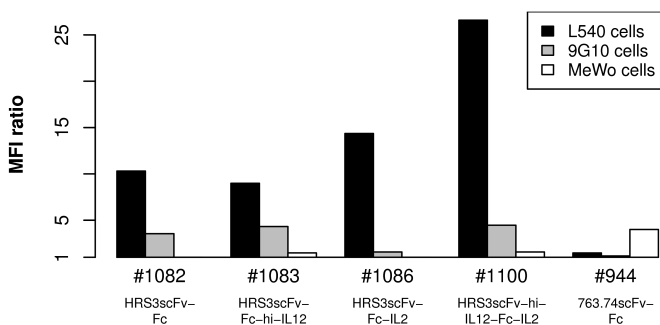


Figure 4.17: Immunocytokines bind to CD30⁺ tumour cells. CD30⁺ HMW-MAA⁻ L540 cells (2×10^5 cells; **black bars**), hybridoma cells producing the anti-idiotypic antibody 9G10 (clone II-G05; 2×10^5 cells; **grey bars**) or HMW-MAA⁺ CD30⁻ MeWo cells (2×10^5 cells; **white bars**) were incubated for 30min with purified immunocytokine, the fusion protein HRS3scFv-Fc or the anti-HMW-MAA fusion protein 763.74scFv-Fc as control (4 pmol each). Bound protein was detected by flow-cytometry using the anti-h-IgG₁-PE antibody. Data represent the ratio of mean fluorescence intensity (**MFI ratio**) between incubation with and without protein. Each bar represents one sample.

incubated with immunocytokines and analysed for proliferation, secretion of IFN- γ and phosphorylation of STAT4.

The anti-CD30 fusion proteins used in this study were generated to aid the eradication of tumour cells. Therefore, we determined the influence of these fusion proteins on the cytolysis of tumour cells by natural killer (NK) cells.

4.3.1 Immunocytokines induce proliferation and IFN- γ secretion in PBMCs

We determined whether the cytokine domains of purified immunocytokines induced proliferation and IFN- γ secretion in peripheral blood mononuclear cells (PBMCs). Pre-activated PBMCs were cultured in absence of IL-2 for 24 hours and incubated with solutions of purified anti-CD30 immunocytokine or the fusion protein HRS3scFv-Fc as control. Alternatively, PBMCs were incubated with anti-CD30 fusion proteins bound to the immobilised anti-idiotypic antibody 9G10 or an isotype-matched control antibody. For control, PBMCs were incubated with IL-2, IL-12 or with medium alone. Proliferation of PBMCs was quantified by incorporation of BrdU and subsequent ELISA (figure 4.18), while IFN- γ secretion of PBMCs was determined from culture supernatants by ELISA (figure 4.19).

Anti-CD30 immunocytokines in solution induced proliferation in PBMCs, whereas the fusion protein HRS3scFv-Fc without cytokine domain did not. Immunocytokines which contain an IL-2 domain significantly increased proliferation when bound to immobilised anti-idiotypic antibody 9G10 compared to immobilised isotype-matched control antibody. After binding to the antibody 9G10, the immunocytokine HRS3scFv-hi-IL12-Fc-IL2 with combined IL-2 and IL-12 domains resulted in significantly increased proliferation of PBMCs compared to immunocytokines with a single cytokine domain or the fusion protein HRS3scFv-Fc. As expected, co-incubation of PBMCs with IL-2 or IL-12 also increased proliferation. The extent of proliferation induced by 4pmol immunocytokine in solution or

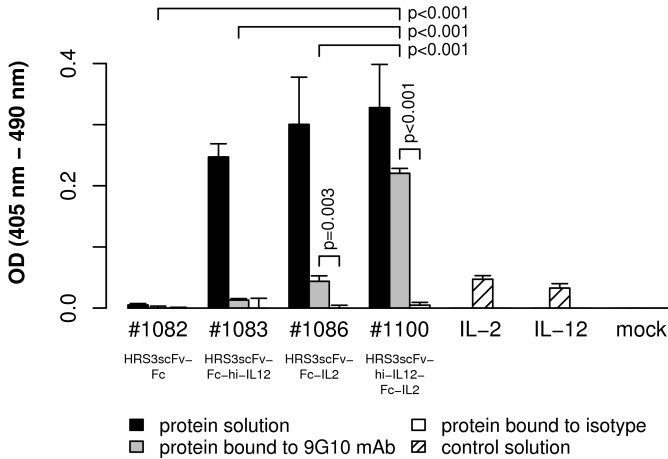


Figure 4.18: Immunocytokines induce proliferation in PBMCs. ELISA plates were coated with the anti-idiotypic antibody 9G10 or an isotype-matched control antibody and incubated for 60 min with purified immunocytokine or the fusion protein HRS3scFv-Fc (4 pmol each). Wells were either washed to remove unbound fusion protein (**grey and white bars**) or not washed (**black bars**). Pre-activated human PBMCs (2.5×10^4 cells) that had been cultured in absence of IL-2 for 24 hours were added to each well and incubated for 96 hours. As controls, PBMCs were incubated with human IL-2 (50 IU), murine IL-12 (100 fmol) or with medium alone (**shaded bars**). Proliferation of PBMCs was quantified by incorporation of BrdU and subsequent ELISA. Data represent the mean of three samples; T-bars indicate standard deviation. Significance of differences in proliferation was determined by an unpaired two-sided Welch-corrected t-test.

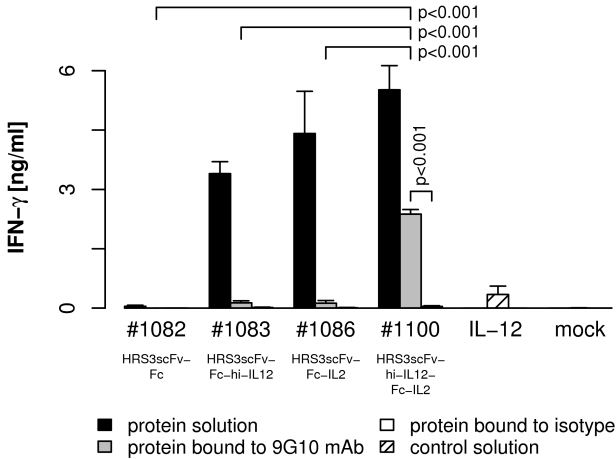


Figure 4.19: Immunocytokines induce IFN- γ secretion in PBMCs. ELISA plates were coated with the anti-idiotypic antibody 9G10 or an isotype-matched control antibody and incubated for 60 min with purified immunocytokine or the fusion protein HRS3scFv-Fc (4 pmol each). Wells were either washed to remove unbound fusion protein (**grey and white bars**) or not washed (**black bars**). Pre-activated human PBMCs (2.5×10^4 cells) that had been cultured in absence of IL-2 for 24 hours were added to each well and incubated for 96 hours. As controls, PBMCs were incubated with murine IL-12 (100 fmol) or with medium alone (**shaded bars**). IFN- γ concentrations in supernatants were determined by ELISA. Data represent the mean of three samples; T-bars indicate standard deviation. Significance of differences in IFN- γ secretion was determined by an unpaired two-sided Welch-corrected t-test.

4 pmol bound immunocytokine HRS3scFv-hi-IL12-Fc-IL2 was 5- to 7-fold that of 50 IU (200 fmol) IL-2 and 7- to 10-fold that of 100 fmol IL-12, indicating 3- to 6-fold less cytokine activity of the immunocytokines compared to the respective recombinant cytokine.

Anti-CD30 immunocytokines in solution induced IFN- γ secretion in PBMCs, whereas the fusion protein HRS3scFv-Fc without cytokine domain did not. The immunocytokine HRS3scFv-hi-IL12-Fc-IL2 with combined IL-2 and IL-12 domains significantly increased secretion of IFN- γ when bound to immobilised anti-idiotypic antibody 9G10 compared to immobilised isotype-matched control antibody. After binding to the antibody 9G10, the immunocytokine HRS3scFv-hi-IL12-Fc-IL2 furthermore resulted in significantly increased IFN- γ secretion compared to immunocytokines with a single cytokine domain or the fusion protein HRS3scFv-Fc. As expected, co-incubation of PBMCs with IL-12 also increased IFN- γ secretion. The amount of IFN- γ secretion induced by 4 pmol immunocytokine in solution or bound immunocytokine HRS3scFv-hi-IL12-Fc-IL2 was 7- to 16-fold that of 100 fmol IL-12, indicating 3- to 6-fold less cytokine activity of the immunocytokines compared to recombinant IL-12.

Purified immunocytokines were active in solution and after binding to surfaces via the HRS3 scFv domain. After binding to the anti-idiotypic antibody 9G10, the immunocytokine HRS3scFv-hi-IL12-Fc-IL2 with combined IL-2 and IL-12 domains resulted in significantly increased proliferation and IFN- γ secretion of PBMCs compared to immunocytokines with a single cytokine domain.

4.3.2 The IL-12 domain of immunocytokines induces phosphorylation of STAT4 in T cells

Signal transducer and activator of transcription-4 (STAT4) is phosphorylated in lymphocytes *in vitro* after stimulation with IL-12, IL-23 or IFN- α (Kaplan, 2005). We determined whether the murine single-chain IL-12 domain of anti-CD30 immunocytokines leads to phosphorylation of STAT4 in human T cells.

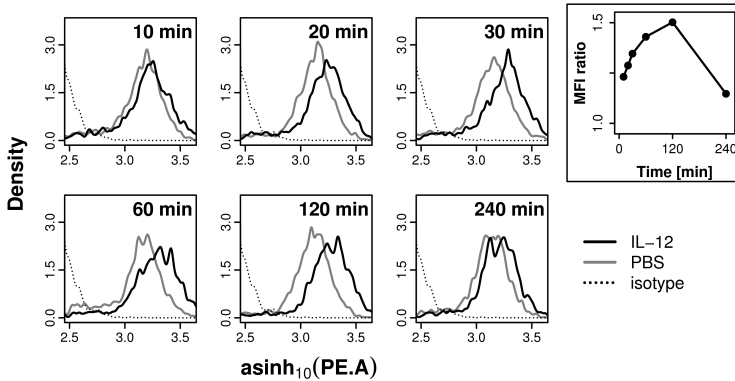


Figure 4.20: Murine IL-12 induces phosphorylation of STAT4 in human T cells. Pre-activated human T cells (5×10^5 cells) that had been cultured in absence of IL-2 for 24 hours were suspended in PBS containing 2% (v/v) FCS. Murine IL-12 (0.2 pmol; **black lines**) or PBS as control (**grey lines**) were added and the reaction tubes were incubated at 37°C. After 10, 20, 30, 60, 120 and 240 min, cells were fixed, permeabilised, stained with either the anti-pSTAT4-PE antibody or an isotype-matched PE-conjugated control antibody (**dotted lines**) and analysed by flow-cytometry. **Inset:** data represent the ratio of mean fluorescence intensity (**MFI ratio**) between incubation with and without murine IL-12 in relation to incubation time.

To determine the incubation time required for phosphorylation of STAT4 by stimulation with murine IL-12, pre-activated human T cells that had been cultured in absence of IL-2 for 24 hours were incubated for different lengths of time with murine IL-12 or PBS as control. T cells were fixed, permeabilised, stained with either the anti-pSTAT4-PE antibody or an isotype-matched PE-conjugated control antibody and analysed by flow-cytometry (figure 4.20). Phosphorylation of STAT4 was detected after 10 min of incubation and increased with incubation time. After reaching a maximum at approximately 120 min, the amount of phosphorylated STAT4 decreased to starting levels (240 min).

We repeated the experiment to determine whether the murine single-chain IL-12 domain of immunocytokines leads to phosphorylation of STAT4.

T cells were incubated for 30 min with purified immunocytokine. The fusion protein HRS3scFv-Fc, murine IL-12 or PBS served as controls (figure 4.21).

The immunocytokine HRS3scFv-Fc-hi-IL12 with IL-12 cytokine domain yielded similar phosphorylation of STAT4 compared to recombinant IL-12, while the immunocytokine HRS3scFv-hi-IL12-Fc-IL2 with combined IL-2 and IL-12 domains led to 1.2-fold higher phosphorylation of STAT4. The immunocytokine HRS3scFv-Fc-IL2 also showed a shift, as did – unexpectedly – the fusion protein HRS3scFv-Fc without cytokine domain. However, STAT4 phosphorylation induced by the fusion protein HRS3scFv-Fc was 4-fold lower compared to the immunocytokine HRS3scFv-hi-IL12-Fc-IL2 or recombinant IL-12.

Purified immunocytokines containing an IL-12 domain induced phosphorylation of STAT4 in human T cells.

4.3.3 Immunocytokines induce NK cells to lyse tumour cells

The cytokines IL-2 and IL-12 enhance cytolysis by NK cells (Thèze, 1999). Furthermore, the Fc γ ₁ domain of immunocytokines can trigger antibody-dependent cellular cytotoxicity (ADCC) by binding to Fc γ receptors on NK cells (Davis and Gillies, 2003). Therefore, we determined the impact of anti-CD30 fusion proteins on the cytolysis of tumour cells by NK cells.

CD30⁺ CEA⁻ MC38 cells stably transfected with pcDNA3.1 CD30 (#841) plasmid DNA or CEA⁺ CD30⁻ C15A3 cells as control (figure 4.22) were incubated with purified immunocytokine or the fusion protein HRS3scFv-Fc. After washing the tumour cells, human NK cells were added and incubated for 24 hours. As control, tumour cells were incubated with NK cells in presence of human IL-2. Viability of NK cells and tumour cells was quantified by colour change of XTT reagent, and cytolysis was calculated (figure 4.23).

Within 24 hours, NK cells lysed CD30⁺ tumour cells coated with anti-CD30

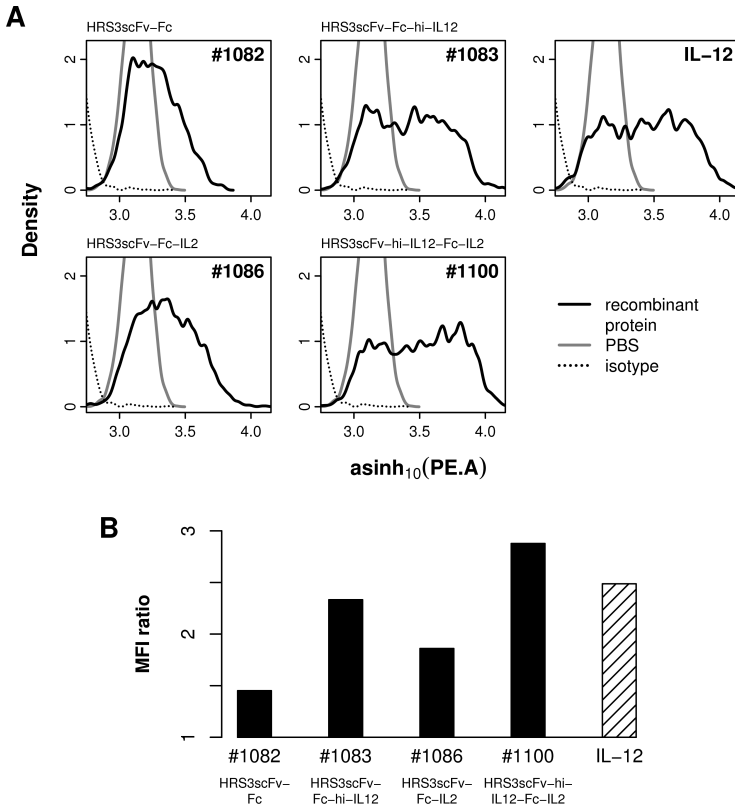


Figure 4.21: The IL-12 domain of immunocytokines induces phosphorylation of STAT4 in T cells. Pre-activated human T cells (2×10^5 cells) that had been cultured in absence of IL-2 for 24 hours were suspended in PBS containing 2% (v/v) FCS. Purified immunocytokine, the fusion protein HRS3scFv-Fc or murine IL-12 as control (0.2 pmol each; **black lines**) were added and the reaction tubes were incubated at 37°C. Purified immunocytokines had been dissolved in PBS containing 3% (v/v) normal mouse serum for storage, therefore this solvent was used as control (**grey lines**). After 30 min, cells were fixed, permeabilised, stained with either the anti-pSTAT4-PE antibody or an isotype-matched PE-conjugated control antibody (**dotted lines**) and analysed by flow-cytometry (A). The ratio of mean fluorescence intensity (**MFI ratio**) between incubation with and without protein was calculated. Each bar corresponds to one sample (B).

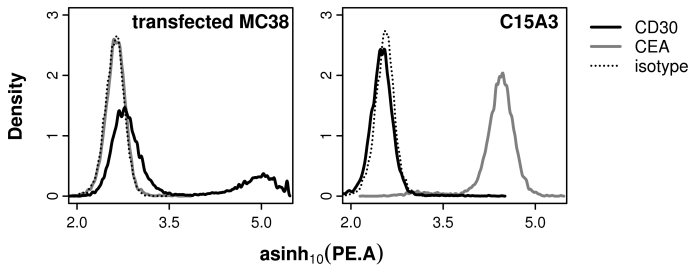


Figure 4.22: Characterisation of modified MC38 and C15A3 cells. CD30⁺ CEA⁻ MC38 cells stably transfected with pcDNA3.1 CD30 (#841) plasmid DNA (2×10^5 cells) or CEA⁺ CD30⁻ C15A3 cells (2×10^5 cells) were stained with either the anti-CD30-PE antibody (**black lines**) or an isotype-matched PE-conjugated control antibody (**dotted lines**). Alternatively, cells were incubated with the anti-CEA antibody HB-8747 (1 μ g) and stained with the anti-m-IgG₁-PE antibody (**grey lines**). Finally, cells were analysed by flow-cytometry.

fusion proteins with an efficiency of 15% to 50%. The effector-to-target cell ratio was 4 : 5. Cytolysis of CD30⁺ tumour cells that were coated with immunocytokines containing an IL-12 domain or the fusion protein HRS3-scFv-Fc was significantly higher than lysis of CD30⁻ tumour cells. Moreover, the immunocytokine HRS3scFv-hi-IL12-Fc-IL2 with combined IL-2 and IL-12 domains significantly increased cytolysis of CD30⁺ tumour cells compared to the fusion protein HRS3scFv-Fc. As expected, co-incubation of NK cells with human IL-2 induced cytolysis of CD30⁺ and CD30⁻ tumour cells, whereas incubation of NK cells without added cytokines did not. In absence of NK cells, anti-CD30 fusion proteins did not induce cytolysis of tumour cells.

In summary, NK cells were induced to specifically lyse CD30⁺ tumour cells coated with anti-CD30 fusion proteins. The immunocytokine HRS3-scFv-hi-IL12-Fc-IL2 with combined IL-2 and IL-12 domains resulted in increased cytolysis of CD30⁺ tumour cells compared to the fusion protein HRS3scFv-Fc without cytokine domain. We conclude that the Fc γ ₁ and cytokine domains of anti-CD30 fusion proteins activate NK cells for the specific lysis of CD30⁺ tumour cells.

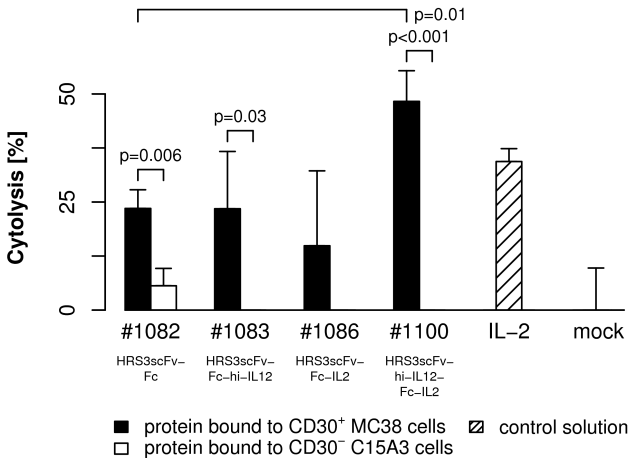


Figure 4.23: Immunocytokines induce NK cells to lyse tumour cells. CD30⁺ CEA⁻ MC38 cells stably transfected with pcDNA3.1 CD30 (#841) plasmid DNA (5×10^4 cells; **black bars**) or CEA⁺ CD30⁻ C15A3 cells as control (5×10^4 cells; **white bars**) were incubated for 60 min with purified immunocytokine or the fusion protein HRS3scFv-Fc (5 ng each). Cells were washed and plated in round-bottom microtitre plates. Human NK cells (4×10^4 cells) were added and plates were incubated at 37°C for 24 hours. As controls, tumour cells were incubated with NK cells either in presence of human IL-2 (100 IU) or with medium alone (**shaded bars**). Viability of NK cells and tumour cells was quantified by colour change of XTT reagent, and cytolysis was calculated. Data represent the mean of three samples; T-bars indicate standard deviation. Significance of differences in cytolysis was determined by an unpaired two-sided Welch-corrected t-test.

4.4 Immunocytokines accumulate at the tumour site

Immunocytokines were designed to target cytokines to specific sites within the body in order to increase local accumulation and decrease administered doses, thereby limiting the severe side effects associated with systemic application of cytokines. We therefore investigated the biodistribution of two anti-CD30 immunocytokines and determined the biological half-life of these proteins.

4.4.1 Immunocytokines retain specificity of binding after radiolabelling

Labelling with Na¹³¹I and chloramine-T leads to modified histidine and tyrosine residues, whereas Bolton-Hunter reagent is coupled to both N-terminus and lysine residues (Coligan, 2005). The N-terminal HRS3 scFv domain of anti-CD30 immunocytokines contains three histidine residues, eleven lysine residues and nineteen tyrosine residues. We therefore assessed binding specificity of immunocytokines after radiolabelling.

Purified immunocytokine HRS3scFv-hi-IL12 or HRS3scFv-Fc-hi-IL12 was radiolabelled with Na¹³¹I and chloramine-T to specific activities ranging from 23 MBq/nmol to 46 MBq/nmol and desalted (figure 4.24). To remove immunocytokine that had lost binding affinity for CD30, labelled immunocytokine was affinity-purified using the anti-idiotypic antibody 9G10 coupled to a HiTrap™ HP column (figure 4.25). Finally, binding of radiolabelled protein to either the anti-idiotypic antibody 9G10 or an isotype-matched control antibody was determined by RIA (figure 4.26).

Immunocytokines that had been radiolabelled with Na¹³¹I and chloramine-T bound to the anti-idiotypic antibody 9G10 in a dose-dependant manner. Maximum binding to the anti-idiotypic antibody 9G10 was 14-fold higher compared to the isotype-matched control antibody. Furthermore, the elution profile during affinity purification of

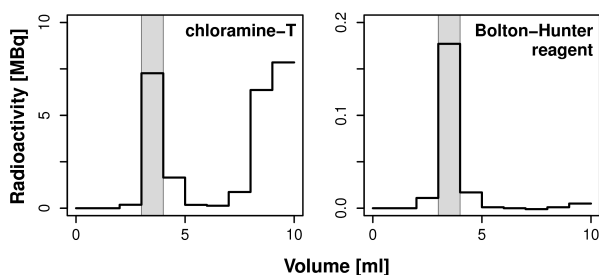


Figure 4.24: Desalting of radiolabelled immunocytokines. Purified immunocytokine HRS3scFv-Fc-hi-IL12 (400 pmol) was radiolabelled with Na^{131}I (31 MBq) and chloramine-T (6 nmol) to a specific activity of 23 MBq/nmol (**chloramine-T**). Alternatively, purified immunocytokine HRS3scFv-Fc-hi-IL12 (400 pmol) was coupled to Bolton-Hunter reagent (300 pmol), yielding a specific activity of 0.5 MBq/nmol (**Bolton-Hunter reagent**). Labelled immunocytokine was desalted using a PD-10TM column to remove chemical reagents and unbound radioactivity. Effluent was collected in 1-ml fractions and radioactivity of each fraction was counted. Finally, fraction #4 of the desalted immunocytokine (**grey sections**) was used for biodistribution experiments.

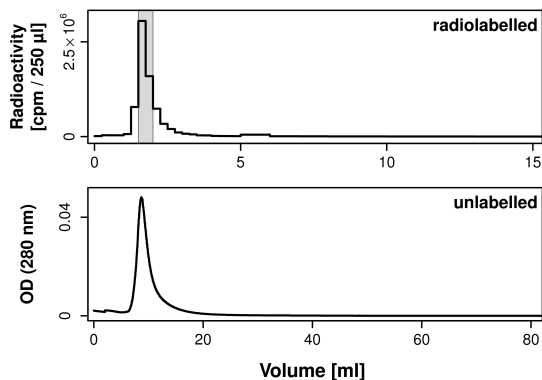


Figure 4.25: Purification of radiolabelled immunocytokine HRS3scFv-hi-IL12.

Purified immunocytokine HRS3scFv-hi-IL12 (1.7 nmol) was radiolabelled with Na^{131}I (17 MBq) and chloramine-T (2.7 nmol) to a specific activity of 0.5 MBq/nmol. After desalting, the immunocytokine was affinity-purified using the anti-idiotypic antibody 9G10 coupled to a HiTrapTM HP column (column volume: 1 ml). The column was washed with PBS until effluent was free from radioactivity. Bound immunocytokine was eluted with 0.1 M glycine buffer (pH 3.0) in steps of 250 µl (first 5 ml) or 1 ml and radioactivity of each fraction was counted. pH of the first twenty fractions was raised by adding 1 M NaHCO_3 (12.5 µl). Finally, fractions #7 and #8 of each batch (**grey section**) were pooled and used for biodistribution experiments (**radiolabelled**). As reference, a characteristic purification of unlabelled immunocytokine HRS3scFv-hi-IL12 from cell culture supernatants (1.5 l) using the anti-idiotypic antibody 9G10 coupled to a HiTrapTM HP column (column volume: 1 ml) and 0.1 M glycine buffer (pH 3.0) is shown. Absorbance of effluent (280 nm) was monitored continuously (**unlabelled**).

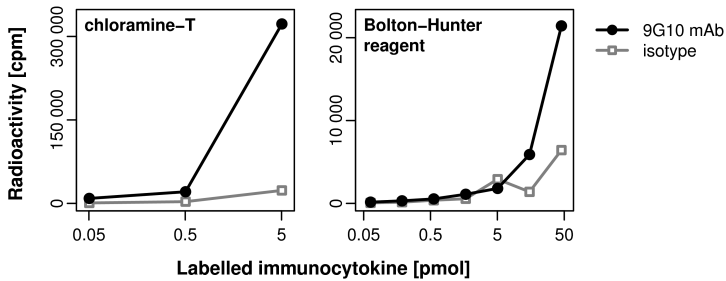


Figure 4.26: Radiolabelled immunocytokines specifically bind to the anti-idiotypic antibody 9G10. Purified immunocytokine HRS3scFv-hi-IL12 (180 pmol) was radiolabelled with Na^{131}I (33 MBq) and chloramine-T (3.6 nmol) to a specific activity of 46 MBq/nmol, desalted and affinity-purified. PolySorp™ tubes were coated with either the anti-idiotypic antibody 9G10 or an isotype-matched control antibody and incubated with serial dilutions of radiolabelled immunocytokine. After washing with PBS, radioactivity in each tube was counted (**chloramine-T**). Alternatively, purified immunocytokine HRS3scFv-Fc-hi-IL12 (400 pmol) was coupled to Bolton-Hunter reagent (95 pmol) and desalted (specific activity: 1.7 MBq/nmol). PolySorp™ LockWell™ strips were coated with either the anti-idiotypic antibody 9G10 or an isotype-matched control antibody and incubated with serial dilutions of radiolabelled immunocytokine. After washing with PBS, radioactivity in each well was counted (**Bolton-Hunter reagent**). Each data point represents one sample.

radiolabelled immunocytokine corresponded to that of unlabelled immunocytokine.

Alternatively, we labelled immunocytokine using the Bolton-Hunter method in order to avoid the harsh conditions of labelling with chloramine-T, thus obviating subsequent affinity purification. Purified immunocytokine HRS3scFv-hi-IL12 or HRS3scFv-Fc-hi-IL12 was radiolabelled to specific activities ranging from 0.7 MBq/nmol to 1.7 MBq/nmol by coupling to Bolton-Hunter reagent. Labelled immunocytokine was desalted (figure 4.24) and binding of radiolabelled protein to either the anti-idiotypic antibody 9G10 or an isotype-matched control antibody was determined by RIA (figure 4.26).

Immunocytokines that had been radiolabelled using the Bolton-Hunter method bound to the anti-idiotypic antibody 9G10 in a dose-dependant manner. Maximum binding to the anti-idiotypic antibody 9G10 was 3.5-fold higher compared to the isotype-matched control antibody.

Purified anti-CD30 immunocytokines radiolabelled either with Na¹³¹I and chloramine-T or by coupling to Bolton-Hunter reagent specifically bound to the anti-idiotypic antibody 9G10.

4.4.2 Immunocytokines accumulate at the tumour site

To determine accumulation at the tumour site, immunocytokines were radiolabelled and their biodistribution was analysed after systemic application in SCID mice which harboured tumours of CD30⁺ L540Cy cells (figure 4.27). The influence of an Fc γ ₁ domain on the biodistribution of immunocytokines was assessed by comparing immunocytokines with and without an Fc γ ₁ domain.

Tumour cells and immunocytokine were injected by Jan-Philipp Hering, who also dissected mice and counted the radioactivity of organs. Biodistribution of the immunocytokine HRS3scFv-Fc-hi-IL12 was determined by

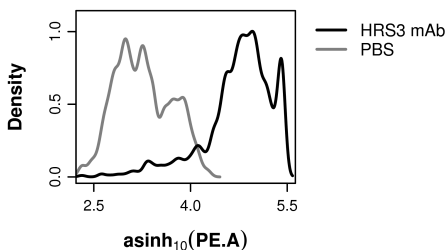


Figure 4.27: L540Cy cells express CD30. L540Cy cells (1×10^5 cells) were incubated with the anti-CD30 antibody HRS3 (400 ng; **black line**) or PBS as control (**grey line**), stained with the anti-m-IgG₁-PE antibody and analysed by flow-cytometry.

PD Dr. Stefan Guhlke and Jan-Philipp Hering, according to my detailed instructions.

Two batches of purified immunocytokine HRS3scFv-hi-IL12 without Fc γ ₁ domain were radiolabelled with Na¹³¹I and chloramine-T. Labelled immunocytokine was desalted (figure 4.24) and affinity-purified using the anti-idiotypic antibody 9G10 coupled to a HiTrapTM HP column in order to remove immunocytokine that had lost binding affinity for CD30 (figure 4.25). Groups of mice ($n = 6$) bearing tumours of CD30⁺ L540Cy cells received *i.v.* injections of 90 pmol (specific activity: 0.5 MBq/nmol) or 11 pmol (specific activity: 3.7 MBq/nmol) radiolabelled immunocytokine. Two mice from each group were sacrificed after 24, 48 or 72 hours. Organs were recovered, weighed and radioactivity was counted. Detected counts were compensated for radioactive decay, and injected dose per gram of tissue (% ID/g) was calculated (figure 4.28).

Tissue retention was calculated as % ID/g (72h) divided by % ID/g (24h). Highest tissue retentions of the immunocytokine HRS3scFv-hi-IL12 were found in small intestine (39%), blood (37%), tumour (35%) and liver (33%). After 21 hours, mice had excreted 32% of total injected radioactivity, as detected in combined litter from all groups.

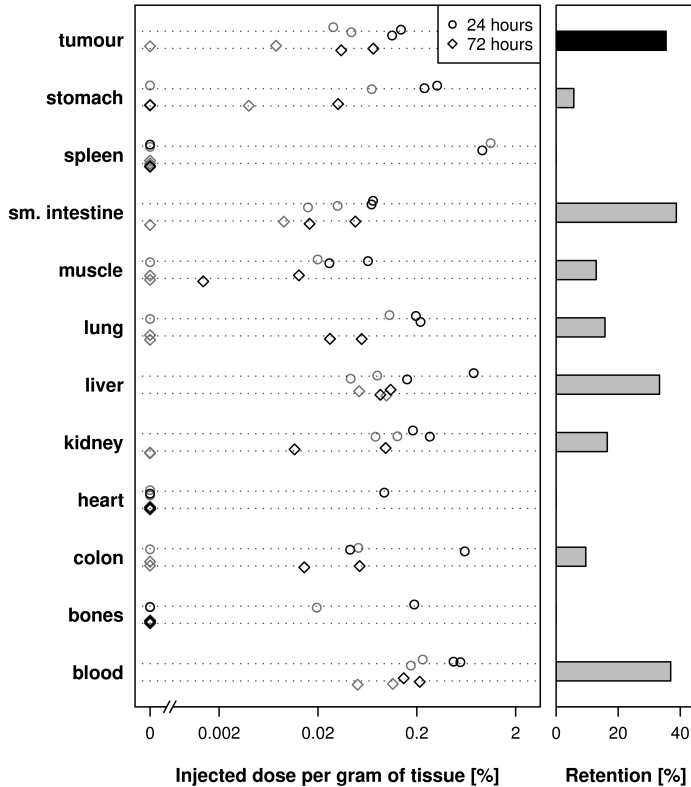


Figure 4.28: Immunocytokine HRS3scFv-hi-IL12 accumulates at the tumour site. Twelve female SCID mice received *s.c.* injections of CD30⁺ L540Cy cells (3×10^7 cells) in the flank. After three weeks, two batches of purified immunocytokine HRS3scFv-hi-IL12 (1.7 nmol / 300 pmol) were labelled with Na¹³¹I (17 MBq / 6 MBq) and chloramine-T (2.7 nmol / 1.4 nmol), desalted and affinity-purified. Groups of mice ($n = 6$) received *i.v.* injections of 90 pmol (0.5 MBq/nmol; **black points**) or 11 pmol immunocytokine (3.7 MBq/nmol; **grey points**). Two mice from each group were sacrificed after 24, 48 or 72 hours. Organs were recovered, weighed and radioactivity was counted. Counts were compensated for radioactive decay, and injected dose per gram of tissue (% ID/g) was calculated. Mean tissue retention was calculated as % ID/g (72 h) divided by % ID/g (24 h).

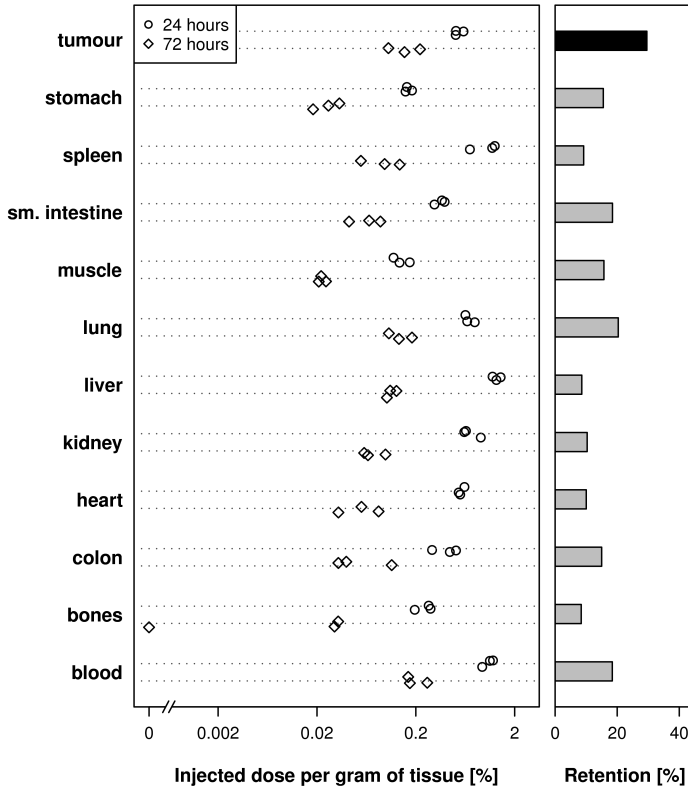


Figure 4.29: Immunocytokine HRS3scFv-Fc-hi-IL12 accumulates at the tumour site. Twelve female SCID mice received s.c. injections of CD30⁺ L540Cy cells (3×10^7 cells) in the flank. After five weeks, purified immunocytokine HRS3scFv-Fc-hi-IL12 (1.2nmol) was coupled to Bolton-Hunter reagent (630pmol) and desalted. Mice received *i.v.* injections of immunocytokine (45 pmol, 1.3 MBq/nmol). Groups of mice ($n = 3$) were sacrificed after 12, 24, 48 or 72 hours. Organs were recovered, weighed and radioactivity was counted. Counts were compensated for radioactive decay, and injected dose per gram of tissue (% ID/g) was calculated. Mean tissue retention was calculated as % ID/g (72 h) divided by % ID/g (24 h).

Alternatively, purified immunocytokine HRS3scFv-Fc-hi-IL12 with Fc γ ₁ domain was coupled to Bolton-Hunter reagent and desalted (figure 4.24). Mice bearing tumours of CD30⁺ L540Cy cells received *i.v.* injections of 45 pmol radiolabelled immunocytokine (specific activity: 1.3 MBq/nmol). Groups of three animals were sacrificed after 12, 24, 48 or 72 hours. Organs were recovered, weighed and radioactivity was counted. Detected counts were compensated for radioactive decay, and injected dose per gram of tissue (% ID/g) was calculated (figure 4.29).

Tissue retention was calculated as % ID/g (72h) divided by % ID/g (24h). Highest tissue retentions of the immunocytokine HRS3scFv-Fc-hi-IL12 were found in tumour (30%), the lungs (20%), small intestine (18%) and blood (18%).

The influence of the Fc γ ₁ domain on biodistribution was assessed by comparing mean tissue retentions of the immunocytokines HRS3scFv-hi-IL12 and HRS3scFv-Fc-hi-IL12. These immunocytokines are identical except for lacking or containing an Fc γ ₁ domain. Mean tissue retentions of both immunocytokines were similar for tumour, muscle and lungs. Tissue retentions of the immunocytokine HRS3scFv-hi-IL12 without Fc γ ₁ domain were 1.6- to 4-fold higher for kidneys, blood, small intestine and liver compared to the immunocytokine HRS3scFv-Fc-hi-IL12 with Fc γ ₁ domain, whereas tissue retentions of colon and stomach were 1.6- to 2.5-fold lower. After 72 hours, radiolabelled immunocytokine HRS3scFv-hi-IL12 without Fc γ ₁ domain was completely cleared from heart, spleen and bones in all animals and from muscle, colon, stomach, kidney and the lungs in at least two animals. In contrast, the immunocytokine HRS3scFv-Fc-hi-IL12 with Fc γ ₁ domain was only cleared from the bones of one animal in this interval. Furthermore, the lowest mean tissue retention of the immunocytokine HRS3scFv-Fc-hi-IL12 with Fc γ ₁ domain amounted to 8.5%.

4.4.3 Biological half-life of immunocytokines

We estimated biological half-life of immunocytokines in blood by linear regression from % ID/g values that were determined in biodistribution

experiments (section 4.4.2), using equations for an *i.v.* bolus in a one-compartment pharmacokinetic model: $\ln(c_t) = \ln(c_0) - k * t$ and $t_{1/2} = \frac{\ln(2)}{k}$ (figure 4.30). These equations are also valid for a two-compartment pharmacokinetic model when drug distribution between central and peripheral compartment has reached equilibrium (β -phase; Schoenwald, 2001).

Biological half-life of radiolabelled immunocytokine HRS3scFv-hi-IL12 was determined as 32 hours (dose: 90pmol; $R^2 = 0.90$, $p = 0.004$) and 34 hours (dose: 11 pmol; $R^2 = 0.51$, not significant), whereas half-life of radiolabelled immunocytokine HRS3scFv-Fc-hi-IL12 amounted to 20 hours ($R^2 = 0.92$, $p < 0.001$). However, when only taking the last 24 hours into account where the β -phase had most likely been reached, half-life of the immunocytokine HRS3scFv-Fc-hi-IL12 was determined as 34 hours ($R^2 = 0.71$, $p = 0.03$).

4.5 Immunocytokine HRS3scFv-hi-IL12-Fc-IL2 inhibits tumour growth in immunocompetent mice

The immunocytokines used in this study were designed to inhibit tumour growth *in vivo*. After finding that hybridoma cells which produce the anti-idiotypic antibody 9G10 grew tumours in immunocompetent Balb/c mice, we determined the influence of the immunocytokine HRS3scFv-hi-IL12-Fc-IL2 with combined IL-2 and IL-12 domains on tumour growth of these cells. Subsequently, mouse sera were tested for the presence of immunocytokine and for antibodies directed against the immunocytokine backbone HRS3scFv-Fc. Finally, we estimated biological half-life of the immunocytokine.

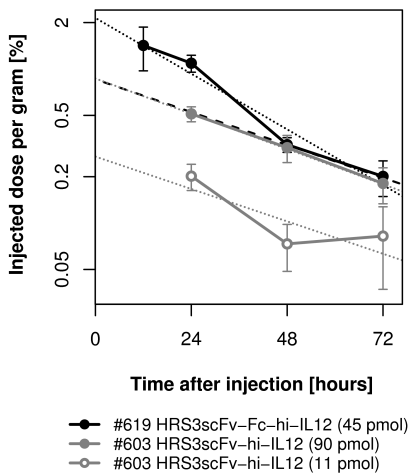


Figure 4.30: Biological half-life of immunocytokines. Two batches of purified immunocytokine HRS3scFv-hi-IL12 (1.7 nmol / 300 pmol) were labelled with Na^{131}I (17 MBq / 6 MBq) and chloramine-T (2.7 nmol / 1.4 nmol), desalted and affinity-purified. Groups of female SCID mice ($n = 6$) bearing *s.c.* tumours of CD30⁺ L540Cy cells received *i.v.* injections of 90 pmol (0.5 MBq/nmol) or 11 pmol immunocytokine (3.7 MBq/nmol). Two mice from each group were sacrificed after 24, 48 or 72 hours (**grey lines**). Alternatively, purified immunocytokine HRS3scFv-Fc-hi-IL12 (1.2 nmol) was coupled to Bolton-Hunter reagent (630 pmol) and desalted. Twelve female SCID mice bearing *s.c.* tumours of CD30⁺ L540Cy cells received *i.v.* injections of immunocytokine (45 pmol, 1.3 MBq/nmol). Groups of mice ($n = 3$) were sacrificed after 12, 24, 48 or 72 hours (**black line**). Blood was recovered, weighed and radioactivity was counted. Counts were compensated for radioactive decay, and injected dose per gram of tissue (% ID/g) was calculated. Data represent the mean of two (HRS3scFv-hi-IL12) or three samples (HRS3scFv-Fc-hi-IL12) \pm standard deviation. **Dotted lines:** linear regression over all points in time. **Dashed line:** linear regression over the last 24 hours.

4.5.1 Immunocytokine HRS3scFv-hi-IL12-Fc-IL2 inhibits tumour growth

To determine the tolerated dose of anti-CD30 immunocytokines in tumour-bearing immunocompetent mice, these animals received escalating doses of the immunocytokine HRS3scFv-hi-IL12-Fc-IL2 with combined IL-2 and IL-12 domains.

Ten female Balb/c mice received *s.c.* injections of 9G10 hybridoma cells (figure 4.16) in the flank. Six animals developed tumours. When tumours were clearly visible after two weeks, mice received escalating doses of purified immunocytokine HRS3scFv-hi-IL12-Fc-IL2 (40 pmol to 500 pmol) three times intravenously at 48-hour intervals. To estimate half-life of the immunocytokine and detect antibodies raised against the immunocytokine, sera were sampled before each injection and, subsequently, additional serum samples were taken. Tumour growth was monitored and mice were sacrificed a week after the last injection or when tumours became necrotic. Mice were grouped by total amount of immunocytokine (figure 4.31). As control, six female Balb/c mice received *s.c.* injections of 9G10 hybridoma cells in the flank, but no subsequent injections of immunocytokine. Five animals developed tumours. Tumour growth was monitored and mice were sacrificed when tumour volumes reached 600 mm³. For statistical analysis, tumour volumes were normalised to the day of first injection of immunocytokine or, for control mice, to the day when visible tumours started to grow (figure 4.32).

Mice tolerated cumulated doses of up to 1 nmol immunocytokine HRS3scFv-hi-IL12-Fc-IL2, the highest single dose being 500 pmol. Observed adverse events were enduring inflammations of the ears in three animals, starting on day 2 to 4 after first injection of immunocytokine. As two animals of the control group displayed the same symptoms, however, we do not consider this a side effect of immunocytokine administration. At days 3 and 7 after first injection of immunocytokine, relative tumour growth was significantly lower in animals that received cumulated doses of 300 pmol immunocytokine and above, compared to animals that received lower doses and control mice. In contrast, tumours of animals which received

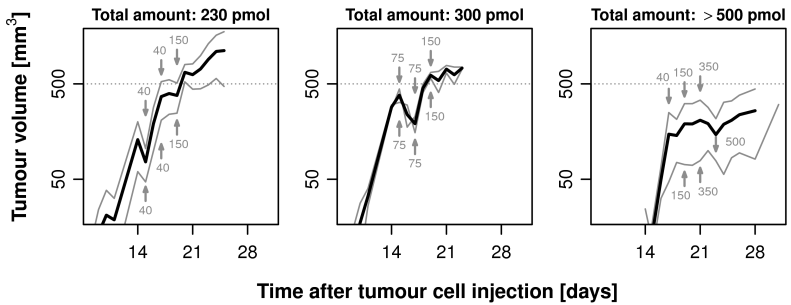


Figure 4.31: Dose escalation of immunocytokine HRS3scFv-hi-IL12-Fc-IL2 in mice. Ten female Balb/c mice received *s.c.* injections of 9G10 hybridoma cells (clone II-G05; 1×10^6 cells) in the flank; six animals developed tumours. When tumours were clearly visible after two weeks, mice received escalating doses of purified immunocytokine HRS3scFv-hi-IL12-Fc-IL2 (40 pmol to 500 pmol) three times intravenously at 48-hour intervals. Sera were sampled before each injection and, subsequently, additional serum samples were taken. Tumour growth was monitored and mice were sacrificed a week after the last injection or when tumours became necrotic. Mice were grouped by total amount of immunocytokine (**230 pmol**, **300 pmol** and **> 500 pmol**; $n = 2$). Each line represents tumour growth in one mouse (**grey lines**) or mean tumour growth for each group (**black lines**). Arrows indicate days of injection; numbers indicate immunocytokine doses in pmol.

less than 300 pmol immunocytokine and tumours of control mice grew at the same rate. Seven days after the first injection of immunocytokine, the tumour volume of animals that received cumulated doses of 300 pmol immunocytokine and above had increased by 1.5-fold compared to a 9.5-fold increase in animals that received lower doses.

Immunocompetent Balb/c mice tolerated single doses of up to 500 pmol and cumulated doses of up to 1 nmol of the immunocytokine HRS3scFv-hi-IL12-Fc-IL2. Tumour growth was inhibited in animals that received cumulated doses of 300 pmol immunocytokine and above. Side effects related to immunocytokine administration were not observed.

4.5.2 Immunocytokine HRS3scFv-hi-IL12-Fc-IL2 accumulates in serum

To determine whether immunocytokine accumulated in the peripheral circulation of mice, sera from two mice that received the immunocytokine HRS3scFv-hi-IL12-Fc-IL2 and one mouse that did not receive immunocytokine as control were analysed by ELISA for presence of the immunocytokine's human Fc γ_1 domain (figure 4.33).

Serum concentrations of immunocytokine increased starting from the day of the first immunocytokine injection, reached its maximum two days after the last injection and decreased again. In contrast, no immunocytokine was detected in sera of the control animal. Biological half-life of the immunocytokine HRS3scFv-hi-IL12-Fc-IL2 was estimated by approximation of calculated to detected serum concentrations, using the equations for an *i.v.* bolus in a one-compartment model: $\ln(c_t) = \ln(c_0) - k * t$ and $t_{1/2} = \frac{\ln(2)}{k}$. As detected serum concentrations of immunocytokine were 13-fold lower than theoretical concentrations, we divided administered doses by 13 prior to calculation. Biological half-life of the immunocytokine HRS3scFv-hi-IL12-Fc-IL2 was estimated to 41 hours for animal #6 and to 32 hours for animal #8.

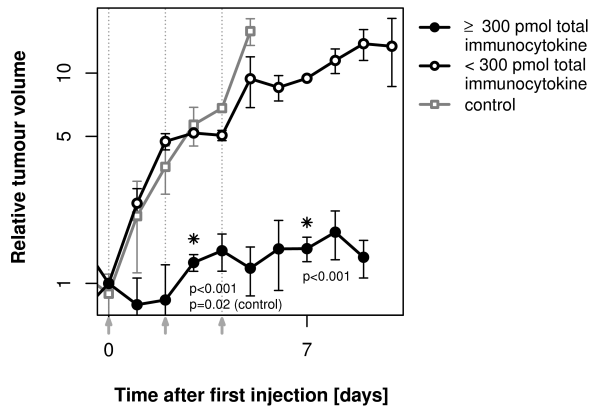


Figure 4.32: Immunocytokine HRS3scFv-hi-IL12-Fc-IL2 inhibits tumour growth in mice. Ten female Balb/c mice received *s.c.* injections of 9G10 hybridoma cells (clone II-G05; 1×10^6 cells) in the flank; six animals developed tumours. When tumours were clearly visible after two weeks, mice received escalating doses of purified immunocytokine HRS3scFv-hi-IL12-Fc-IL2 (40 pmol to 500 pmol) three times intravenously at 48-hour intervals. Tumour growth was monitored and mice were sacrificed a week after the last injection or when tumours became necrotic. Mice were grouped by total amount of immunocytokine (≥ 300 pmol ($n = 4$) and < 300 pmol ($n = 2$); **black lines**). As control, six female Balb/c mice received *s.c.* injections of 9G10 hybridoma cells (5×10^6 cells) in the flank, but no subsequent injections of immunocytokine. Five animals developed tumours. Tumour growth was monitored and mice were sacrificed when tumour volumes reached 600 mm^3 ($n = 5$; **grey line**). Time is given as days since first injection of immunocytokine or, for control mice, since start of tumour growth. Tumour volume at day 0 was set to 1. Arrows indicate days of injection. Data represent mean relative tumour volume \pm standard deviation. Significance of differences in relative tumour volume was determined at days 3 and 7 by an unpaired two-sided Welch-corrected t-test. Difference between ≥ 300 pmol immunocytokine and < 300 pmol immunocytokine: $p < 0.001$ (days 3 and 7); difference between ≥ 300 pmol immunocytokine and control: $p = 0.02$ (day 3); difference between < 300 pmol immunocytokine and control: not significant (day 3).

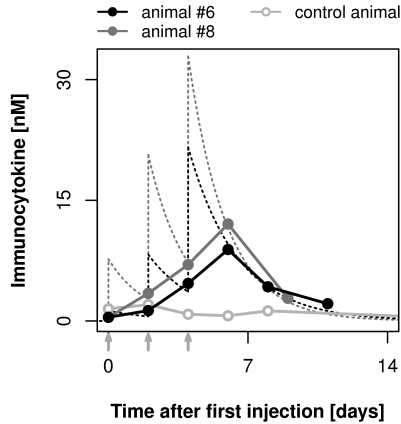


Figure 4.33: Immunocytokine HRS3scFv-hi-IL12-Fc-IL2 accumulates in serum.

Sera from two mice that received the immunocytokine HRS3scFv-hi-IL12-Fc-IL2 (> 500 pmol in three doses; figure 4.31; **filled points**) and one mouse that did not receive immunocytokine as control (**open points**) were diluted in PBS (1 : 100). ELISA plates were coated with the anti-h-IgG antibody and incubated with serial dilutions of pre-diluted sera. Bound protein was probed with the biotinylated anti-h-IgG antibody and detected by streptavidin- β -peroxidase and ABTS as substrate. Biological half-life of the immunocytokine was estimated by approximation of calculated to detected serum concentrations, using the equations for an *i.v.* bolus in a one-compartment model (**dotted black line:** animal #6, $t_{1/2} = 41$ hours, **dotted grey line:** animal #8, $t_{1/2} = 32$ hours). As detected serum concentrations of immunocytokine were 13-fold lower than theoretical concentrations, administered doses were divided by 13 prior to calculation. Each line represents serum samples from one mouse. Arrows indicate days of injection.

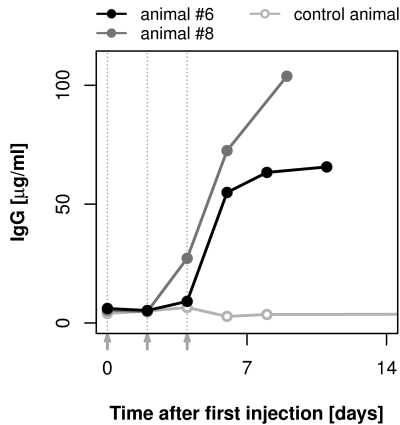


Figure 4.34: Mice raise antibodies directed against the immunocytokine HRS3-scFv-hi-IL12-Fc-IL2. Sera from two mice that received the immunocytokine HRS3-scFv-hi-IL12-Fc-IL2 (> 500 pmol in three doses; figure 4.31; **filled points**) and one mouse that did not receive immunocytokine as control (**open points**) were diluted in PBS (1 : 100). ELISA plates were coated with purified fusion protein HRS3scFv-Fc and incubated with serial dilutions of pre-diluted sera. Bound mouse antibodies were probed with the biotinylated anti-m-IgG antibody and detected by streptavidin- β -peroxidase and ABTS as substrate. Each line represents serum samples from one mouse. Arrows indicate days of injection.

4.5.3 Mice raise antibodies directed against the immunocytokine HRS3scFv-hi-IL12-Fc-IL2

To determine whether mice had raised anti-immunocytokine antibodies, sera from two mice that received the immunocytokine HRS3scFv-hi-IL12-Fc-IL2 and one mouse that did not receive immunocytokine as control were analysed by ELISA for IgG antibodies binding to the fusion protein HRS3scFv-Fc. This fusion protein forms the backbone of all anti-CD30 immunocytokines. We used an anti-IgG antibody that had been cross-adsorbed to both pooled human sera and purified human paraproteins by the manufacturer, thus allowing us to detect murine IgG antibodies in

presence of the fusion protein HRS3scFv-Fc which contains a human Fc γ ₁ domain (figure 4.34).

Serum concentrations of murine IgG antibodies directed against the immunocytokine backbone HRS3scFv-Fc increased with time, starting from day 4 after the first injection. In contrast, no IgG antibodies directed against the immunocytokine backbone were detected in sera of the control animal.

5 Discussion

Researchers have proposed to treat cancer with a combination of IL-2 and IL-12, as these cytokines activate separate pathways, reciprocally up-regulate each other's receptors and induce complimentary biological effects (Weiss *et al.*, 2007). Accordingly, our group has found that the combination of an immunocytokine with IL-2 domain and an immunocytokine with IL-12 domain enhances activation of resting NK cells and tumour cell lysis *in vitro*, compared to a single immunocytokine alone (Hombach *et al.*, 2005). As the simultaneous administration of two immunocytokines may induce problems such as competition on binding to CD30, we have generated the novel anti-CD30 immunocytokine HRS3scFv-hi-IL12-Fc-IL2. This immunocytokine has been designed for the therapy of classical Hodgkin's lymphoma, targets CD30 on the surface of the malignant Hodgkin-Reed-Sternberg cells and combines human IL-2 and single-chain murine IL-12 in one molecule.

Production of immunocytokines has turned out to be a major issue. In order to compare different immunocytokines at the same time, it has been necessary to express and purify large amounts of protein within a reasonable time frame. Therefore, we have expressed anti-CD30 fusion proteins in the SL2 cell line derived from *Drosophila melanogaster*. Moreover, we have chosen to use the FibraStage™ bioreactor for its ability to culture cells in high densities and simultaneously express up to four recombinant proteins. In this bioreactor, bottles filled with fibre disks for cell adhesion are locked in a holder and medium is pumped through the disk layer by the programmable vertical motion of a platform.

We have inserted the expression cassettes coding for anti-CD30 fusion proteins into the *Drosophila* Expression System™ DNA vector pMT/BiP V5-

His A (#1070) and stably transfected SL2 cells with the generated plasmids using the transfection reagent Fugene™ HD. This transfection reagent has been chosen for delivering high transfection efficiencies while retaining the morphology of transfected SL2 cells. In the FibraStage™ bioreactor, stably transfected SL2 clones produce 2 mg/l to 8 mg/l recombinant fusion protein within three days at an estimated cell density of 5×10^6 cells/ml. Protein expression has been constant over the observation time of four to five weeks.

Baxter *et al.* (2006) have reported that SL2 cells cultured in a bioreactor at cell densities of 1.5×10^7 cells/ml yield up to 27 mg/l recombinant soluble human IL-5 receptor- α per day and compare this with a 17 mg/l yield of the same protein produced in a shaker culture (3×10^7 cells/ml). Furthermore, SL2 cells cultured in spinner flasks at cell densities of 8×10^6 cells/ml have been reported to produce from 10 mg/l to 15 mg/l recombinant human plasminogen within three days (Nilsen and Castellino, 1999). After normalising these protein yields to one day and cell densities of 5×10^6 cells/ml, our yields of 1 mg/l to 5 mg/l immunocytokine per day compare well to the reported 4 mg/l to 18 mg/l recombinant protein per day. Such yields facilitate bulk production of immunocytokines for clinical trials, especially as the FibraStage™ system can be operated according to GMP guidelines, may easily be scaled up and needs minimal maintenance.

In our group, immunocytokines have previously been affinity purified using pre-packed columns, which is a time-consuming process taking three to four days from thawing of supernatants to freezing of the concentrated protein. Pumping supernatants through the column at low flow rates is the time-determining step of this process, taking from one to two days for 1.5l of supernatant. By incubating supernatants with antibody-coupled Sepharose™ beads in a moving roller bottle for 4 hours and packing an empty column with the centrifuged beads, we have shortened the affinity purification process to one and a half days, at the cost of losing approximately 10% of the Sepharose™ beads – including bound protein – per purification. Finally, we have completely automated the äktaPrime™ chromatograph that has been used for affinity purification, thereby minimising operator intervention and producing consistent purification results.

We have routinely obtained 0.5 mg to 2.0 mg purified immunocytokine or fusion protein from 1.5 l of supernatant, this being only a sixth of the 3 mg to 12 mg protein present in the supernatant. As we have re-used supernatants until purifications yielded no more protein, loss of protein is probably due to unspecific adsorption during clarification of crude samples and application of supernatants to either columns or Sepharose™ beads.

For stabilisation, we have supplemented purified immunocytokines and the fusion protein HRS3scFv-Fc with 3% (v/v) of either heat-inactivated FCS (*in vitro* studies) or heat-inactivated normal mouse serum (studies in mice) and stored the protein solutions at -80°C until use. We have chosen not to use protease inhibitors, as they may interfere with cell growth *in vitro* or exhibit toxicity *in vivo*. Neither the addition of sera, nor freezing to -80°C influence binding of purified proteins to the anti-idiotypic antibody 9G10 or the biotinylated anti-h-IgG, anti-h-IL-2 or anti-m-IL-12 (p40/p70) antibodies as detected by ELISA (data not shown). We therefore conclude that the used animal sera do not interact with the anti-CD30 fusion proteins. Furthermore, storage at -80°C does not alter the basic characteristics of these proteins.

Specific binding of immunocytokines is essential for targeted drug delivery. We have therefore analysed the binding of anti-CD30 immunocytokines to immobilised antigen and tumour cells, as well as competition between soluble CD30 and surface-bound antigen in binding to immunocytokines. Purified anti-CD30 fusion proteins specifically bind to the immobilised anti-idiotypic antibody 9G10 in a dose-dependant manner. This internal-image antibody mimics the HRS3-binding epitope on CD30 (Pohl *et al.*, 1992). Interestingly, binding of the immunocytokine HRS3scFv-Fc-IL2 to the antibody 9G10 is 3- to 4-fold lower compared to the other anti-CD30 fusion proteins. These results are consistent with those published by our group (Hombach *et al.*, 2005).

Co-incubation of immunocytokines with CD30 results in dose-dependent inhibition of binding to the immobilised anti-idiotypic antibody 9G10. Thus, anti-CD30 fusion proteins specifically bind via the HRS3 scFv domain, and the anti-idiotypic antibody 9G10 is a valid substitute for CD30

to capture these fusion proteins. The recorded binding inhibitions of 34% to 54% are lower than what would be expected for a 3-fold molar excess of CD30 over fusion protein. We conclude that the anti-CD30 fusion proteins, particularly the immunocytokine HRS3scFv-hi-IL12-Fc-IL2, preferentially bind to surface-bound antigen in presence of solute CD30. Immunotherapy of Hodgkin's lymphoma would benefit from this property, as Hodgkin-Reed-Sternberg cells shed CD30 in large quantities (Matthey *et al.*, 2004). Recorded binding inhibitions are lower than those published by our group (Hombach *et al.*, 2005). This discrepancy may be due to the fact that immunocytokine concentrations in the aforementioned publication have been determined using "Advanced Protein Assay Reagent" (Cytoskeleton, Denver, CO, USA). We have found that this reagent results in a 2- to 3-fold overestimate of immunocytokine concentrations compared to the prediction of molar absorption coefficients used in this study. When taking this into account, the results of this study are consistent with published data.

Anti-CD30 fusion proteins specifically bind to CD30⁺ tumour cells and to hybridoma cells that secrete the anti-idiotypic antibody 9G10. Unexpectedly, fusion proteins containing an IL-2 domain bind 1.5- to 3-fold stronger to L540 cells compared to fusion proteins without IL-2 domain. In contrast, binding of the anti-CD30 immunocytokines to hybridoma cells secreting the anti-idiotypic antibody 9G10 is equally strong. In both cases, binding of the immunocytokine HRS3scFv-Fc-IL2 is decreased twofold compared to HRS3scFv-hi-IL12-Fc-IL2, which is in accordance with the observed decrease in binding to immobilised antibody 9G10. Excess binding of IL-2-containing immunocytokines to L540 cells may result from binding to IL-2 receptors found on these cells. Interestingly, the Hodgkin-derived cell line L540 rapidly internalises IL-2 after binding to the receptor, but does not respond to IL-2 stimuli with increased proliferation (Tesch *et al.*, 1990). Thus, binding of immunocytokines to IL-2 receptors on malignant cells will not endanger therapeutic success by inducing these cells to grow, but might necessitate higher doses for efficient immunotherapy of Hodgkin's lymphoma.

Decreased binding of the immunocytokine HRS3scFv-Fc-IL2 to cells and surface-bound antigen compared to the other anti-CD30 immunocy-

tokines might be due to protein degradation or differences in protein folding. It does not originate from production in insect cells, however, as this immunocytokine shows a similar decrease in binding when produced in mammalian cells. The immunocytokine HRS3scFv-hi-IL12-Fc-IL2 with combined IL-2 and IL-12 domains exhibits unobstructed binding and thus presents itself as a substitute for the immunocytokine HRS3scFv-Fc-IL2.

The cytokines IL-2 and IL-12 induce proliferation and IFN- γ secretion in activated T and natural killer (NK) cells *in vitro* (Thèze, 1999). Accordingly, pre-activated peripheral blood mononuclear cells (PBMCs) proliferate and secrete IFN- γ when stimulated by purified immunocytokines in solution. After specific binding via the HRS3 scFv domain, the immunocytokine HRS3scFv-hi-IL12-Fc-IL2 with combined IL-2 and IL-12 domains increases proliferation and IFN- γ secretion of PBMCs compared to immunocytokines with a single cytokine domain. As expected, the fusion protein HRS3scFv-Fc without cytokine domain does not activate PBMCs. Immunocytokines that contain a murine IL-12 cytokine domain also induce phosphorylation of signal transducer and activator of transcription-4 (STAT4) in pre-activated T cells (cf. figure 4.21). This is consistent with a publication that reports phosphorylation of STAT4 in lymphocytes after stimulation with IL-12, IL-23 or IFN- α (Kaplan, 2005).

Anti-CD30 immunocytokines in solution and the bound immunocytokine HRS3scFv-hi-IL12-Fc-IL2 show 3- to 6-fold less cytokine activity in respect to induction of proliferation and IFN- γ secretion compared to the respective recombinant cytokine. This concurs with Gillies *et al.* (1992, 2002) who have reported 3- to 4-fold diminished cytokine activity for immunocytokines. In contrast, the immunocytokine HRS3scFv-Fc-hi-IL12 yields the same amount of phosphorylation of STAT4 as recombinant IL-12, while the immunocytokine HRS3scFv-hi-IL12-Fc-IL2 with combined IL-2 and IL-12 domains leads to 1.2-fold increased phosphorylation of STAT4. To our best knowledge, no reports on the influence of immunocytokines on the phosphorylation status of STAT4 have been published.

The cytokines IL-2 and IL-12 enhance cytotoxicity by NK cells (Thèze, 1999). In addition, the Fc γ ₁ domain of immunocytokines can trigger antibody-dependent cellular cytotoxicity (ADCC) by binding to Fc γ receptors on NK

cells and other lymphocytes (Davis and Gillies, 2003). Accordingly, resting NK cells are induced to specifically lyse CD30⁺ tumour cells after coating with anti-CD30 immunocytokines or the fusion protein HRS3scFv-Fc without cytokine domain. As the immunocytokine HRS3scFv-hi-IL12-Fc-IL2 with combined IL-2 and IL-12 domains induces higher cytolysis than the fusion protein HRS3scFv-Fc, we conclude that immunocytokines induce cytolysis by both antibody-dependent cellular cytotoxicity via binding to Fc γ receptors and cytokine-mediated cytotoxicity. This conclusion is substantiated by the fact that we have used 5 ng anti-CD30 fusion protein instead of equimolar amounts, thus 44 fmol (5 ng) of the immunocytokine HRS3scFv-Fc-hi-IL12 or 72 fmol of the immunocytokine HRS3scFv-Fc-IL2 induce the same amount of cytolysis as 93 fmol of the fusion protein HRS3scFv-Fc. Within 24 hours, efficiency of cytolysis ranges between 15% and 50% for an effector-to-target cell ratio of 4 : 5. It is not possible to directly compare our results to other publications due to differing incubation times (from hours to days) and effector-to-target cell ratios (from 10 : 1 to 1 : 100). Despite these differences, however, reported cytolysis of immunocytokines usually lies between 20% and 70% (Anderson *et al.*, 1997; Hornick *et al.*, 1997; Peng *et al.*, 1999), which corresponds with our data.

Immunocytokines have been designed to target cytokines to specific sites within the body in order to decrease administered doses, thus limiting the severe side effects associated with systemic application of cytokines. To determine accumulation at the tumour site, we have radiolabelled two immunocytokines. Radiolabelling leads to modified amino acids, and thus may change the properties of proteins. As radiolabelled anti-CD30 immunocytokines specifically bind to the anti-idiotypic antibody 9G10 and the elution profile of radiolabelled immunocytokine during affinity purification corresponds to that of unlabelled immunocytokine, however, we conclude that radiolabelling has not changed the binding affinities of immunocytokines.

We have analysed the biodistribution of radiolabelled immunocytokines after systemic application in SCID mice harbouring tumours of the CD30⁺ Hodgkin-derived cell line L540Cy. The substantial excretion of injected radioactivity within a day as well as high tissue retentions in small intestine may result from dehalogenation and accord with the known elimina-

tion routes of free iodine (Bakker *et al.*, 1991; Riccobene *et al.*, 2003). We have recorded decreased injected dose per gram of tissue (% ID/g) values in tumours and increased % ID/g values in the blood compared to data published by Hornick *et al.* (1997) and Kaspar *et al.* (2007). This may be due to shedding of CD30 from the surface of L540Cy cells (Matthey *et al.*, 2004). Nevertheless, highest tissue retention of the immunocytokine HRS3scFv-Fc-hi-IL12 is found at the tumour (30%) compared to healthy tissues ($\leq 20\%$). In case of the immunocytokine HRS3scFv-hi-IL12, retention at the tumour amounts to 35% and is among the three highest observed tissue retentions (small intestine: 39%, blood: 37%). We therefore conclude that anti-CD30 immunocytokines specifically accumulate at the tumour site.

We have determined the influence of dimerisation mediated by the Fc γ_1 domain on biodistribution by using two immunocytokines that are identical except for lacking or containing an Fc γ_1 domain. The immunocytokine HRS3scFv-hi-IL12 without Fc γ_1 domain is secreted as a monomer of 110kDa (Heuser *et al.*, 2003), while the immunocytokine HRS3scFv-Fc-hi-IL12 is secreted as a homodimer of 260kDa (Hombach *et al.*, 2005). Despite the difference in molecular weight, however, neither biological half-life in β -phase, nor retention at the tumour site of these immunocytokines differ significantly. This concurs with Rennen *et al.* (2001), who have reported slow blood clearance for proteins of intermediate size (70kDa to 210kDa) compared to rapid clearance of smaller (< 30kDa) and larger (> 660kDa) proteins. On the other hand, the tested immunocytokines show different distribution to tissues. After 72 hours, the immunocytokine HRS3scFv-Fc-hi-IL12 with Fc γ_1 domain is detected in all tissues, whereas the immunocytokine HRS3scFv-hi-IL12 without Fc γ_1 domain is cleared within 72 hours from heart, spleen and bones in all animals and from muscle, colon, stomach, kidney and the lungs in at least two animals. While both immunocytokines are retained at the tumour, our results are clearly in favour of the immunocytokine HRS3scFv-hi-IL12 without Fc γ_1 domain, as it combines fast clearance in off-target tissues with retention at the tumour site, thus adding tumour selectivity to cytokine therapy.

Biological half-life in β -phase of radiolabelled immunocytokines in SCID mice amounts to 33 hours (HRS3scFv-hi-IL12) and 34 hours (HRS3scFv-

Fc-hi-IL12), while we have estimated half-life of the immunocytokine HRS3scFv-hi-IL12-Fc-IL2 in two Balb/c mice to 32 hours and 41 hours. These values are close to each other and thus justify calculation of a mean value. The mean biological half-life of anti-CD30 immunocytokines amounts to 35 hours and lies well within the reported half-life of 30 hours (Hornick *et al.*, 1997), 31 hours (Xu *et al.*, 2000) and 37 hours (Powers *et al.*, 2001) for immunocytokines and scFv-Fc fusion proteins. Moreover, biological half-life in β -phase of immunocytokines is much higher than that of recombinant cytokine in humans (human IL-2: 0.4 hours; human IL-12: 5 hours to 10 hours; Atkins *et al.*, 1986, 1997). An increased biological half-life allows to decrease administered doses. If the drug also selectively accumulates at the target site, administered doses may be lowered even further, thus decreasing side effects. We therefore expect anti-CD30 immunocytokines to require lower doses and elicit less side effects compared to conventional cytokine therapy.

The anti-CD30 immunocytokines used in this study have been designed to inhibit tumour growth *in vivo*. We have therefore assessed influence of the immunocytokine HRS3scFv-hi-IL12-Fc-IL2 with combined IL-2 and IL-12 domains on the growth of established tumours in immunocompetent mice. Mice tolerate single doses of up to 500 pmol (3.3 mg/kg body weight) and cumulated doses of up to 1 nmol (6.5 mg/kg) of this immunocytokine. Cumulated immunocytokine doses of 300 pmol (1.9 mg/kg) and above inhibit tumour growth in immunocompetent mice when administered three times intravenously at 48-hour intervals. In contrast, tumour growth is not inhibited by lower cumulated doses or in control animals. This concurs with Gillies *et al.* (2002) who have reported that an immunocytokine with combined IL-2 and IL-12 domains delays tumour growth, but does not lead to tumour regression unless injected directly into the tumour (cumulated dose: \approx 5 mg/kg). Finally, we have not observed side effects related to immunocytokine administration.

Within certain limits, drug doses can be translated from mice to human adults by normalisation to average body surface area (Reagan-Shaw *et al.*, 2008). The minimum effective cumulated dose in mice (1.9 mg/kg administered in three doses) translates to 160 μ g/kg for human adults. Thus, a third of this dose (i.e. 55 μ g/kg) might be a feasible single dose for tumour

therapy. This dose is much lower than the 0.8 mg/kg to 7.5 mg/kg dosing regimes used in current clinical trials of immunocytokines (Ribas *et al.*, 2009), which might be attributed to synergism mediated by the combined cytokine domains of the immunocytokine HRS3scFv-hi-IL12-Fc-IL2. However, Hodgkin-Reed-Sternberg cells as well as the tumour-infiltrating lymphocytes produce a complex pattern of cytokines and chemokines (Skinnider and Mak, 2002). This situation cannot be reproduced in laboratory animals and might necessitate increased immunocytokine doses for effective therapy. In addition, antibodies directed against the immunocytokine might limit the clinical use of this protein. On the other hand, immunogenicity of the immunocytokine may be minimised by humanising the HRS3 scFv and exchanging the murine single-chain IL-12 domain with its human counterpart. Moreover, many patients with classical Hodgkin's lymphoma display signs of immunosuppression (Romagnani *et al.*, 1985) and might thus exhibit enhanced tolerance to foreign proteins.

We have recorded 13-fold lower immunocytokine concentrations in the peripheral circulation of mice compared to concentrations calculated from administered doses for a pharmacokinetic one-compartment model. Thus, large amounts of immunocytokine are either retained in tissues and at the tumour, as shown by the biodistribution experiment, or cleared from the body. While we cannot quantify distribution and clearance, it is obvious that at least a fraction of the administered immunocytokine reaches the tumour, as tumour growth has been effectively inhibited. As expected, immunocompetent mice raise antibodies directed against the immunocytokine backbone consisting of the scFv HRS3 and human IgG₁. However, antibodies first appeared on day 4 after the first injection, therefore clearance by antibodies does not account for the low immunocytokine concentrations in peripheral blood.

Classical Hodgkin's lymphoma is characterised by an immunosuppression in patients that is attributed to an overproduction of T_H2 cytokines. As the balance between T_H1 and T_H2 cytokines determines which immune response results from infection with a pathogen, the defective immune response might be turned into an efficient anti-tumour response by the administration of T_H1 cytokines. In this study, we have demonstrated that the anti-CD30 immunocytokine HRS3scFv-hi-IL12-Fc-IL2 with combined IL-2

and IL-12 domains selectively binds to CD30⁺ cells derived from Hodgkin's lymphoma and induces secretion of the T_H1 cytokine IFN- γ in resting NK cells and pre-activated PBMCs. IFN- γ and IL-12 are potent immunomodulators that drive immune reactions to the T_H1 type, and the endogenous production of IFN- γ is required for an effective anti-tumour response. The immunocytokine HRS3scFv-hi-IL12-Fc-IL2 enhances IFN- γ secretion of effector cells compared to immunocytokines with a single cytokine domain and induces resting natural killer cells to cytolysis of tumour cells, while its IL-2 domain is thought to prevent the immunosuppression mediated by IL-12 monotherapy. Thus, the misguided T_H2 immune reaction could be overcome by the immunocytokine HRS3scFv-hi-IL12-Fc-IL2, resulting in an efficient anti-tumour response against the malignant Hodgkin-Reed-Sternberg cells.

The ideal anti-cancer drug combines high tumour selectivity with long biological half-life and fast clearance in off-target tissues. Anti-CD30 immunocytokines selectively bind to CD30⁺ tumour tissue *in vivo* and have a prolonged biological half-life compared to recombinant cytokines. These properties allow to decrease administered immunocytokine doses, thereby decreasing the incidence of side effects. This is reflected by the fact that effective doses of the immunocytokine HRS3scFv-hi-IL12-Fc-IL2 do not elicit noticeable side effects in immunocompetent mice. Our data suggest that immunocytokines without an Fc γ ₁ domain are cleared faster from off-target tissues than immunocytokines which contain an Fc γ ₁ domain. On the other hand, an Fc γ ₁ domain mediates antibody-dependent cellular cytotoxicity, thus adding to anti-tumour activity, and allows convenient purification and detection of immunocytokines using anti-IgG antibodies. Currently, clinical trials of immunocytokines with and without Fc domain are under way and may reveal the benefits of either configuration (Schliemann *et al.*, 2009; Ribas *et al.*, 2009).

In clinical studies, immunocytokines with an IL-2 domain have led to stable disease in 81% ($n = 16$) or 24% ($n = 33$) of cancer patients, whereas trials with 27 pediatric patients and 9 adults have not shown clinical response. However, most patients have shown immunologic response to immunocytokine therapy such as lymphopenia followed by rebound lymphocytosis, increased NK cell activity, antibody-dependent cellular cytotoxicity and

increased levels of soluble IL-2 receptor- α in peripheral blood. Although a large number of patients has developed antibodies against immunocytokines, these antibodies have not negatively influenced therapy, except for anaphylaxis in one patient. Toxicities induced by immunocytokines with an IL-2 domain have been reversible and mostly resemble those of therapy with IL-2 or monoclonal antibodies. Dose-limiting toxicities include hypotension, hypoxia, allergic reactions, vascular leak syndrome and pain requiring morphine. (Johannsen *et al.*, 2008; King *et al.*, 2004; Ko *et al.*, 2004; Osenga *et al.*, 2006; Ribas *et al.*, 2009). In contrast to high-dose IL-2 therapy, however, no grade 4 events or treatment-related deaths have been reported (Dutcher *et al.*, 2001). Thus, treatment with immunocytokines elicits manageable and reversible toxicities, which is a definite improvement over conventional cytokine therapy. Even though case numbers are small, it also seems that a higher proportion of patients responds to therapy with immunocytokines compared to the 5% to 10% that respond to high-dose IL-2 therapy (Atkins, 2009; Dutcher *et al.*, 2001).

Current efforts in cancer therapy aim to specifically target the malignant cells in a tumour lesion. Already, monoclonal antibodies, anti-estrogens and tyrosine kinase inhibitors have revolutionised cancer therapy. Immunotherapy aspires to activate a patient's immune system and elicit an immune response directed against the tumour without inducing autoimmunity. Promising approaches with regard to targeted immunotherapy are bispecific antibodies that exert their anti-tumour activity by cross-linking malignant cells and effector cells (Deckert, 2009), and adoptive immunotherapy that aims to kill tumour cells by expressing recombinant receptors on the surface of T cells (Hombach and Abken, 2007). In the case of classical Hodgkin's lymphoma, however, these approaches may be limited by the inherent immunosuppression and T cell anergy in patients. On the other hand, combining bispecific antibodies or adoptive immunotherapy with immunocytokines makes for an intriguing prospect, as immunosuppression and T cell anergy may be overcome and synergetic anti-tumour reactivity ensue, especially if competition in binding to malignant cells is circumvented by targeting different antigens or epitopes on these cells.

In summary, the immunocytokine concept has matured in the last years and the first immunocytokines are being tested in clinical trials. Im-

munocytokines elicit immunological and clinical response in patients with advanced stages of cancer, while toxicities are manageable and reversible. This improvement over conventional cytokine therapy may facilitate that more patients benefit from cytokine-based immunotherapy. We have adopted the immunocytokine concept for the therapy of classical Hodgkin's lymphoma and generated the immunocytokine HRS3scFv-hi-IL12-Fc-IL2. This recombinant protein shares the favourable properties of immunocytokines, which are specific binding to tumour cells, retained cytokine activity and accumulation at the tumour lesion. In addition, the immunocytokine HRS3scFv-hi-IL12-Fc-IL2 combines IL-2 and IL-12 domains in one molecule and thus exhibits enhanced anti-tumour reactivity compared to immunocytokines with each cytokine domain. The resulting activation of resting NK cells might be able to overcome the immunosuppression in classical Hodgkin's lymphoma. Moreover, the immunocytokine HRS3scFv-hi-IL12-Fc-IL2 inhibits tumour growth in immunocompetent mice without noticeable side effects, thus presenting itself as a well-tolerated and potent new drug for the therapy of classical Hodgkin's lymphoma.

6 Summary

Classical Hodgkin's lymphoma is one of the most curable cancers. However, non-responders, tumour relapses and long-term toxicities of the treatment make it necessary to look for alternative drugs. Immunotherapy with cytokines could result in an immune response against the malignant Hodgkin-Reed-Sternberg cells, while antibody-cytokine conjugates (immunocytokines) may reduce side effects by directing cytokine activity to the tumour. As combining the cytokines IL-2 and IL-12 elicits strong synergistic anti-tumour activity, we have generated the novel immunocytokine HRS3scFv-hi-IL12-Fc-IL2 that targets CD30 on the surface of Hodgkin-Reed-Sternberg cells and combines IL-2 and IL-12 domains in one molecule. We have characterised this immunocytokine for binding and activity, both *in vitro* and *in vivo*. Furthermore, we have compared the biodistribution of two immunocytokines that are identical except for lacking or containing the Fc domain of human IgG₁.

In this study, we have established bulk production of immunocytokines in insect cells and purified recombinant protein in the milligramme range. Anti-CD30 immunocytokines specifically bind to CD30⁺ tumour cells, activate peripheral blood mononuclear cells and induce resting natural killer cells to specific lysis of CD30⁺ tumour cells. The immunocytokine HRS3scFv-hi-IL12-Fc-IL2 with combined IL-2 and IL-12 domains has proved superior to immunocytokines with a single cytokine domain by exhibiting higher cytokine activity, and increases lysis of tumour cells compared to the fusion protein HRS3scFv-Fc without cytokine domain. *In vivo*, anti-CD30 immunocytokines accumulate at the tumour site and have a long biological half-life of 1.5 days, while the immunocytokine HRS3scFv-hi-IL12-Fc-IL2 inhibits tumour growth in immunocompetent mice without noticeable side effects. Data suggest that immunocytokines without an Fc do-

Summary

main may be superior to those containing an Fc domain due to faster clearance in off-target tissues. In summary, the immunocytokine HRS3scFv-hi-IL12-Fc-IL2 with combined IL-2 and IL-12 domains exhibits enhanced anti-tumour reactivity, might overcome the T cell anergy in Hodgkin's lymphoma by activating tumour-infiltrating natural killer cells and may decrease side effects by accumulation at the tumour lesion. Thus, this immunocytokine presents itself as a well-tolerated and potent new drug for the therapy of Hodgkin's lymphoma.

7 Acknowledgements

I am indebted to Prof. Dr. Hinrich Abken, not only for providing the topic of my work, but also for his consistent support and dedication, and for making me feel that my problems were more important than his schedule. I must also thank Prof. Dr. Klaus Mohr for his supervision and advice, and for his “Color Atlas of Pharmacology” textbook. I’d further like to thank Prof. Dr. Evi Kostenis and Prof. Dr. Waldemar Kolanus who kindly agreed to join the *Promotionskommission*.

Sincere thanks are also due to Dr. Andreas Hombach for his supervision, and to PD Dr. Stefan Guhlke and Jan-Philipp Hering for helping me with the biodistribution experiments. I’d like to thank PD Dr. Hinrich Hansen, Vijaya Simhadri, Prof. Dr. Thomas Blankenstein, Prof. Dr. Soldano Ferrone, Prof. Dr. Naomi Taylor and Dr. Ralph Willemsen for kindly providing me with cell lines, plasmids, antibodies and recombinant proteins. I must also thank everyone in our group, especially Markus Chmielewski, Claudia Ederer, Caroline Kopecky and Tobias Riët, who became dear friends as they helped me through the problems I faced. A special thank-you is due to Danuta Chrobok and Frank Steiger for their excellent work. I’d also like to thank both Samir-Ghali Tawadros, who gave up his free time and week-ends to help me, and PD Dr. Martin Hellmich of the *Institut für Medizinische Statistik, Informatik und Epidemiologie* for reviewing my statistical analyses. Finally, I want to thank everyone in the LFI building who supported me with advice and cheerful conversation.

I must also express my gratitude to the open source community, whose software has been used extensively to create this document. In particular, I want to thank the many people behind the statistical software package *R* and the \LaTeX typesetting system.

Acknowledgements

Thanks also to Claudia Ederer and Mark Hill for proof-reading parts of my manuscript. I want to thank Ole Löding for being a real friend and for adding to the soundtrack of my life. And in this last, but prominent place I want to thank my parents, my brother and my friends for everything else. Without you, I wouldn't be who or where I am.



A Abbreviations

ABTS

diazanium(2Z)-3-ethyl-2-[(Z)-(3-ethyl-6-sulfonato-1,3-benzothiazol-2-ylidene)hydrazinyliidene]-1,3-benzothiazole-6-sulfonate

ABVD adriamycin (doxorubicin), bleomycin, vinblastine, dacarbazine

ADCC antibody-dependent cellular cytotoxicity

AEC 9-ethylcarbazol-3-amine

AKT protein kinase B

asinh *area sinus hyperbolicus*

ATCC American type culture collection

ATTACK Adoptive engineered T cell targeting to activate cancer killing

BEACOPP bleomycin, etoposide, adriamycin (doxorubicin), cyclophosphamide, oncovin (vincristine), procarbazine, prednisone

BiP immunoglobulin heavy chain binding protein

bp base pairs

BrdU 5-bromo-2'-deoxyuridine (5-bromo-1-[(2R,4S,5R)-4-hydroxy-5-(hydroxymethyl)oxolan-2-yl]pyrimidine-2,4-dione)

Abbreviations

BSA bovine serum albumin

CD cluster of differentiation

CEA carcinoembryonic antigen

cpm counts per minute

Da Dalton

ddH₂O double distilled water

DMSO dimethylsulfinylmethane

DNA deoxyribonucleic acid

dNTP deoxynucleoside triphosphate

ED effective dose

EDTA

2-[2-[bis(carboxymethyl)amino]ethyl-(carboxymethyl)amino]acetic acid

ELISA enzyme-linked immunosorbent assay

FCS foetal calf serum

Fab antigen-binding fragment

Fc crystallisable fragment

FITC fluorescein (mistakenly abbreviated by its commonly-used reactive form fluorescein-5-isothiocyanate)

GMP good manufacturing practise

hi hinge

HEPES 2-[4-(2-hydroxyethyl)piperazin-1-yl]ethanesulfonic acid

HMW-MAA high-molecular-weight melanoma-associated antigen

HRS Hodgkin-Reed-Sternberg

ID identification number / injected dose

IFN interferon

IL interleukin

IU international unit

Jak Janus family tyrosine kinase

kb kilo base pairs

LB Luria broth (also known as Lenox broth)

Lk Lkappa

mAb monoclonal antibody

MACS magnetic cell separation

MAP kinase mitogen-activated protein kinase

MCS multiple cloning site

MFI mean fluorescence intensity

MHC major histocompatibility complex

MOPS 3-morpholin-4-ylpropane-1-sulfonic acid

Abbreviations

MW molecular weight

MWCO molecular weight cut-off

n.d. not detected

NHS 1-hydroxy-2,5-pyrrolidinedione

NK cell natural killer cell

OAc acetate

OD optical density

PAGE polyacrylamide gel electrophoresis

PBMC peripheral blood mononuclear cell

PBS phosphate buffered saline

PCR polymerase chain reaction

PE phycoerythrin

PHA-L leucoagglutinin

PI3 kinase phosphatidyl inositol 3 kinase

pMT *Drosophila* metallothionein promotor

RIA radioimmunoassay

RPMI Roswell Park Memorial Institute medium

rpm revolutions per minute

scFv single-chain fragment variant

SCID severe combined immunodeficiency

SDS sodium dodecyl sulfate

SL2 Schneider's *Drosophila* line 2

SPF specific pathogen free

STAT signal transducer and activator of transcription

TAE TRIS / acetate / EDTA buffer

TGF transforming growth factor

tm transmembrane

TRIS 2-amino-2-(hydroxymethyl)propane-1,3-diol

Tyk tyrosine kinase

U unit

UV ultraviolet

WHO World Health Organization

XTT 4-methoxy-5-[3-(2-methoxy-4-nitro-5-sulfophenyl)-5-(phenylcarbamoyl)tetrazol-3-ium-2-yl]-2-nitrobenzenesulfonate

B DNA sequence data

B.1 pBullet HRS3scFv-CD3 ζ (#1078)

<u>Begin</u>	<u>End</u>	<u>Domain</u>
1973bp	2713bp	HRS3 scFv
2720bp	3127bp	CD3 ζ

NcoI (1968)
| **HRS3 scFv (1973-2713)**
| |

```
1964 CTGCCATGG GTGGCCAG GTGCAACTG CAGCAGTCA GGGGCTGAG CTGGCTAGA CCTGGGGCT
      V A Q V Q L Q Q S G A E L A R P G A
2027 TCAGTGAAG ATGTCTGC AAGGCTTCT GGCTACACC TTTACTACC TACACAATA CACTGGGTA
      S V K M S C K A S G Y T F T T Y T I H W V
2090 AGACAGAGG CCTGGACAC GATCTGAA TGGATTGGA TACATTAAT CCTAGCAGT GGATATTCT
      R Q R P G H D L E W I G Y I N P S S G Y S
2153 GACTACAAT CAAAATTC AAGGGCAAG ACCACATTG ACTGCAGAC AAGTCTCC AACACAGCC
      D Y N Q N F K G K T T L T A D K S S N T A
2216 TACATGCAA CTGAACAGC CTGACATCT GAGGACTCT GCGGTCTAT TACTGTGCA AGAAGAGCG
      Y M Q L N S L T S E D S A V Y Y C A R R A
2279 GACTATGGT AACTACGAA TATACTGG TTTGCTTAC TGGGGCCAA GGGACCACG GTCACCGCC
      D Y G N Y E Y T W F A Y W G Q G T T V T A
```

DNA sequence data

2342 S S S G G G S G G G G G S G G G G S D I E L
TCCTCAAGT GGAGGCGGT TCAGGTGGA GGTGGCTCT GGCGGTGGC GGATCGGAC ATCGAGCTC

2405 T Q S P K F M S T S V G D R V N V T Y K A
ACTCAGTCT CCAAAATTC ATGTCCACA TCAGTAGGA GACAGGGTC AACGTACC TACAAGGCC

2468 S Q N V G T N V A W F Q Q K P G Q S P K V
AGTCAGAAT GTGGTACT AATGTAGCC TGGTTTCAA CAAAAACCA GGGCAATCT CCTAAAGTT

2531 L I Y S A S Y R Y S G V P D R F T G S G S
CTGATTAC TCGGCATCT TACCGATAC AGTGGAGTC CCTGATCGC TTCACAGGC AGTGGATCT

2594 G T D F T L T I S N V Q S E D L A E Y F C
GGAACAGAT TTCACTCTC ACCATCAGC AATGTGCAG TCTGAAGAC TTGGCAGAG TATTCTGTG

2657 Q Q Y H T Y P L T F G G G T K L E I K R A
CAGCAATAT CACACCTAT CCTCTCACG TTCGGAGGG GGCACCAAG CTGGAAATC AAACGGGCG

CD3 ζ (2720-3127)

BamHI (2720)

|

2720 D P K L C Y L L D G I L F I Y G V I L T A
GATCCAAA CTCTGTAC CTGCTGGAT GGAATCCTC TTCATCTAT GGTGTCATT CTCACTGCC

2783 L F L R V K F S R S A D A P A Y Q Q G Q N
TTGTTCTG AGAGTGAAG TTCAGCAGG AGCGCAGAC GCCCCCGC TACCAGCAG GGCCAGAAC

2846 Q L Y N E L N L G R R E E Y D V L D K R R
CAGCTCTAT AACGAGCTC AATCTAGGA CGAAGAGAG GAGTACGAT GTTTTGAC AAGAGACGT

2909 G R D P E M G G K P R R K N P Q E G L Y N
GGCCGGGAC CCTGAGATG GGGGAAAG CCGAGAAGG AAGAACCCT CAGGAAGGC CTGTACAAT

2972 E L Q K D K M A E A Y S E I G M K G E R R
GAACTGCAG AAAGATAAG ATGGCGGAG GCCTACAGT GAGATTGGG ATGAAAGGC GAGCGCCGG

3035 R G K G H D G L Y Q G L S T A T K D T Y D
AGGGGCAAG GGGCACGAT GGCCTTAC CAGGGTCTC AGTACAGCC ACCAAGGAC ACCTACGAC

NotI (3148)

|

3098 A L H M Q A L P P R *
GCCCTTAC ATGCAGGCC CTGCCCCCT CGCTAACAG GTCGACAGA TCCGCGGCC GCTCGGCAC

XhoI (3161)

|

3161 TCGAGAGAT CCGGATTAG TC CAATTG TTAAAGACA GGATATCAG TGGTCCAGG CTCTAGTTT

B.2 pMT/BiP HRS3scFv-Fc (#1082)

Begin	End	Domain
851 bp	904 bp	BiP signal sequence
917 bp	1657 bp	HRS3 scFv
1670 bp	2368 bp	human Fc γ ₁

BiP signal sequence (851-904)

|
M K L C I L L A V V A F V G L S L G
842 GATCTCAAT ATGAAGTTA TGCATATTA CTGGCCGTC GTGGCCCTTT GTTGGCCTC TCGTCTGGG

NcoI (912)

| HRS3 scFv (917-1657)
| |
R S P W V A Q V Q L Q Q S G A E L A R P G
905 AGATCTCCA TGGGTGGCC CAGGTGCAA CTGCAGCAG TCAGGGGCT GAGCTGGCT AGACCTGGG
A S V K M S C K A S G Y T F T T Y T I H W
968 GCTTCAGTG AAGATGTCC TGCAAGGCT TCTGGCTAC ACCTTTACT ACCTACACA ATACACTGG
V R Q R P G H D L E W I G Y I N P S S G Y
1031 GTAAGACAG AGGCCCTGGA CACGATCTG GAATGGATT GGATACATT AATCCTAGC AGTGGATAT
S D Y N Q N F K G K T T L T A D K S S N T
1094 TCTGACTAC AATCAAAA TCAAGGGC AAGACCACA TTGACTGCA GACAAGTCC TCCAACACA
A Y M Q L N S L T S E D S A V Y Y C A R R
1157 GCCTACATG CAACTGAAC AGCCTGACA TCTGAGGAC TCTGCGGTC TATTACTGT GCAAGAAGA
A D Y G N Y E Y T W F A Y W G Q G T T V T
1220 GCGGACTAT GGTAACTAC GAATATACC TGGTTTGCT TACTGGGGC CAAGGGACC ACGGTCACC
A S S S G G G S G G G G G S G G G G S D I E
1283 GCCTCTCA AGTGGAGGC GGTTCAGGT GGAGGTGGC TCTGGCGGT GGCGGATCG GACATCGAG
L T Q S P K F M S T S V G D R V N V T Y K
1346 CTCACTCAG TCTCAAAA TTCATGTCC ACATCAGTA GGAGACAGG GTCAACGTC ACCTACAAG

1409 A S Q N V G T N V A W F Q Q K P G Q S P K
GCCAGTCAG AATGTGGGT ACTAATGTA GCCTGGTTT CAACAAAAA CCAGGGCAA TCTCTAAA
1472 V L I Y S A S Y R Y S G V P D R F T G S G
GTTCTGATT TACTCGGA TCTTACCGA TACAGTGA GTCCTGAT CGCTTACA GGCAGTGA
1535 S G T D F T L T I S N V Q S E D L A E Y F
TCTGGAACA GATTCACT CTCACCATC AGCAATGTG CAGCTGAA GACTTGGCA GAGTATTC
1598 C Q Q Y H T Y P L T F G G G T K L E I K R
TGTCAGCAA TATCACACC TATCCTCTC ACGTTCGGA GGGGGCACC AAGCTGGAA ATCAAACGG

BamHI (1664)

| h-Fc γ 1 (1670-2368)
| |

1661 A D P A E P K S P D K T H T C P P C P A P
GGGATCCC GCCGAGCC AAATCTCT GACAAAAC CACACATG CCACCGTG CCAGCACCT
1724 E L L G G P S V F L F P P K P K D T L M I
GAACTCTG GGGGACCG TCAGTCTT CTCTTCCC CCAAAACC AAGGACCC CTCATGATC
1787 S R T P E V T C V V V D V S H E D P E V K
TCCGGACC CCTGAGTC ACATGCGTG GTGGTGGAC GTGAGCCAC GAAGACCCT GAGGTCAAG
1850 F N W Y V D G V E V H N A K T K P R E E Q
TTCAACTGG TACGTGGAC GCGTGGAG GTGCATAAT GCCAAGACA AAGCCGCG GAGGAGCAG
1913 Y N S T Y R V V S V L T V L H Q D W L N G
TACAACAGC ACGTACCGT GTGGTCAGC GTCCCTACC GTCCTGCAC CAGGACTGG CTGAATGGC
1976 K E Y K C K V S N K A L P A P I E K T I S
AAGGAGTAC AAGTGCAAG GTCTCCAAC AAAGCCCTC CCAGCCCCC ATCGAGAAA ACCATCTCC
2039 K A K G Q P R E P Q V Y T L P P S R D E L
AAAGCCAAA GGCAGCCC CGAGAACCA CAGGTGTAC ACCCTGCC CCATCCCGG GATGAGCTG
2102 T K N Q V S L T C L V K G F Y S S D I A V
ACCAAGAAC CAGGTGAGC CTGACCTGC CTGGTCAAA GGTTCTAT TCCAGCGAC ATCGCCGTG
2165 E W E S N G Q P E N N Y K T T P P V L D S
GAGTGGGAG AGCAATGGG CAGCCGGAG AACAACTAC AAGACCAG CCTCCCGTG CTGGACTCC
2228 D G S F F L Y S K L T V D K S R W Q Q G N
GACGGCTCC TTCTTCTC TACAGCAAG CTCACCGTG GACAAGAGC AGGTGGCAG CAGGGGAAC

DNA sequence data

2291 V F S C S V M H G A L H N H Y T Q K S L S
GTCTTCTCA TGCTCCGTG ATGCATGGG GCTCTGCAC AACCACTAC ACGCAGAAG AGCCTCTCC

XhoI (2376)

|

2354 L S P G K I *
CTGTCTCCG GGTAAGATC TAGCTCGAG TCTAGAGGG CCCTTCGAA GGTAAGCCT ATCCCTAAC

B.3 pMT/BiP HRS3scFv-Fc-hi-IL12 (#1083)

Begin	End	Domain
851 bp	904 bp	BiP signal sequence
917 bp	1657 bp	HRS3 scFv
1670 bp	2368 bp	human Fc γ ₁
2381 bp	2416 bp	hinge (human IgG ₁)
2420 bp	3358 bp	murine IL-12 (p40)
3359 bp	3403 bp	murine IL-12 (linker)
3404 bp	3982 bp	murine IL-12 (Δ p35)

BiP signal sequence (851-904)

|
M K L C I L L A V V A F V G L S L G
842 GATCTCAAT ATGAAGTTA TGCATATTA CTGGCCGTC GTGGCCTTT GTTGGCCTC TCGCTCGGG

NcoI (912)

| HRS3 scFv (917-1657)
| |
R S P W V A Q V Q L Q Q S G A E L A R P G
905 AGATCTCCA TGGGTGGCC CAGGTGCAA CTGCAGCAG TCAGGGGCT GAGCTGGCT AGACCTGGG
A S V K M S C K A S G Y T F T T Y T I H W
968 GCTTCAGTG AAGATGTCC TGCAAGGCT TCTGGCTAC ACCTTTACT ACCTACACA ATACACTGG
V R Q R P G H D L E W I G Y I N P S S G Y
1031 GTAAGACAG AGGCCTGGA CACGATCTG GAATGGATT GGATACATT AATCCTAGC AGTGGATAT
S D Y N Q N F K G K T T L T A D K S S N T
1094 TCTGACTAC AATCAAAAC TTCAAGGGC AAGACCACA TTGACTGCA GACAAGTCC TCCAACACA
A Y M Q L N S L T S E D S A V Y Y C A R R
1157 GCCTACATG CAACTGAAC AGCCTGACA TCTGAGGAC TCTGCGGTC TATTACTGT GCAAGAAGA
A D Y G N Y E Y T W F A Y W G Q G T T V T
1220 CCGGACTAT GGTAACACT GAATATACC TGGTTTGCT TACTGGGGC CAAGGGACC ACGGTCACC
A S S S G G G S G G G G G S G G G G S D I E
1283 GCCTCTCA AGTGGAGGC GGTTCAGGT GGAGGTGGC TCTGGCGGT GCGGATCG GACATCGAG

DNA sequence data

1346 L T Q S P K F M S T S V G D R V N V T Y K
CTCACTCAG TCTCCAAA TTCATGTC ACATCAGTA GGAGACAGG GTCAACGTC ACCTACAAG

1409 A S Q N V G T N V A W F Q Q K P G Q S P K
GCCAGTCAG AATGTGGGT ACTAATGTA GCCTGGTTT CAACAAAA CCAGGGCAA TCTCTAAA

1472 V L I Y S A S Y R Y S G V P D R F T G S G
GTTCTGATT TACTCGCA TCTTACCGA TACAGTGA GTCCCTGAT CGCTTCACA GGCAGTGA

1535 S G T D F T L T I S N V Q S E D L A E Y F
TCTGGAACA GATTTCACT CTCACCATC AGCAATGTG CAGTCTGAA GACTTGCA GAGTATTTT

1598 C Q Q Y H T Y P L T F G G G T K L E I K R
TGTCAGCAA TATCACACC TATCCTCTC ACGTTCGGA GGGGGCACC AAGCTGGAA ATCAAACGG

BanHI (1664)
| **h-Fcγ1 (1670-2368)**
| |

1661 A D P A E P K S P D K T H T C P P C P A P
GCGGATCCC GCCGAGCCC AAATCTCCT GACAAAAC T CACACATGC CCACCGTGC CCAGCACCT

1724 E L L G G P S V F L F P P K P K D T L M I
GAACTCTG GGGGACCG TCAGTCTTC CTCTTCCCC CCAAAACCC AAGGACACC CTCATGATC

1787 S R T P E V T C V V V D V S H E D P E V K
TCCCGGACC CCTGAGGTC ACATGCGTG GTGGTGGAC GTGAGCCAC GAAGACCCT GAGGTC AAG

1850 F N W Y V D G V E V H N A K T K P R E E Q
TTCAACTGG TACGTGGAC GCGGTGGAG GTGCATAAT GCCAAGACA AAGCCGCGG GAGGAGCAG

1913 Y N S T Y R V V S V L T V L H Q D W L N G
TACAACAGC ACGTACCGT GTGGTCAGC GTCCTCACC GTCCTGCAC CAGGACTGG CTGAATGGC

1976 K E Y K C K V S N K A L P A P I E K T I S
AAGGAGTAC AAGTGCAAG GTCCTCAAC AAAGCCCTC CCAGCCCCC ATCGAGAAA ACCATCTCC

2039 K A K G Q P R E P Q V Y T L P P S R D E L
AAAGCCAAA GGGCAGCCC CGAGAACCA CAGGTGTAC ACCCTGCCC CCATCCCGG GATGAGCTG

2102 T K N Q V S L T C L V K G F Y S S D I A V
ACCAAGAAC CAGGTCAGC CTGACCTGC CTGGTCAAA GGCTTCTAT TCCAGCGAC ATCGCCGTG

2165 E W E S N G Q P E N N Y K T T P P V L D S
GAGTGGGAG AGCAATGGG CAGCCGGAG AACAACTAC AAGACCAGC CCTCCCGTG CTGACTCC

2228 D G S F F L Y S K L T V D K S R W Q Q G N
GACGGCTCC TTCTTCTCTACAGCAAG CTCACCGTG GACAAGAGC AGGTGGCAG CAGGGGAAC

2291 V F S C S V M H G A L H N H Y T Q K S L S
GTCTTCTCA TGCTCCGTG ATGCATGGG GCTCTGCAC AACCACTAC ACGCAGAAG AGCCTCTCC

hinge (h-IgG1) (2381-2416)

|
2354 L S P G K K D P A E P K S P D K T H T C P
CTGTCTCCG GGTAACAAA GATCCCGCC GAGCCCAA TCTCTGAC AAAACTCAT ACATGCCCA

m-IL12 (p40) (2420-3358)

| **BstXI (2422)**

| |
2417 P M W E L E K D V Y V V E V D W T P D A P
CCAATGTGG GAGCTGGAG AAAGACGTT TATGTGTGA GAGGTGGAC TGGACTCCC GATGCCCTT

2480 G E T V N L T C D T P E E D D I T W T S D
GGAGAAACA GTGAACCTC ACCTGTGAC ACGCCTGAA GAAGATGAC ATCACCTGG ACCTCAGAC

BstXI (2550)

|
2543 Q R H G V I G S G K T L T I T V K E F L D
CAGAGACAT GGAGTCATA GGCTCTGGA AAGACCCCTG ACCATCACT GTCAAAGAG TTTCTAGAT

2606 A G Q Y T C H K G G E T L S H S H L L L H
GCTGGCCAG TACACCTGC CACAAAGGA GCGGAGACT CTGAGCCAC TCACATCTG CTGCTCCAC

2669 K K E N G I W S T E I L K N F K N K T F L
AAGAAGGAA AATGGAATT TGGTCCACT GAAATTTA AAAAATTC AAAACAAG ACTTTCCTG

2732 K C E A P N Y S G R F T C S W L V Q R N M
AAGTGTGAA GCACCAAAT TACTCCGGA CGGTTCACG TGCTCATGG CTGGTGCAA AGAAACATG

2795 D L K F N I K S S S S P P D S R A V T C G
GACTTGAAG TTCAACATC AAGAGCAGT AGCAGTCCC CCCGACTCT CGGGCAGTG ACATGTGGA

2858 M A S L S A E K V T L D Q R D Y E K Y S V
ATGGCGTCT CTGTCTGCA GAGAAGGTC ACACCTGGAC CAAAGGAC TATGAGAAG TATTCACTG

BstXI (2975)

|
2921 S C Q E D V T C P T A E E T L P I E L A L
TCCTGCCAG GAGGATGTC ACCTGCCCA ACTGCCGAG GAGACCCTG CCCATTGAA CTGGCGTTG

DNA sequence data

2984 E A R Q Q N K Y E N Y S T S F F I R D I I
GAAGCACGG CAGCAGAAT AAATATGAG AACTACAGC ACCAGCTTC TTCATCAGG GACATCATC

3047 K P D P P K N L Q M K P L K N S Q V E V S
AAACCAGAC CCGCCCAAG AACTTGCAG ATGAAGCCT TTGAAGAAC TCACAGGTG GAGGTCAGC

3110 W E Y P D S W S T P H S Y F S L K F F V R
TGGGAGTAC CCTGACTCC TGGAGCACT CCCCATTC TACTTCTCC CTCAAGTTC TTTGTTCTGA

3173 I Q R K K E K M K E T E E G C N Q K G A F
ATCCAGCGC AAGAAAGAA AAGATGAAG GAGACAGAG GAGGGGTGT AACCAGAAA GGTGCGTTC

3236 L V E K T S T E V Q C K G G N V C V Q A Q
CTCGTAGAG AAGACATCT ACCGAAGTC CAATGCAAA GCGGGGAAT GTCTGCGTG CAAGCTCAG

m-IL12 (linker) (3359-3403)

3299 D R Y Y N S S C S K W A C V P C R V R S G
GATCGTAT TACAATTC TCATGCAGC AAGTGGCA TGTGTTCC TGCAAGGTC CGATCCGGT

m-IL12 (Δ p35) (3404-3982)

3362 G G G S G G G G S G G G G S R V I P V S G
GGCGGTGGC TCGGGCGGT GGTGGGTCG GGTGGCGGC GGATCTAGG GTCATTCCA GTCTCTGGA

3425 P A R C L S Q S R N L L K T T D D M V K T
CCTGCCAGG TGTCTTAGC CAGTCCCGA AACCTGCTG AAGACCACA GATGACATG GTGAAGACG

3488 A R E K L K H Y S C T A E D I D H E D I T
GCCAGAGAA AAGCTGAAA CATTATTCC TGCACTGCT GAAGACATC GATCATGAA GACATCACA

3551 R D Q T S T L K T C L P L E L H K N E S C
CGGGACCAA ACCAGCACA TTGAAGACC TGTTTACCA CTGGAAC TAACAAGAAC GAGAGTTGC

3614 L A T R E T S S T T R G S C L P P Q K T S
CTGGCTACT AGAGAGACT TCTTCCACA ACAAGAGGG AGTGCCCTG CCCCCACAG AAGACGTCT

3677 L M M T L C L G S I Y E D L K M Y Q T E F
TTGATGATG ACCCTGTGC CTGTTAGC ATCTATGAG GACTTGAAG ATGTACCAG ACAGAGTTC

3740 Q A I N A A L Q N H N H Q Q I I L D K G M
CAGGCCATC AACGCAGCA CTTCAGAAT CACAACCAT CAGCAGATC ATTCTAGAC AAGGGCATG

3803 L V A I D E L M Q S L N H N G E T L R Q K
CTGGTGGCC ATCGATGAG CTGATGCAG TCTCTGAAT CATAATGGC GAGACTCTG CGCCAGAAA

pMT/BiP HRS3scFv-Fc-hi-IL12 (#1083)

3866 P P V G E A D P Y R V K M K L C I L L H A
CCTCCTGTG GGAGAAGCA GACCCTTAC AGAGTGAAA ATGAAGCTC TGCATCCTG CTTCACGCC

XhoI (3987)

F S T R V V T I N R V M G Y L S S A *
3929 TTCAGCACC CGCGTCGTG ACCATCAAC AGGGTGATG GGCTATCTG AGCTCCGCC TGACTCGAG

B.4 pMT/BiP HRS3scFv-Fc-IL2 (#1086)

Begin	End	Domain
851 bp	904 bp	BiP signal sequence
917 bp	1657 bp	HRS3 scFv
1670 bp	2368 bp	human Fc γ ₁
2378 bp	2776 bp	human IL-2

BiP signal sequence (851-904)

|
M K L C I L L A V V A F V G L S L G
842 GATCTCAAT ATGAAGTTA TGCATATTA CTGGCCGTC GTGGCCCTTT GTTGGCCCTC TCGCTCGGG

NcoI (912)

| HRS3 scFv (917-1657)
| |
R S P W V A Q V Q L Q Q S G A E L A R P G
905 AGATCTCCA TGGGTGGCC CAGGTGCAA CTGCAGCAG TCAGGGGCT GAGCTGGCT AGACCTGGG
A S V K M S C K A S G Y T F T T Y T I H W
968 GCTTCAGTG AAGATGTC TGAAGGCT TCTGGCTAC ACCTTTACT ACCTACACA ATACACTGG
V R Q R P G H D L E W I G Y I N P S S G Y
1031 GTAAGACAG AGGCCTGGA CACGATCTG GAATGGATT GGATACATT AATCCTAGC AGTGGATAT
S D Y N Q N F K G K T T L T A D K S S N T
1094 TCTGACTAC AATCAAAAC TTCAAGGGC AAGACCACA TTGACTGCA GACAAGTCC TCCAACACA
A Y M Q L N S L T S E D S A V Y Y C A R R
1157 GCCTACATG CAACTGAAC AGCCTGACA TCTGAGGAC TCTGCGGTC TATTACTGT GCAAGAAGA
A D Y G N Y E Y T W F A Y W G Q G T T V T
1220 GCGGACTAT GGTAACTAC GAATATACC TGGTTTGCT TACTGGGGC CAAGGGACC ACGGTACC
A S S S G G G S G G G G G S G G G G S D I E
1283 GCCTCTCA AGTGGAGGC GGTTCAGGT GGAGGTGGC TCTGGCGGT GCGGATCG GACATCGAG
L T Q S P K F M S T S V G D R V N V T Y K
1346 CTCACTCAG TCTC AAAA TTCATGTCC ACATCAGTA GGAGACAGG GTCAACGTC ACCTACAAG

1409 A S Q N V G T N V A W F Q Q K P G Q S P K
GCCAGTCAG AATGTGGGT ACTAATGTA GCCTGGTTT CAACAAAAA CCAGGGCAA TCTCTAAA
1472 V L I Y S A S Y R Y S G V P D R F T G S G
GTTCTGATT TACTCGGA TCTTACCGA TACAGTGA GTCCTGAT CGCTTACA GGCAGTGA
1535 S G T D F T L T I S N V Q S E D L A E Y F
TCTGGAACA GATTCACT CTCACCATC AGCAATGTG CAGTCTGAA GACTTGGCA GAGTATTC
1598 C Q Q Y H T Y P L T F G G G T K L E I K R
TGTCAGCAA TATCACACC TATCCTCTC ACGTTCGGA GGGGGCACC AAGCTGGAA ATCAAACGG

BamHI (1664)

| h-Fc γ 1 (1670-2368)
| |

1661 A D P A E P K S P D K T H T C P P C P A P
GGGATCCC GCCGAGCC AAATCTCCT GACAAAAC CACACATG CCACCGTG CCAGCACCT
1724 E L L G G P S V F L F P P K P K D T L M I
GAACTCTG GGGGACCG TCAGTCTTC CTCTTCCCC CCAAAACCC AAGGACACC CTCATGATC
1787 S R T P E V T C V V V D V S H E G P E V K
TCCCGGACC CCTGAGGTC ACATGCGTG GTGGTGGAC GTGAGCCAC GAAGGCCT GAGGTCAAG
1850 F N W Y V D G V E V H N A K T K P R E E Q
TTCAACTGG TACGTGGAC GCGTGGAG GTGCATAAT GCCAAGACA AAGCCGCG GAGGAGCAG
1913 Y N S T Y R V V S V L T V L H Q D W L N G
TACAACAGC ACGTACCGT GTGGTCAGC GTCCCTACC GTCCTGCAC CAGGACTGG CTGAATGGC
1976 K E Y K C K V S N K A L P A P I E K T I S
AAGGAGTAC AAGTGCAAG GTCTCCAAC AAAGCCCTC CCAGCCCCC ATCGAGAAA ACCATCTCC
2039 K A K G Q P R E P Q V Y T L P P S R D E L
AAAGCCAAA GGCAGCCC CGAGAACCA CAGGTGTAC ACCCTGCC CCATCCCGG GATGAGCTG
2102 T K N Q V S L T C L V K G F Y P S D I A V
ACCAAGAAC CAGGTGAGC CTGACCTGC CTGGTCAAA GGCTTCTAT CCCAGCGAC ATCGCCGTG
2165 E W E S N G Q P E N N Y K T T P P V L D S
GAGTGGGAG AGCAATGGG CAGCCGGAG AACAACTAC AAGACCAG CCTCCCGTG CTGGACTCC
2228 D G S F F L Y S K L T V D K S R W Q Q G N
GACGGCTCC TTCTTCTC TACAGCAAG CTCACCGTG GACAAGAGC AGGTGGCAG CAGGGGAAC

DNA sequence data

2291 V F S C S V M H E A L H N H Y T Q K S L S
GTCTTCTCA TGCTCCGTG ATGCATGAG GCTCTGCAC AACCACTAC ACGCAGAAG AGCCTCTCC

h-IL2 (2378-2776)

|
2354 L S P G K K D P A P T S S S T K K T Q L Q
CTGTCTCCG GGTAAAAA GATCTGCA CCTACTTCA AGTTCTACA AAGAAAAACA CAGTACTAA

2417 L E H L L L D L Q M I L N G I N N Y K N P
CTGGAGCAT TTACTGCTG GATTACAG ATGATTTTG AATGGAATT AATAATTAC AAGAATCCC

2480 K L T R V L T F K F Y M P K K A T E L K H
AAACTCACC AGGGTGCTC ACATTTAAG TTTTACATG CCCAAGAAG GCCACAGAA CTGAAACAT

2543 L Q C L E E E L K P L E E V L N L A Q S K
CTTCAGTGT CTAGAGAA GAACTCAA CCTCTGGAG GAAGTGCTA AATTTAGCT CAAAGCAAA

2606 N F H L R P R D L I S N I N V I V L E L K
AACTTTCAC TTAAGACCC AGGGACTTA ATCAGCAAT ATCAACGTA ATAGTTCTG GAACTAAAG

2669 G S E T T F M C E Y A D E T A T I V E F L
GGATCTGAA ACAACATTC ATGTGTGAA TATGCTGAT GAGACAGCA ACCATTGTA GAATTTCTA

XhoI (2786)

|
2732 N R W I T F C Q S I I S T L T *
AACAGATGG ATTACCTTT TGTCAAAGC ATCATCTCA AACTGACT TGAGTCGAC TCGAGTCTA

B.5 pMT/BiP HRS3scFv-hi-IL12-Fc-IL2 (#1100)

Begin	End	Domain
851 bp	904 bp	BiP signal sequence
917 bp	1657 bp	HRS3 scFv
1673 bp	1708 bp	hinge (human IgG ₁)
1712 bp	2650 bp	murine IL-12 (p40)
2651 bp	2695 bp	murine IL-12 (linker)
2696 bp	3274 bp	murine IL-12 (Δ p35)
3284 bp	3982 bp	human Fc γ ₁
3992 bp	4390 bp	human IL-2

BiP signal sequence (851-904)

|
M K L C I L L A V V A F V G L S L G
842 GATCTCAAT ATGAAGTTA TGCATATTA CTGGCCGTC GTGGCCTTT GTTGGCCTC TCGCTCGGG

NcoI (912)

| HRS3 scFv (917-1657)
| |
R S P W V A Q V Q L Q Q S G A E L A R P G
905 AGATCTCCA TGGGTGCC CAGGTGCAA CTGCAGCAG TCAGGGGCT GAGCTGGCT AGACCTGGG
A S V K M S C K A S G Y T F T T Y T I H W
968 GCTTCAGTG AAGATGTC TGCAAGGCT TCTGGCTAC ACCTTACT ACCTACACA ATACACTGG
V R Q R P G H D L E W I G Y I N P S S G Y
1031 GTAAGACAG AGGCCTGGA CACGATCTG GAATGGATT GGATACATT AATCCTAGC AGTGGATAT
S D Y N Q N F K G K T T L T A D K S S N T
1094 TCTGACTAC AATCAAAAC TTCAAGGCC AAGACCACA TTGACTGCA GACAAGTCC TCCAACACA
A Y M Q L N S L T S E D S A V Y Y C A R R
1157 GCCTACATG CAACTGAAC AGCCTGACA TCTGAGGAC TCTCGGTC TATTACTGT GCAAGAAGA
A D Y G N Y E Y T W F A Y W G Q G T T V T
1220 CCGGACTAT GGTAACTAC GAATATACC TGGTTTGCT TACTGGGGC CAAGGGACC ACGGTCAAC

DNA sequence data

1283 V S S S G G G S G G G G G S G G G G S D I E
 GTCTCTCA AGTGGAGGC GGTTCAGGT GGAGGTGGC TCTGGCGGT GGCGGATCG GACATCGAG

1346 L T Q S P K F M S T S V G D R V N V T Y K
 CTCACTCAG TCTCAAAA TTCATGTCC ACATCAGTA GGAGACAGG GTCAACGTC ACCTACAAG

1409 A S Q N V G T N V A W F Q Q K P G Q S P K
 GCCAGTCAG AATGTGGGT ACTAATGTA GCCTGGTTT CAACAAAAA CCAGGGCAA TCTCTAAA

1472 V L I Y S A S Y R Y S G V P D R F T G S G
 GTTCTGATT TACTCGGCA TCTTACCGA TACAGTGGG GTCCTGAT CGCTTACA GGCAGTGGG

1535 S G T D F T L T I S N V Q S E D L A E Y F
 TCTGGAACA GATTTCACT CTCACCATC AGCAATGTG CAGTCTGAA GACTTGGCA GAGTATTTT

1598 C Q Q Y H T Y P L T F G G G T K L E I K R
 TGTCAGCAA TATCACACC TATCCTCTC ACGTTCGGA GGGGGCACC AAGCTGGAA ATCAAAACGG

BamHI (1664) **m-IL12 (p40) (1712-2650)**
 | **hinge (h-IgG1) (1673-1708)** | **BstXI (1714)**
 | | |

1661 A D P T E P K S P D K T H T C P P M W E L
 GCGGATCCC ACCGAGCCC AAATCTCCT GACAAAAC TATACATGC CCACCAATG TGGGAGCTG

1724 E K D V Y V V E V D W T P D A P G E T V N
 GAGAAAGAC GTTTATGTT GTAGAGGTG GACTGGACT CCCGATGCC CCTGGAGAA ACAGTGAAC

BstXI (1842)

1787 L T C D T P E E D D I T W T S D Q R H G V
 CTCACCTGT GACACGCTT GAAGAAGAT GACATCACC TGGACCTCA GACCAGAGA CATGGAGTC

1850 I G S G K T L T I T V K E F L D A G Q Y T
 ATAGGCTCT GGAAAGACC CTGACCATC ACTGTCAAA GAGTTTCTA GATGCTGGC CAGTACACC

1913 C H K G G E T L S H S H L L L H K K E N G
 TGCCACAAA GGAGGCGAG ACTCTGAGC CACTCACAT CTGCTGCTC CACAAGAAG GAAAATGGA

1976 I W S T E I L K N F K N K T F L K C E A P
 ATTTGGTCC ACTGAAATT TTAAAAAAT TTCAAAAAC AAGACTTTC CTGAAGTGT GAAGCACCA

2039 N Y S G R F A C S W L V Q R N M D L K F N
 AATTACTCC GGACGGTTC GCGTGCTCA TGGCTGGTG CAAAGAAAC ATGGACTTG AAGTTCAAC

pMT/BiP HRS3scFv-hi-IL12-Fc-IL2 (#1100)

2102 I K S S S S P P D S R A V T C G M A S L S
ATCAAGAGC AGTAGCAGT CCCCCGAC TCTCGGGCA GTGACATGT GGAATGGCG TCTCTGTCT

2165 A E K V T L D Q R D Y E K Y S V S C Q E D
GCAGAGAAG GTCACACTG GACCAAAGG GACTATGAG AAGTATTCA GTGTCCTGC CAGGAGGAT

BstXI (2267)

2228 V T C P T A E E T L P I E L A L E A R Q Q
GTCACCTGC CCAACTGCC GAGGAGACC CTGCCATT GAAGTGGCG TTGGAAGCA CGGCAGCAG

2291 N K Y E N Y S T S F F I R D I I K P D P P
AATAAATAT GAGAACTAC AGCACCAGC TTCTTCATC AGGACATC ATCAAACCA GACCCGCC

2354 K N L Q M K P L K N S Q V E V S W E Y P D
AAGAACTTG CAGATGAAG CCTTTGAAG AACTCACAG GTGGAGGTC AGCTGGGAG TACCCTGAC

2417 S W S T P H S Y F S L K F F V R I Q R K K
TCCTGGAGC ACTCCCAT TCCTACTTC TCCCTCAAG TTCTTTGTT CGAATCCAG CGCAAGAAA

2480 E K M K E T E E G C N Q K G A F L V E K T
GAAAAGATG AAGGAGACA GAGGAGGG TGTAACCAG AAAGTGGCG TTCCTCGTA GAGAAGACA

2543 S T E V Q C K G G N V C V Q A Q D R Y Y N
TCTACCGAA GTCCAATGC AAAGCGGG AATGTCTGC GTGCAAGCT CAGGATCGC TATTACAAT

m-IL12 (linker) (2651-2695)

2606 S S C S K W A C V P C R V R S G G G G S G
TCCTCATGC AGCAAGTGG GCATGTGTT CCCTGCAGG GTCCGATCC GGTGGCGGT GGCTCGGG

m-IL12 (Δ p35) (2696-3274)

2669 G G G S G G G G S R V I P V S G P A R C L
GGTGGTGGG TCGGGTGGC GCGGATCT AGGGTCATT CCAGTCTCT GGACCTGCC AGGTGTCTT

2732 S Q S R N L L K T T D D M V K T A R E K L
AGCCAGTCC CGAAACCTG CTGAAGACC ACAGATGAC ATGGTGAAG ACGGCCAGA GAAAAGCTG

2795 K H Y S C T A E D I D H E D I T R D Q T S
AAACATTAT TCCTGCACT GCTGAAGAC ATCGATCAT GAAGACATC ACACGGGAC CAAACCAGC

2858 T L K T C L P L E L H K N E S C L A T R E
ACATTGAAG ACCTGTTTA CCACTGGAA CTACACAAG AACGAGAGT TGCTTGCT ACTAGAGAG

DNA sequence data

2921 T S S T T R G S C L P P Q K T S L M M T L
ACTTCTTC ACAACAAGA GGGAGCTGC CTGCCCCCA CAGAAGACG TCTTTGATG ATGACCCTG

2984 C L G S I Y E D L K M Y Q T E F Q A I N A
TGCCTTGGT AGCATCTAT GAGGACTTG AAGATGTAC CAGACAGAG TTCCAGGCC ATCAACGCA

3047 A L Q N H N H Q Q I I L D K G M L V A I D
GCACTTCAG AATCACAAC CATCAGCAG ATCATTCTA GACAAGGGC ATGCTGGTG GCCATCGAT

3110 E L M Q S L N H N G E T L R Q K P P V G E
GAGCTGATG CAGTCTCTG AATCATAAT GGCGAGACT CTGCGCCAG AAACCTCCT GTGGGAGAA

3173 A D P Y R V K M K L C I L L H A F S T R V
GCAGACCCT TACAGAGTG AAAATGAAG CTCTGCATC CTGCTTAC GCCTTCAGC ACCCGCGTC

h-Fcγ1 (3284–3982)

|

3236 V T I N R V M G Y L S S A G D P A E P K S
GTGACCATC AACAGGGTG ATGGGCTAT CTGAGCTCC GCCGGAGAT CCCGCCGAG CCCAAATCT

3299 P D K T H T C P P C P A P E L L G G P S V
CCTGACAAA ACTCACACA TGCCACCG TGCCAGCA CCTGAACTC CTGGGGGA CCGTCAGTC

3362 F L F P P K P K D T L M I S R T P E V T C
TTCCTTTC CCCCCAAA CCCAAGGAC ACCCTCATG ATCTCCCGG ACCCCTGAG GTCACATGC

3425 V V V D V S H E G P E V K F N W Y V D G V
GTGGTGGTG GACGTGAGC CACGAAGGC CTGAGGTC AAGTTCAAC TGGTACGTG GACGGCGTG

3488 E V H N A K T K P R E E Q Y N S T Y R V V
GAGGTGCAT AATGCCAAG ACAAAGCCG CGGGAGGAG CAGTACAAC AGCACGTAC CGTGTGGTC

3551 S V L T V L H Q D W L N G K E Y K C K V S
AGCGTCTC ACCGTCCTG CACCAGGAC TGGCTGAAT GGCAAGGAG TACAAGTGC AAGTCTCC

3614 N K A L P A P I E K T I S K A K G Q P R E
AACAAAGCC CTCCAGCC CCCATCGAG AAAACCATC TCCAAAGCC AAAGGGCAG CCCCAGAA

3677 P Q V Y T L P P S R D E L T K N Q V S L T
CCACAGGTG TACACCCTG CCCCATCC CGGGATGAG CTGACCAAG AACCAAGTC AGCCTGACC

3740 C L V K G F Y P S D I A V E W E S N G Q P
TGCTGGTC AAAGGCTTC TATCCAGC GACATCGCC GTGGAGTGG GAGAGCAAT GGGCAGCCG

pMT/BiP HRS3scFv-hi-IL12-Fc-IL2 (#1100)

3803 E N N Y K T T P P V L D S D G S F F L Y S
GAGAACAAC TACAAGACC ACGCCTCCC GTGCTGGAC TCCGACGGC TCCTTCTTC CTCTACAGC

3866 K L T V D K S R W Q Q G N V F S C S V M H
AAGCTCACC GTGACAAG AGCAGGTGG CAGCAGGGG AACGCTTTC TCATGTCTC GTGATGCAT

3929 E A L H N H Y T Q K S L S L S P G K K D P
GAGGCTCTG CACAACCAC TACACGCAG AAGAGCCTC TCCCTGTCT CCGGGTAAA AAAGATCCT

h-IL2 (3992-4390)

|
3992 A P T S S S T K K T Q L Q L E H L L L D L
GCACCTACT TCAAGTCTT ACAAGAAA ACACAGCTA CAACTGGAG CATTTACTG CTGATTTA

4055 Q M I L N G I N N Y K N P K L T R V L T F
CAGATGATT TTGAATGGA ATTAATAAT TACAAGAAT CCCAAACTC ACCAGGGTG CTCACATTI

4118 K F Y M P K K A T E L K H L Q C L E E E L
AAGTTTTAC ATGCCCAAG AAGGCCACA GAAGTAAA CATCTTCAG TGCTAGAA GAAGAACTC

4181 K P L E E V L N L A Q S K N F H L R P R D
AAACCTCTG GAGGAAGTG CTAAATTTA GCTCAAAGC AAAAACTTT CACTTAAGA CCCAGGGAC

4244 L I S N I N V I V L E L K G S E T T F M C
TTAATCAGC AATATCAAC GTAATAGTT CTGGAACTA AAGGGATCT GAAACAACA TTCATGTGT

4307 E Y A D E T A T I V E F L N R W I T F C Q
GAATATGCT GATGAGACA GCAACCATT GTAGAATT CTAAACAGA TGGATTACC TTTGTCAA

XhoI (4400)

|
4370 S I I S T L T *
AGCATCATC TCAACACTG ACTTGAGTC GACTCGAGT CTAGAGGGC CCTTCGAAG GTAAGCCTA

B.6 pMT/BiP SCA431scFv-Fc (#1103)

Begin	End	Domain
851 bp	904 bp	BiP signal sequence
917 bp	1660 bp	SCA431 scFv
1661 bp	2341 bp	murine Fc γ ₁

BiP signal sequence (851-904)

|
M K L C I L L A V V A F V G L S L G
842 GATCTCAAT ATGAAGTTA TGCATATTA CTGGCCGTC GTGGCCCTTT GTTGGCCTC TCGCTCGGG

NcoI (912)

| SCA431 scFv (917-1660)
| |
R S P W R G V H S Q V Q L Q E S G P D L V
905 AGATCTCCA TGGAGAGGT GTCCACTCC CAGGTCCAA CTGCAGGAG TCAGGACCT GACCTGGTG
K P S Q S L S L T C T V T G Y S I T S G Y
968 AAACCTTCT CAGTCACTT TCACTCACC TGCCTGTG ACTGGCTAC TCATCACC AGTGGTTAT

BamHI (1042)

|
S W H W I R Q F P G N K L E W M G Y I Q Y
1031 AGCTGGCAC TGGATCCGG CAGTTTCCA GGAAACAAA CTGGAATGG ATGGGCTAC ATACAATAC

XhoI (1144)

|
S G I T N Y N P S L K S R I S I T R D T S
1094 AGTGGTATC ACTAACTAC AACCCCTCT CTCAAAAGT CGAATCTCT ATCACTCGA GACACATCC

EcoRI (1181)

|
K N Q F F L Q L N S V T T E D T A T Y Y C
1157 AAGAACCAG TTCTTCCTG CAGTTGAAT TCTGTGACT ACTGAGGAC ACAGCCACA TATTACTGT
A R E D Y D Y H W Y F D V W G Q G T T V T
1220 GCAAGAGAA GACTATGAT TACCACTGG TACTTCGAT GTCTGGGGC CAAGGGACC ACGGTCACC

1283 V S S G G G G S G G G G G S G G G G S D I Q
GTCTCCTCA GGAGGTGGT GGATCGGGC GGTGGCGGG TCGGGTGGC GGCGGATCT GACATCCAG

1346 L T Q S P A I M S A S L G E E I T L T C S
CTGACCCAG TCTCCAGCA ATCATGTCT GCATCTCTA GGGGAGGAG ATCACCCCTA ACCTGCAGT

XhoI (1415)

|
1409 A S S S V S Y M H W Y Q Q K S G T S P K L
GCCAGCTCG AGTGTAAGT TACATGCAC TGGTACCAG CAGAAGTCA GGCACTTCT CCCAAACTC

1472 L I Y S T S N L A S G V P S R F S G S G S
TTGATTAT AGCACATCC AACCTGGCT TCTGGAGTC CCTTCTCGC TTCAGTGGC AGTGGGTCT

1535 G T F Y S L T I S S V E A E D A A D Y Y C
GGGACCTTT TATCTCTC ACAATCAGC AGTGTGGAG GCTGAAGAT GCTGCCGAT TATTACTGC

1598 H Q W S S Y P T F G G G T K L E I K V D P
CATCAGTGG AGTAGTTAT CCCACGTTT GGAGGGGGG ACCAAGCTG GAGATCAAA GTAGATCCT

m-Fcγ1 (1661-2341)

|
1661 V P R D G G C K P C I C T V P E V S S V F
GTGCCCAGG GATGGTGGT TGTAAGCCT TGCATATGT ACAGTCCCA GAAGTATCA TCTGTCTTC

1724 I F P P K P K D V L T I T L T P K V T C V
ATCTTCCCC CCAAAGCCC AAGGATGTG CTCACCATT ACTCTGACT CCTAAGGTC ACGTGTGTT

1787 V V D I S K D D P E V Q F S W F V D D V E
GTGGTAGAC ATCAGCAAG GATGATCCC GAGGTCCAG TTCAGCTGG TTTGTAGAT GATGTGGAG

1850 V H T A Q T Q P R E E Q F N S T F R S V S
GTGCACACA GCTCAGACG CAACCCCGG GAGGAGCAG TTCAACAGC ACTTTCGCG TCAGTCAGT

1913 E L P I M H Q D W L N G K E F K C R V N S
GAACTTCCC ATCATGCAC CAGGACTGG CTCAATGGC AAGGAGTTC AAATGCAGG GTCAACAGT

1976 A A F P A P I E K T I S K T K G R P K A P
GCAGCTTTC CCTGCCCC ATCGAGAAA ACCATCTCC AAAACCAA GGCAGACCG AAGGCTCCA

2039 Q V C T I P P P K E Q M A K D K V S L T C
CAGTGTGTC ACCATTCCA CCTCCCAAG GAGCAGATG GCCAAGGAT AAAGTCAGT CTGACCTGC

2102 M I T D F F P E D I T V E W Q W N G Q P A
ATGATAACA GACTTCTTC CCTGAAGAC ATTACTGTG GAGTGGCAG TGAATGGG CAGCCAGCG

DNA sequence data

2165 E N Y K N T Q P I M D T D G S Y F V Y S K
GAGAACTAC AAGAACT CAGCCATC ATGGACACA GATGGCTCT TACTTCGTC TACAGCAAG

2228 L N V Q K S N W E A G N T F T C S V L H E
CTCAATGTG CAGAAGAGC AACTGGGAG GCAGGAAAT ACTTTCACC TGCTCTGTG TTACATGAG

XhoI (2353)

NotI (2347) |

BstXI (2334) | |

2291 G L H N H H T E K S L S H S P G K *
GGCCTGCAC AACCAACAT ACTGAGAAG AGCCTCTCC CACTCTCCT GGTAAGTGA GCGGCCGCT

B.7 pMT/BiP SCA431scFv-Fc-IL7 (#1117)

Begin	End	Domain
851 bp	904 bp	BiP signal sequence
917 bp	1660 bp	SCA431 scFv
1661 bp	2341 bp	murine Fc γ ₁
2342 bp	2728 bp	murine IL-7

BiP signal sequence (851-904)

|
M K L C I L L A V V A F V G L S L G
842 GATCTCAAT ATGAAGTTA TGCATATTA CTGGCCGTC GTGGCCCTT GTTGGCCTC TCGCTCGGG

NcoI (912)

| SCA431 scFv (917-1660)
| |
R S P W R G V H S Q V Q L Q E S G P D L V
905 AGATCTCCA TGGAGAGGT GTCCACTCC CAGGTCCAA CTGCAGGAG TCAGGACCT GACCTGGTG
K P S Q S L S L T C T V T G Y S I T S G Y
968 AAACCTTCT CAGTCACTT TCACTCACC TGCAGTGTG ACTGGCTAC TCCATCACC AGTGGTTAT

BamHI (1042)

|
S W H W I R Q F P G N K L E W M G Y I Q Y
1031 AGCTGGCAC TGGATCCGG CAGTTTCCA GAAACAAA CTGGAATGG ATGGGCTAC ATACAATAC

XhoI (1144)

|
S G I T N Y N P S L K S R I S I T R D T S
1094 AGTGGTATC ACTAACTAC AACCCCTCT CTCAAAAGT CGAATCTCT ATCACTCGA GACACATCC

EcoRI (1181)

|
K N Q F F L Q L N S V T T E D T A T Y Y C
1157 AAGAACCAG TTCTTCTGT CAGTTGAAT TCTGTGACT ACTGAGGAC ACAGCCACA TATTACTGT
A R E D Y D Y H W Y F D V W G Q G T T V T
1220 GCAAGAGAA GACTATGAT TACCACTGG TACTTCGAT GTCTGGGGC CAAGGGACC ACGGTCACC

DNA sequence data

1283 V S S G G G G S S G G G G S G G G G S D I Q
GTCTCTCA GGAGGTGGT GGATCGGGC GGTGGCGGG TCGGGTGGC GCGCGATCT GACATCCAG

1346 L T Q S P A I M S A S L G E E I T L T C S
CTGACCCAG TCTCCAGCA ATCATGTCT GCATCTCTA GGGGAGGAG ATCACCTA ACCTGCAGT

XhoI (1415)

|

1409 A S S S V S Y M H W Y Q Q K S G T S P K L
GCCAGCTCG AGTGTAAGT TACATGCAC TGGTACCAG CAGAAGTCA GGCACCTCT CCCAAACTC

1472 L I Y S T S N L A S G V P S R F S G S G S
TTGATTAT AGCACATCC AACCTGGCT TCTGGAGTC CCTTCTCGC TTCAGTGGC AGTGGGTCT

1535 G T F Y S L T I S S V E A E D A A D Y Y C
GGGACTTT TATTCTCTC ACAATCAGC AGTGTGGAG GCTGAAGAT GCTGCCGAT TATTACTGC

1598 H Q W S S Y P T F G G G T K L E I K V D P
CATCAGTGG AGTAGTTAT CCCACGTTC GGAGGGGGG ACCAAGCTG GAGATCAAA GTAGATCTT

m-Fcγ1 (1661-2341)

|

1661 V P R D G G C K P C I C T V P E V S S V F
GTGCCCAGG GATGGTGGT TGTAAGCCT TGCATATGT ACAGTCCCA GAAGTATCA TCTGTCTTC

1724 I F P P K P K D V L T I T L T P K V T C V
ATCTTCCC CCAAAGCCC AAGGATGTG CTCACCATT ACTCTGACT CCTAAGGTC ACGTGTGTT

1787 V V D I S K D D P E V Q F S W F V D D V E
GTGGTAGAC ATCAGCAAG GATGATCCC GAGGTCCAG TTCAGCTGG TTTGTAGAT GATGTGGAG

1850 V H T A Q T Q P R E E Q F N S T F R S V S
GTGCACACA GCTCAGACG CAACCCCGG GAGGAGCAG TTCAACAGC ACTTTCCGC TCAGTCAGT

1913 E L P I M H Q D W L N G K E F K C R V N S
GAACTTCCC ATCATGCAC CAGGACTGG CTCAATGGC AAGGAGTTC AAATGCAGG GTCAACAGT

1976 A A F P A P I E K T I S K T K G R P K A P
GCAGCTTTC CCTGCCCC ATCGAGAAA ACCATCTCC AAAACCAA GGCAGACCG AAGGCTCCA

2039 Q V C T I P P P K E Q M A K D K V S L T C
CAGGTGTGC ACCATTCCA CCTCCAAG GAGCAGATG GCCAAGGAT AAAGTCAGT CTGACCTGC

2102 M I T D F F P E D I T V E W Q W N G Q P A
ATGATAACA GACTTCTTC CCTGAAGAC ATTACTGTG GAGTGGCAG TGAATGGG CAGCCAGCG

2165 E N Y K N T Q P I M D T D G S Y F V Y S K
GAGAACTAC AAGAACACT CAGCCCATC ATGGACACA GATGGCTCT TACTTCGTC TACAGCAAG

2228 L N V Q K S N W E A G N T F T C S V L H E
CTCAATGTG CAGAAGAGC AACTGGGAG GCAGGAAAT ACTTTCACC TGCTCTGTG TTACATGAG

BstXI (2334)

| m-IL7 (2342-2728)

|

|

2291 G L H N H H T E K S L S H S P G K E C H I
GGCCTGCAC AACCACCAT ACTGAGAAG AGCCTCTCC CACTCTCCT GGTAAGGAG TGCACATT

2354 K D K E G K A Y E S V L M I S I D E L D K
AAAGACAAA GAAGGTAAA GCATATGAG AGTGTACTG ATGATCAGC ATCGATGAA TTGGACAAA

2417 M T G T D S N C P N N E P N F F R K H V C
ATGACAGGA ACTGATAGT AATTGCCCG AATAATGAA CCAAACHTT TTTAGAAAA CATGTATGT

2480 D D T K E A A F L N R A A R K L K Q F L K
GATGATACA AAGGAAGCT GCTTTTCTA AATCGTGCT GCTCGCAAG TTGAAGCAA TTTCTTAAA

EcoRI (2559)

|

2543 M N I S E E F N V H L L T V S Q G T Q T L
ATGAATATC AGTGAAGAA TTCAATGTC CACTTACTA ACAGTATCA CAAGGCACA CAAACACTG

2606 V N C T S K E E K N V K E Q K K N D A C F
GTGAACTGC ACAAGTAAG GAAGAAAA AACGTAAAG GAACAGAAA AAGAATGAT GCATGTTC

2669 L K R L L R E I K T C W N K I L K G S I *
CTAAAGAGA CTA CTACTGAGA GAAATAAAA ACTTGTGTG AATAAAAT TTTGAAGGC AGTATATGA

NotI (2734)

| XhoI (2740)

|

|

2732 GCGGCCGCT CGAGTCTAG AGGGCCCTT CGAAGGTAA GCCTATCCC TAACCCTCT CCTCGGTCT

B.8 pMT/BiP SCA431scFv-Fc-IL15 (#1118)

Begin	End	Domain
851 bp	904 bp	BiP signal sequence
917 bp	1660 bp	SCA431 scFv
1661 bp	2341 bp	murine Fc γ ₁
2342 bp	2683 bp	human IL-15

BiP signal sequence (851-904)

|
M K L C I L L A V V A F V G L S L G
842 GATCTCAAT ATGAAGTTA TGCATATTA CTGGCCGTC GTGGCCTTT GTTGGCCTC TCGCTCGGG

NcoI (912)

| SCA431 scFv (917-1660)
| |
R S P W R G V H S Q V Q L Q E S G P D L V
905 AGATCTCCA TGGAGAGGT GTCCACTCC CAGGTCCAA CTGCAGGAG TCAGGACCT GACCTGGTG
K P S Q S L S L T C T V T G Y S I T S G Y
968 AAACCTTCT CAGTCACTT TCACTCACC TGCCTGTG ACTGGCTAC TCCATCACC AGTGGTTAT

BamHI (1042)

|
S W H W I R Q F P G N K L E W M G Y I Q Y
1031 AGCTGGCAC TGGATCCGG CAGTTTCCA GGAAACAAA CTGGAATGG ATGGGCTAC ATACAATAC

XhoI (1144)

|
S G I T N Y N P S L K S R I S I T R D T S
1094 AGTGGTATC ACTAACTAC AACCCCTCT CTCAAAAGT CGAATCTCT ATCACTCGA GACACATCC

EcoRI (1181)

|
K N Q F F L Q L N S V T T E D T A T Y Y C
1157 AAGAACCAG TTCTTCCTG CAGTTGAAT TCTGTGACT ACTGAGGAC ACAGCCACA TATTACTGT
A R E D Y D Y H W Y F D V W G Q G T T V T
1220 GCAAGAGAA GACTATGAT TACCACTGG TACTTCGAT GTCTGGGGC CAAGGGACC ACGGTCACC

1283 V S S G G G G S G G G G G S G G G G S D I Q
GTCTCTCA GGAGGTGGT GGATCGGC GGTGGCGGG TCGGGTGGC GGCGGATCT GACATCCAG

1346 L T Q S P A I M S A S L G E E I T L T C S
CTGACCCAG TCTCCAGCA ATCATGTCT GCATCTCTA GGGGAGGAG ATCACCCCTA ACCTGCAGT

XhoI (1415)

|
1409 A S S S V S Y M H W Y Q Q K S G T S P K L
GCCAGCTCG AGTGTAAGT TACATGCAC TGGTACCAG CAGAAGTCA GGCACTTCT CCCAAACTC

1472 L I Y S T S N L A S G V P S R F S G S G S
TTGATTAT AGCACATCC AACCTGGCT TCTGGAGTC CCTTCTCGC TTCAGTGGC AGTGGGTCT

1535 G T F Y S L T I S S V E A E D A A D Y Y C
GGGACCTTT TATCTCTC ACAATCAGC AGTGTGGAG GCTGAAGAT GCTGCCGAT TATTACTGC

1598 H Q W S S Y P T F G G G T K L E I K V D P
CATCAGTGG AGTAGTTAT CCCACGTTT GGAGGGGGG ACCAAGCTG GAGATCAAA GTAGATCCT

m-Fcγ1 (1661-2341)

|
1661 V P R D G G C K P C I C T V P E V S S V F
GTGCCCAGG GATGGTGGT TGTAAGCCT TGCATATGT ACAGTCCCA GAAGTATCA TCTGTCTTC

1724 I F P P K P K D V L T I T L T P K V T C V
ATCTTCCCC CCAAAGCCC AAGGATGTG CTCACCATT ACTCTGACT CCTAAGGTC ACGTGTGTT

1787 V V D I S K D D P E V Q F S W F V D D V E
GTGGTAGAC ATCAGCAAG GATGATCCC GAGGTCCAG TTCAGCTGG TTTGTAGAT GATGTGGAG

1850 V H T A Q T Q P R E E Q F N S T F R S V S
GTGCACACA GCTCAGACG CAACCCCGG GAGGAGCAG TTCAACAGC ACTTTCGCG TCAGTCAGT

1913 E L P I M H Q D W L N G K E F K C R V N S
GAACTTCCC ATCATGCAC CAGGACTGG CTCAATGGC AAGGAGTTC AAATGCAGG GTCAACAGT

1976 A A F P A P I E K T I S K T K G R P K A P
GCAGCTTTC CCTGCCCC ATCGAGAAA ACCATCTCC AAAACCAA GGCAGACCG AAGGCTCCA

2039 Q V C T I P P P K E Q M A K D K V S L T C
CAGTGTGC ACCATTCCA CCTCCAAG GAGCAGATG GCCAAGGAT AAAGTCAGT CTGACCTGC

2102 M I T D F F P E D I T V E W Q W N G Q P A
ATGATAACA GACTTCTTC CCTGAAGAC ATTACTGTG GAGTGGCAG TGAATGGG CAGCCAGCG

DNA sequence data

2165 E N Y K N T Q P I M D T D G S Y F V Y S K
GAGAACTAC AAGAACT CAGCCATC ATGGACACA GATGGCTCT TACTTCGTC TACAGCAAG

2228 L N V Q K S N W E A G N T F T C S V L H E
CTCAATGTG CAGAAGAGC AACTGGGAG GCAGGAAAT ACTTTCACC TGCTCTGTG TTACATGAG

BstXI (2334)

| h-IL15 (2342-2683)

| |

2291 G L H N H H T E K S L S H S P G K N W V N
GGCCTGCAC AACCACCAT ACTGAGAAG AGCCTCTCC CACTCTCCT GGTAAGAAC TGGGTGAAT

2354 V I S D L K K I E D L I Q S M H I D A T L
GTAATAAGT GATTTGAAA AAAATTGAA GATCTTATT CAATCTATG CATATTGAT GCTACTTTA

2417 Y T E S D V H P S C K V T A M K C F L L E
TATACGGAA AGTGATGTT CACCCAGT TGCAAAGTA ACAGCAATG AAGTGCTTT CTCTTGGAG

2480 L Q V I S L E S G D A S I H D T V E N L I
TTACAAGTT ATTTCACTT GAGTCCGGA GATGCAAGT ATTCATGAT ACAGTAGAA AATCTGATC

2543 I L A N N S L S S N G N V T E S G C K E C
ATCCTAGCA AACAACAGT TTGTCTTCT AATGGGAAT GTAACAGAA TCTGGATGC AAAGAATGT

2606 E E L E E K N I K E F L Q S F V H I V Q M
GAGGAACTG GAGGAAAAA AATATTA AAATTTTGT CAGAGTTT GTACATATT GTCCAAATG

NotI (2689)

| XhoI (2695)

| |

2669 F I N T S *
TTCATCAAC ACTTCTTGA GCGGCCGCT CGAGTCTAG AGGGCCCTT CGAAGGTAA GCCTATCCC

C äktaPrime™ methods

Methods for the äktaPrime™ chromatograph can be stored as plain text files in the directory C:\UNICORN\Bin\Prime\. Such methods are run from the main menu with the commands Run Stored Method, OK, From PC and OK. The method number is entered and OK is pressed twice to start the method. The äktaPrime™ should be set-up as follows:

Injection Valve: 2 connected to column output
4 blocked with a stop plug
6 connected to column input

Buffer inlets: A1 PBS
B 100 mM glycine buffer (pH 3.0)

Each run is split into two parts so that an operator may respond to problems during conditioning. The method “conditioning” flushes inlet tubing with the connected buffers to remove trapped air bubbles and save time during elution. When the procedure has finished, buffer inlet A1 has to be immersed in a flask containing PBS with 0.1% (w/v) sodium azide. The “elution” method then elutes the protein and washes the column.

C.1 Purification of immunocytokines

C.1.1 1 ml HiTrap™ HP column (Conditioning)

```

1 *****
2 ** Method Dump
3 **
4 ** AKTAprime Ver , V2.01
5 **
6 ** Dump Format Ver , V1.00
7 **
8 *****
9
10
11 *****
12 ** Method Settings
13 *****
14 Method Type , -
15 Method , -
16 Method base , ml
17 Frac base , ml
18 Max pressure (kPa) , 500
19 Alarm (min/ml) , 0.0
20
21 *****
22 ** Method Breakpoints
23 *****
24
25 Brkp Volume Conc Flow Frac Buff Inj Peak Autozero Eventmark
26 (mAu/min)
27
28 ,1 ,0.0 ,100 ,50.0 ,0.0 ,1 ,Waste ,0 ,N ,N
29 ,2 ,19.9 ,100 ,50.0 ,0.0 ,1 ,Waste ,0 ,N ,N
30 ,3 ,20.0 ,0 ,50.0 ,0.0 ,1 ,Waste ,0 ,N ,N
31 ,4 ,69.5 ,0 ,1.0 ,0.0 ,1 ,Waste ,0 ,N ,N
32 ,5 ,70.0 ,0 ,1.0 ,0.0 ,1 ,Inj ,0 ,N ,Y
33 ,6 ,80.0 ,0 ,1.0 ,0.0 ,1 ,Inj ,0 ,Y ,Y
34 ,7 ,90.0 ,0 ,1.0 ,0.0 ,1 ,Inj ,0 ,Y ,N

```

C.1.2 1 ml HiTrap™ HP column (Elution)

```

1  ****
2  ** Method Dump
3  **
4  ** AKTAprime Ver , V2.01
5  **
6  ** Dump Format Ver , V1.00
7  **
8  ****
9
10
11 ****
12 ** Method Settings
13 ****
14 Method Type , -
15 Method , -
16 Method base , ml
17 Frac base , ml
18 Max pressure (kPa) , 500
19 Alarm (min/ml) , 0.0
20
21 ****
22 ** Method Breakpoints
23 ****
24
25 Brkpk Volume Conc Flow Frac Buff Inj Peak Autozero Eventmark
26 (mAu/min)
27
28 ,1 ,0.0 ,100 ,1.0 ,0.0 ,1 ,Inj ,0 ,N ,Y
29 ,2 ,1.0 ,100 ,1.0 ,0.0 ,1 ,Inj ,0 ,Y ,Y
30 ,3 ,5.0 ,100 ,1.0 ,1.5 ,1 ,Inj ,10.0 ,N ,Y
31 ,4 ,25.0 ,100 ,1.0 ,0.0 ,1 ,Inj ,0 ,N ,Y
32 ,5 ,39.9 ,100 ,1.0 ,0.0 ,1 ,Inj ,0 ,N ,N
33 ,6 ,40.0 ,0 ,1.0 ,0.0 ,1 ,Inj ,0 ,N ,Y
34 ,7 ,70.0 ,0 ,1.0 ,0.0 ,1 ,Waste ,0 ,N ,N

```

C.1.3 5ml HiTrap™ HP column (Conditioning)

```
1 *****
2 ** Method Dump
3 **
4 ** AKTAprime Ver , V2.01
5 **
6 ** Dump Format Ver , V1.00
7 **
8 *****
9
10
11 *****
12 ** Method Settings
13 *****
14 Method Type , -
15 Method , -
16 Method base , ml
17 Frac base , ml
18 Max pressure (kPa) , 500
19 Alarm (min/ml) , 0.0
20
21 *****
22 ** Method Breakpoints
23 *****
24
25 Brkp Volume Conc Flow Frac Buff Inj Peak Autozero Eventmark
26 (mAu/min)
27
28 ,1 ,0.0 ,100 ,50.0 ,0.0 ,1 ,Waste ,0 ,N ,N
29 ,2 ,19.9 ,100 ,50.0 ,0.0 ,1 ,Waste ,0 ,N ,N
30 ,3 ,20.0 ,0 ,50.0 ,0.0 ,1 ,Waste ,0 ,N ,N
31 ,4 ,69.0 ,0 ,2.5 ,0.0 ,1 ,Waste ,0 ,N ,N
32 ,5 ,70.0 ,0 ,2.5 ,0.0 ,1 ,Inj ,0 ,N ,Y
33 ,6 ,95.0 ,0 ,2.5 ,0.0 ,1 ,Inj ,0 ,Y ,Y
34 ,7 ,120.0 ,0 ,2.5 ,0.0 ,1 ,Inj ,0 ,Y ,N
```

C.1.4 5 ml HiTrap™ HP column (Elution)

```

1  *****
2  ** Method Dump
3  **
4  ** AKTAprime   Ver   , V2.01
5  **
6  ** Dump Format Ver   , V1.00
7  **
8  *****
9
10
11 *****
12 ** Method Settings
13 *****
14 Method Type      ,-
15 Method           ,-
16 Method base     ,ml
17 Frac base       ,ml
18 Max pressure (kPa) ,500
19 Alarm (min/ml)  ,0.0
20
21 *****
22 ** Method Breakpoints
23 *****
24
25 Brkpk Volume    Conc Flow  Frac   Buff Inj   Peak   Autozero Eventmark
26                                     (mAu/min)
27
28 ,1  ,0.0      ,100 ,2.5 ,0.0  ,1  ,Inj  ,0    ,N    ,Y
29 ,2  ,1.0      ,100 ,2.5 ,0.0  ,1  ,Inj  ,0    ,Y    ,Y
30 ,3  ,5.0      ,100 ,2.5 ,1.5  ,1  ,Inj  ,20.0 ,N    ,Y
31 ,4  ,50.0     ,100 ,2.5 ,0.0  ,1  ,Inj  ,0    ,N    ,Y
32 ,5  ,99.9     ,100 ,2.5 ,0.0  ,1  ,Inj  ,0    ,N    ,N
33 ,6  ,100.0    ,0   ,2.5 ,0.0  ,1  ,Inj  ,0    ,N    ,Y
34 ,7  ,250.0    ,0   ,2.5 ,0.0  ,1  ,Waste ,0    ,N    ,N

```

C.1.5 C10/10™ column packed with Sepharose™ beads (Conditioning)

```

1 *****
2 ** Method Dump
3 **
4 ** AKTAprime Ver , V2.01
5 **
6 ** Dump Format Ver , V1.00
7 **
8 *****
9
10
11 *****
12 ** Method Settings
13 *****
14 Method Type , -
15 Method , -
16 Method base , ml
17 Frac base , ml
18 Max pressure (kPa) , 500
19 Alarm (min/ml) , 0.0
20
21 *****
22 ** Method Breakpoints
23 *****
24
25 Brkp Volume Conc Flow Frac Buff Inj Peak Autozero Eventmark
26 (mAu/min)
27
28 ,1 ,0.0 ,100 ,50.0 ,0.0 ,1 ,Waste ,0 ,N ,N
29 ,2 ,19.9 ,100 ,50.0 ,0.0 ,1 ,Waste ,0 ,N ,N
30 ,3 ,20.0 ,0 ,50.0 ,0.0 ,1 ,Waste ,0 ,N ,N
31 ,4 ,69.0 ,0 ,2.0 ,0.0 ,1 ,Waste ,0 ,N ,N

```


**C.1.6 C10/10™ column packed with Sepharose™ beads
(Elution)**

```
1 *****
2 ** Method Dump
3 **
4 ** AKTAprime Ver , V2.01
5 **
6 ** Dump Format Ver , V1.00
7 **
8 *****
9
10
11 *****
12 ** Method Settings
13 *****
14 Method Type , -
15 Method , -
16 Method base , ml
17 Frac base , ml
18 Max pressure (kPa) , 500
19 Alarm (min/ml) , 0.0
20
21 *****
22 ** Method Breakpoints
23 *****
24
25 Brkp Volume Conc Flow Frac Buff Inj Peak Autozero Eventmark
26 (mAu/min)
27
28 ,1 ,0.0 ,100 ,2.0 ,0.0 ,1 ,Inj ,0 ,N ,Y
29 ,2 ,1.0 ,100 ,2.0 ,0.0 ,1 ,Inj ,0 ,Y ,Y
30 ,3 ,5.0 ,100 ,2.0 ,1.5 ,1 ,Inj ,20.0 ,N ,Y
31 ,4 ,60.0 ,100 ,2.0 ,0.0 ,1 ,Inj ,0 ,N ,Y
32 ,5 ,119.9 ,100 ,2.0 ,0.0 ,1 ,Inj ,0 ,N ,N
33 ,6 ,120.0 ,0 ,2.0 ,0.0 ,1 ,Inj ,0 ,N ,Y
34 ,7 ,170.0 ,0 ,2.0 ,0.0 ,1 ,Waste ,0 ,N ,N
```

C.2 Purification of antibodies

C.2.1 C10/10™ column (Conditioning)

```

1 *****
2 ** Method Dump
3 **
4 ** AKTAprime Ver , V2.01
5 **
6 ** Dump Format Ver , V1.00
7 **
8 *****
9
10
11 *****
12 ** Method Settings
13 *****
14 Method Type , -
15 Method , -
16 Method base , ml
17 Frac base , ml
18 Max pressure (kPa) , 300
19 Alarm (min/ml) , 0.0
20
21 *****
22 ** Method Breakpoints
23 *****
24
25 Brkp Volume Conc Flow Frac Buff Inj Peak Autozero Eventmark
26 (mAu/min)
27
28 ,1 ,0.0 ,100 ,50.0 ,0.0 ,1 ,Waste ,0 ,N ,N
29 ,2 ,19.9 ,100 ,50.0 ,0.0 ,1 ,Waste ,0 ,N ,N
30 ,3 ,20.0 ,0 ,50.0 ,0.0 ,1 ,Waste ,0 ,N ,N
31 ,4 ,69.0 ,0 ,1.0 ,0.0 ,1 ,Waste ,0 ,N ,N
32 ,5 ,70.0 ,0 ,1.0 ,0.0 ,1 ,Inj ,0 ,N ,Y
33 ,6 ,95.0 ,0 ,1.0 ,0.0 ,1 ,Inj ,0 ,Y ,Y
34 ,7 ,120.0 ,0 ,1.0 ,0.0 ,1 ,Inj ,0 ,Y ,N

```

C.2.2 C10/10™ column (Elution)

```

1  *****
2  ** Method Dump
3  **
4  ** AKTAprime Ver , V2.01
5  **
6  ** Dump Format Ver , V1.00
7  **
8  *****
9
10
11 *****
12 ** Method Settings
13 *****
14 Method Type , -
15 Method , -
16 Method base , ml
17 Frac base , ml
18 Max pressure (kPa) , 300
19 Alarm (min/ml) , 0.0
20
21 *****
22 ** Method Breakpoints
23 *****
24
25 Brkpk Volume Conc Flow Frac Buff Inj Peak Autozero Eventmark
26 (mAu/min)
27
28 ,1 ,0.0 ,100 ,1.0 ,0.0 ,1 ,Inj ,0 ,N ,Y
29 ,2 ,1.0 ,100 ,1.0 ,0.0 ,1 ,Inj ,0 ,Y ,Y
30 ,3 ,5.0 ,100 ,1.0 ,1.5 ,1 ,Inj ,20.0 ,N ,Y
31 ,4 ,60.0 ,100 ,1.0 ,0.0 ,1 ,Inj ,0 ,N ,Y
32 ,5 ,119.9 ,100 ,1.0 ,0.0 ,1 ,Inj ,0 ,N ,N
33 ,6 ,120.0 ,0 ,1.0 ,0.0 ,1 ,Inj ,0 ,N ,Y
34 ,7 ,170.0 ,0 ,1.0 ,0.0 ,1 ,Waste ,0 ,N ,N

```


Bibliography

- Anderson R, Macdonald I, Corbett T, Hacking G, Lowdell MW and Prentice HG.** Construction and biological characterization of an interleukin-12 fusion protein (Flexi-12): delivery to acute myeloid leukemic blasts using adeno-associated virus. *Hum Gene Ther*, **8**(9):1125–1135, 1997.
- Atkins MB.** Treatment selection for patients with metastatic renal cell carcinoma: identification of features favoring upfront IL-2-based immunotherapy. *Med Oncol*, **26 Suppl 1**:18–22, 2009.
- Atkins MB, Gould JA, Allegretta M, Li JJ, Dempsey RA, Rudders RA, Parkinson DR, Reichlin S and Mier JW.** Phase I evaluation of recombinant interleukin-2 in patients with advanced malignant disease. *J Clin Oncol*, **4**(9):1380–1391, 1986.
- Atkins MB, Robertson MJ, Gordon M, Lotze MT, DeCoste M, DuBois JS, Ritz J, Sandler AB, Edington HD, Garzone PD, Mier JW, Canning CM, Battiato L, Tahara H and Sherman ML.** Phase I evaluation of intravenous recombinant human interleukin 12 in patients with advanced malignancies. *Clin Cancer Res*, **3**(3):409–417, 1997.
- Ausubel FM (ed.).** *Current Protocols in Molecular Biology*. Wiley-Interscience, Brooklyn, NY, USA, online edn., 2005.
- Bakker WH, Krenning EP, Breeman WA, Kooij PP, Reubi JC, Koper JW, de Jong M, Laméris JS, Visser TJ and Lamberts SW.** In vivo use of a radioiodinated somatostatin analogue: dynamics, metabolism, and binding to somatostatin receptor-positive tumors in man. *J Nucl Med*, **32**(6):1184–1189, 1991.

- Baxter SC, Panarello D, Ajith S, Bhattacharya M and Chaiken IM.** Recombinant-protein production in insect cells utilizing a hollow-fibre bioreactor. *Biotechnol Appl Biochem*, **45**(Pt 3):167–172, 2006.
- Bean MA, Bloom BR, Herberman RB, Old LJ, Oettgen HF, Klein G and Terry WD.** Cell-mediated cytotoxicity for bladder carcinoma: evaluation of a workshop. *Cancer Res*, **35**(10):2902–2913, 1975.
- Bolton AE and Hunter WM.** The labelling of proteins to high specific radioactivities by conjugation to a ¹²⁵I-containing acylating agent. *Biochem J*, **133**(3):529–539, 1973.
- Chiarle R, Podda A, Prolla G, Gong J, Thorbecke GJ and Inghirami G.** CD30 in normal and neoplastic cells. *Clin Immunol*, **90**(2):157–164, 1999.
- Chmielewski M.** *Antigen-spezifische T-Zellaktivierung durch rekombinante Immunrezeptoren: Evaluierung in einem immunkompetenten Maus-Modell.* Ph.D. thesis, Mathematisch-naturwissenschaftliche Fakultät der Universität zu Köln, 2007.
- Coligan JE** (ed.). *Current Protocols in Protein Science.* Wiley-Interscience, Brooklyn, NY, USA, online edn., 2005.
- Corbett TH, Griswold DP, Roberts BJ, Peckham JC and Schabel FM.** Tumor induction relationships in development of transplantable cancers of the colon in mice for chemotherapy assays, with a note on carcinogen structure. *Cancer Res*, **35**(9):2434–2439, 1975. MC38.
- Davis CB and Gillies SD.** Immunocytokines: amplification of anti-cancer immunity. *Cancer Immunol Immunother*, **52**(5):297–308, 2003.
- Deckert PM.** Current constructs and targets in clinical development for antibody-based cancer therapy. *Curr Drug Targets*, **10**(2):158–175, 2009.
- Diehl V, Kirchner HH, Burrichter H, Stein H, Fonatsch C, Gerdes J, Schaadt M, Heit W, Uchanska-Ziegler B, Ziegler A, Heintz F and Sueno K.** Characteristics of Hodgkin's disease-derived cell lines. *Cancer Treat Rep*, **66**(4):615–632, 1982.

- DuBridge RB, Tang P, Hsia HC, Leong PM, Miller JH and Calos MP.** Analysis of mutation in human cells by using an Epstein-Barr virus shuttle system. *Mol Cell Biol*, **7**(1):379–387, 1987. MC38.
- Dutcher J, Atkins MB, Margolin K, Weiss G, Clark J, Sosman J, Logan T, Aronson F, Mier J and Group CW.** Kidney cancer: the Cytokine Working Group experience (1986-2001): part II. Management of IL-2 toxicity and studies with other cytokines. *Med Oncol*, **18**(3):209–219, 2001.
- Engvall E and Perlmann P.** Enzyme-linked immunosorbent assay (ELISA). Quantitative assay of immunoglobulin G. *Immunochemistry*, **8**(9):871–874, 1971.
- Ettre LS.** Nomenclature for chromatography (IUPAC Recommendations 1993). *Pure and Applied Chemistry*, **65**(4):819–872, 1993.
- Felgner PL, Gadek TR, Holm M, Roman R, Chan HW, Wenz M, Northrop JP, Ringold GM and Danielsen M.** Lipofection: a highly efficient, lipid-mediated DNA-transfection procedure. *Proc Natl Acad Sci U S A*, **84**(21):7413–7417, 1987.
- Fuchs M, Diehl V and Re D.** Current strategies and new approaches in the treatment of Hodgkin's lymphoma. *Pathobiology*, **73**(3):126–140, 2006.
- Gentleman RC, Carey VJ, Bates DM, Bolstad B, Dettling M, Dudoit S, Ellis B, Gautier L, Ge Y, Gentry J, Hornik K, Hothorn T, Huber W, Iacus S, Irizarry R, Leisch F, Li C, Maechler M, Rossini AJ, Sawitzki G, Smyth G, Tierney L, Yang JYH and Zhang J.** Bioconductor: open software development for computational biology and bioinformatics. *Genome Biol*, **5**(10):R80, 2004.
- Gerber DE.** Targeted therapies: a new generation of cancer treatments. *Am Fam Physician*, **77**(3):311–319, 2008.
- Gillies SD, Lan Y, Brunkhorst B, Wong WK, Li Y and Lo KM.** Bi-functional cytokine fusion proteins for gene therapy and antibody-targeted treatment of cancer. *Cancer Immunol Immunother*, **51**(8):449–460, 2002.
- Gillies SD, Reilly EB, Lo KM and Reisfeld RA.** Antibody-targeted interleukin 2 stimulates T-cell killing of autologous tumor cells. *Proc Natl Acad Sci U S A*, **89**(4):1428–1432, 1992.

- Greenwood FC, Hunter WM and Glover JS.** The preparation of I-131-labelled human growth hormone of high specific radioactivity. *Biochem J*, **89**:114–123, 1963.
- Hanahan D.** Studies on transformation of Escherichia coli with plasmids. *J Mol Biol*, **166**(4):557–580, 1983.
- Hanahan D.** *DNA Cloning: a practical approach*, vol. 1, pp. 109–135. IRL Press Limited, Oxford, 1985.
- Heuser C, Diehl V, Abken H and Hombach A.** Anti-CD30-IL-12 antibody-cytokine fusion protein that induces IFN-gamma secretion of T cells and NK cell-mediated lysis of Hodgkin's lymphoma-derived tumor cells. *Int J Cancer*, **106**(4):545–552, 2003.
- Heuser C, Guhlke S, Matthies A, Bender H, Barth S, Diehl V, Abken H and Hombach A.** Anti-CD30-scFv-Fc-IL-2 antibody-cytokine fusion protein that induces resting NK cells to highly efficient cytolysis of Hodgkin's lymphoma derived tumour cells. *Int J Cancer*, **110**(3):386–394, 2004.
- Hock H, Dorsch M, Diamantstein T and Blankenstein T.** Interleukin 7 induces CD4+ T cell-dependent tumor rejection. *J Exp Med*, **174**(6):1291–1298, 1991.
- Hoffmann P, Mueller N, Shively JE, Fleischer B and Neumaier M.** Fusion proteins of B7.1 and a carcinoembryonic antigen (CEA)-specific antibody fragment opsonize CEA-expressing tumor cells and coactivate T-cell immunity. *Int J Cancer*, **92**(5):725–732, 2001.
- Hombach A and Abken H.** Costimulation tunes tumor-specific activation of redirected T cells in adoptive immunotherapy. *Cancer Immunol Immunother*, **56**(5):731–737, 2007.
- Hombach A, Heuser C and Abken H.** Simultaneous targeting of IL2 and IL12 to Hodgkin's lymphoma cells enhances activation of resting NK cells and tumor cell lysis. *Int J Cancer*, **115**(2):241–247, 2005.
- Hombach A, Sircar R, Heuser C, Tillmann T, Diehl V, Kruis W, Pohl C and Abken H.** Chimeric anti-TAG72 receptors with immunoglobulin constant Fc domains and gamma or zeta signalling chains. *Int J Mol Med*, **2**(1):99–103, 1998.

- Hornick JL, Khawli LA, Hu P, Lynch M, Anderson PM and Epstein AL.** Chimeric CLL-1 antibody fusion proteins containing granulocyte-macrophage colony-stimulating factor or interleukin-2 with specificity for B-cell malignancies exhibit enhanced effector functions while retaining tumor targeting properties. *Blood*, **89**(12):4437–4447, 1997.
- Hölscher C.** The power of combinatorial immunology: IL-12 and IL-12-related dimeric cytokines in infectious diseases. *Med Microbiol Immunol*, **193**(1):1–17, 2004.
- Johannsen M, Roemer A, Spitaleri G, Curigliano G, Giovannoni L, Menssen HD, Zardi L, Neri D, Miller K and de Braud FG.** Phase I/II study of the tumor-targeting human L19-IL2 monoclonal antibody-cytokine fusion protein in patients with advanced renal cell carcinoma. *ASCO Meeting Abstracts*, **26**(15S):16032, 2008.
- Jost LM, Kirkwood JM and Whiteside TL.** Improved short- and long-term XTT-based colorimetric cellular cytotoxicity assay for melanoma and other tumor cells. *J Immunol Methods*, **147**(2):153–165, 1992.
- von Kalle C, Wolf J, Becker A, Scaer A, Munck M, Engert A, Kapp U, Fonatsch C, Komitowski D and de Lacroix WF.** Growth of Hodgkin cell lines in severely combined immunodeficient mice. *Int J Cancer*, **52**(6):887–891, 1992.
- Kaplan MH.** STAT4: a critical regulator of inflammation in vivo. *Immunol Res*, **31**(3):231–242, 2005.
- Kaspar M, Trachsel E and Neri D.** The antibody-mediated targeted delivery of interleukin-15 and GM-CSF to the tumor neovasculature inhibits tumor growth and metastasis. *Cancer Res*, **67**(10):4940–4948, 2007.
- King DM, Albertini MR, Schalch H, Hank JA, Gan J, Surfus J, Mahvi D, Schiller JH, Warner T, Kim K, Eickhoff J, Kendra K, Reisfeld R, Gillies SD and Sondel P.** Phase I clinical trial of the immunocytokine EMD 273063 in melanoma patients. *J Clin Oncol*, **22**(22):4463–4473, 2004.
- Ko YJ, Bublely GJ, Weber R, Redfern C, Gold DP, Finke L, Kovar A, Dahl T and Gillies SD.** Safety, pharmacokinetics, and biological pharmacodynamics of the immunocytokine EMD 273066 (huKS-IL2): results of a

phase I trial in patients with prostate cancer. *J Immunother*, **27**(3):232–239, 2004.

Koprowski H, Steplewski Z, Mitchell K, Herlyn M, Herlyn D and Fuhrer P. Colorectal carcinoma antigens detected by hybridoma antibodies. *Somatic Cell Genet*, **5**(6):957–971, 1979.

Kung P, Goldstein G, Reinherz EL and Schlossman SF. Monoclonal antibodies defining distinctive human T cell surface antigens. *Science*, **206**(4416):347–349, 1979.

Köhler G and Milstein C. Continuous cultures of fused cells secreting antibody of predefined specificity. *Nature*, **256**(5517):495–497, 1975.

Ma A, Koka R and Burkett P. Diverse functions of IL-2, IL-15, and IL-7 in lymphoid homeostasis. *Annu Rev Immunol*, **24**:657–679, 2006.

Matthey B, Borchmann P, Schnell R, Tawadros S, Lange H, Huhn M, Klimka A, Tur MK, Barth S, Engert A and Hansen HP. Metalloproteinase inhibition augments antitumor efficacy of the anti-CD30 immunotoxin Ki-3(scFv)-ETA' against human lymphomas in vivo. *Int J Cancer*, **111**(4):568–574, 2004.

Mosmann TR, Yokota T, Kastelein R, Zurawski SM, Arai N and Takebe Y. Species-specificity of T cell stimulating activities of IL 2 and BSF-1 (IL 4): comparison of normal and recombinant, mouse and human IL 2 and BSF-1 (IL 4). *J Immunol*, **138**(6):1813–1816, 1987.

Murphy K, Travers P and Walport M. *Janeway's immunobiology*. Garland Science, 7th edn., 2008.

Nilsen SL and Castellino FJ. Expression of human plasminogen in *Drosophila* Schneider S2 cells. *Protein Expr Purif*, **16**(1):136–143, 1999.

Osenga KL, Hank JA, Albertini MR, Gan J, Sternberg AG, Eickhoff J, Seeger RC, Matthey KK, Reynolds CP, Twist C, Krailo M, Adamson PC, Reisfeld RA, Gillies SD, Sondel PM and Group CO. A phase I clinical trial of the hu14.18-IL2 (EMD 273063) as a treatment for children with refractory or recurrent neuroblastoma and melanoma: a study of the Children's Oncology Group. *Clin Cancer Res*, **12**(6):1750–1759, 2006.

- Pace CN, Vajdos F, Fee L, Grimsley G and Gray T.** How to measure and predict the molar absorption coefficient of a protein. *Protein Sci*, **4**(11):2411–2423, 1995.
- Peng LS, Penichet ML and Morrison SL.** A single-chain IL-12 IgG3 antibody fusion protein retains antibody specificity and IL-12 bioactivity and demonstrates antitumor activity. *J Immunol*, **163**(1):250–258, 1999.
- Pfreundschuh M.** *Leucocyte typing IV: white cell differentiation antigens; Vienna 21 - 25 Febr. 1989*, vol. 4, pp. 419–22. Oxford University Press, Oxford, 1989.
- Pohl C, Renner C, Schwonzen M, Sieber M, Lorenz P, Pfreundschuh M and Diehl V.** Anti-idiotypic vaccine against Hodgkin's lymphoma: induction of B- and T-cell immunity across species barriers against CD30 antigen by murine monoclonal internal image antibodies. *Int J Cancer*, **50**(6):958–967, 1992.
- Powers DB, Amersdorfer P, Poul M, Nielsen UB, Shalaby MR, Adams GP, Weiner LM and Marks JD.** Expression of single-chain Fv-Fc fusions in *Pichia pastoris*. *J Immunol Methods*, **251**(1-2):123–135, 2001.
- R Development Core Team.** *R: A Language and Environment for Statistical Computing*. R Foundation for Statistical Computing, Vienna, Austria, 2009. ISBN 3-900051-07-0.
- Reagan-Shaw S, Nihal M and Ahmad N.** Dose translation from animal to human studies revisited. *FASEB J*, **22**(3):659–661, 2008.
- Rennen HJ, Makarewicz J, Oyen WJ, Laverman P, Corstens FH and Boerman OC.** The effect of molecular weight on nonspecific accumulation of (99m)T-labeled proteins in inflammatory foci. *Nucl Med Biol*, **28**(4):401–408, 2001.
- Ribas A, Kirkwood JM, Atkins MB, Whiteside TL, Gooding W, Kovar A, Gillies SD, Kashala O and Morse MA.** Phase I/II open-label study of the biologic effects of the interleukin-2 immunocytokine EMD 273063 (hu14.18-IL2) in patients with metastatic malignant melanoma. *J Transl Med*, **7**:68, 2009.

- Riccobene TA, Miceli RC, Lincoln C, Knight Y, Meadows J, Stabin MG and Sung C.** Rapid and specific targeting of 125I-labeled B lymphocyte stimulator to lymphoid tissues and B cell tumors in mice. *J Nucl Med*, **44**(3):422–433, 2003.
- Ritz C and Streibig JC.** Bioassay Analysis using R. *Journal of Statistical Software*, **12**, 2005.
- Romagnani S, Ferrini PL and Ricci M.** The immune derangement in Hodgkin's disease. *Semin Hematol*, **22**(1):41–55, 1985.
- Schliemann C, Palumbo A, Zuberbühler K, Villa A, Kaspar M, Trachsel E, Klapper W, Messen HD and Neri D.** Complete eradication of human B-cell lymphoma xenografts using rituximab in combination with the immunocytokine L19-IL2. *Blood*, **113**(10):2275–2283, 2009.
- Schneider I.** Cell lines derived from late embryonic stages of *Drosophila melanogaster*. *J Embryol Exp Morphol*, **27**(2):353–365, 1972.
- Schoenhaut DS, Chua AO, Wolitzky AG, Quinn PM, Dwyer CM, McComas W, Familletti PC, Gately MK and Gubler U.** Cloning and expression of murine IL-12. *J Immunol*, **148**(11):3433–3440, 1992.
- Schoenwald RD.** *Pharmacokinetic principles of dosing adjustments : understanding the basics*. Technomic Publishing Company, Lancaster, PA, USA, 2001. ISBN ISBN: 1566768993.
- Schrama D, Reisfeld RA and Becker JC.** Antibody targeted drugs as cancer therapeutics. *Nat Rev Drug Discov*, **5**(2):147–159, 2006.
- Sjöblom T, Jones S, Wood LD, Parsons DW, Lin J, Barber TD, Mandelker D, Leary RJ, Ptak J, Silliman N, Szabo S, Buckhaults P, Farrell C, Meeh P, Markowitz SD, Willis J, Dawson D, Willson JKV, Gazdar AF, Hartigan J, Wu L, Liu C, Parmigiani G, Park BH, Bachman KE, Papadopoulos N, Vogelstein B, Kinzler KW and Velculescu VE.** The consensus coding sequences of human breast and colorectal cancers. *Science*, **314**(5797):268–274, 2006.
- Skinnider BF and Mak TW.** The role of cytokines in classical Hodgkin lymphoma. *Blood*, **99**(12):4283–4297, 2002.

- Stallmach A, Marth T, Weiss B, Wittig BM, Hombac A, Schmidt C, Neurath M, Zeitz M, Zeuzem S and Abken H.** An interleukin 12 p40-IgG2b fusion protein abrogates T cell mediated inflammation: anti-inflammatory activity in Crohn's disease and experimental colitis in vivo. *Gut*, **53**(3):339–345, 2004.
- Tesch H, Herrmann T, Abts H, Diamantstein T and Diehl V.** High affinity IL-2 receptors on a Hodgkin's derived cell line. *Leuk Res*, **14**(11-12):953–960, 1990.
- Thomson AW and Lotze MT** (eds.). *The cytokine handbook*. Academic Press, London, UK, 4th edn., 2003.
- Thèze J** (ed.). *The cytokine network and immune functions*. Oxford University Press, Oxford, UK, 1st edn., 1999.
- Uzel G, Frucht DM, Fleisher TA and Holland SM.** Detection of intracellular phosphorylated STAT-4 by flow cytometry. *Clin Immunol*, **100**(3):270–276, 2001.
- Voltz E and Gronemeyer H.** A new era of cancer therapy: cancer cell targeted therapies are coming of age. *Int J Biochem Cell Biol*, **40**(1):1–8, 2008.
- Wagener C, Clark BR, Rickard KJ and Shively JE.** Monoclonal antibodies for carcinoembryonic antigen and related antigens as a model system: determination of affinities and specificities of monoclonal antibodies by using biotin-labeled antibodies and avidin as precipitating agent in a solution phase immunoassay. *J Immunol*, **130**(5):2302–2307, 1983.
- Weiss JM, Subleski JJ, Wigginton JM and Wiltrout RH.** Immunotherapy of cancer by IL-12-based cytokine combinations. *Expert Opin Biol Ther*, **7**(11):1705–1721, 2007.
- Wigginton JM and Wiltrout RH.** IL-12/IL-2 combination cytokine therapy for solid tumours: translation from bench to bedside. *Expert Opin Biol Ther*, **2**(5):513–524, 2002.
- World Health Organization** (ed.). *The global burden of disease : 2004 update*. WHO Press, 2008.

Xu X, Clarke P, Szalai G, Shively JE, Williams LE, Shyr Y, Shi E and Primus FJ. Targeting and therapy of carcinoembryonic antigen-expressing tumors in transgenic mice with an antibody-interleukin 2 fusion protein. *Cancer Res*, **60**(16):4475–4484, 2000.

Yalow RS and Berson SA. Immunoassay of endogenous plasma insulin in man. *J Clin Invest*, **39**:1157–1175, 1960.

Young GAR and Iland HJ. Clinical perspectives in lymphoma. *Intern Med J*, **37**(7):478–484, 2007.